UNIVERSIDAD DE SALAMANCA

CENTRO DE INVESTIGACIÓN DEL CÁNCER

INSTITUTO DE BIOLOGÍA MOLECULAR Y CELULAR DEL CÁNCER (CSIC-USAL)

Role of C3G in the differentiation and maturation of megakaryocytes

MEMORIA PARA OPTAR AL GRADO DE DOCTOR
PRESENTADA POR

Sara Ortiz Rivero

Bajo la dirección de la Doctora
Carmen Guerrero Arroyo

Salamanca, 2017

Dra. CARMEN GUERRERO ARROYO, Profesora Titular del Departamento de Medicina, Instituto de Biología Molecular y Celular del Cáncer (IBMCC, CSIC-Universidad de Salamanca).

CERTIFICA:

Que Dña. Sara Ortiz Rivero, licenciada en Biología por la Universidad de Salamanca, ha realizado bajo su dirección el trabajo de Tesis Doctoral que lleva por título "*Role of C3G in the differentiation and maturation of megakaryocytes*", y considera que éste reúne originalidad y contenidos suficientes para que sea presentada ante el Tribunal correspondiente y optar al Grado de Doctor por la Universidad de Salamanca con Mención de Doctorado Internacional.

Y para que conste, y a los efectos oportunos, expide el presente certificado en Salamanca a 28 de junio de 2017.

Fdo, Dra. Carmen Guerrero Arroyo

Directora de la Tesis

Este trabajo se ha enmarcado dentro de los proyectos del Plan nacional I+D+i "*Análisis in vitro e in vivo de la función de C3G en diferentes tipos celulares y su impacto en patologías cardiovasculares y en metástasis"* (SAF2013-48210-C2-1-R) y "*Función de C3G en el desarrollo tumoral y en la patofisiología del hígado. Implicación del C3G plaquetario en la angiogénesis y en enfermedades hepáticas y cardiovasculares*" (SAF2016-76588-C2-2-R) financiados por el Ministerio de Economía y Competitividad y el Fondo Europeo de Desarrollo Regional; y de los proyectos del Programa de apoyo a proyectos de investigación de la Consejería de Educación de la junta de Castilla y León titulados "*Estudio del papel de C3G y p38 MAPK en la función plaquetaria y el desarrollo de neutrófilos: implicaciones en la regulación de la leucemia mieloide crónica*" (SA157A12-1) y "*Papel de C3G en la regulación de la función plaquetaria: Implicaciones en angiogénesis y aplicación al diagnóstico y tratamiento de la enfermedad trombótica*" (SA017U16).

Sara Ortiz Rivero realizó parte del trabajo de esta tesis durante una estancia de seis meses en el laboratorio del Prof. Jacob Iasha Sznajder en la Northwestern University de Chicago, IL (USA), financiada por una *Visiting Predoctoral Fellowship* de la Northwestern University.

List of Abbreviations

aa	Amino Acid
ADP	Adenosine Diphosphate
APC	Allophycocyanin
ATP	Adenosine Triphosphate
BFU-MK	Burst-Forming Unit-Megakaryocyte
Bis	Bisindolylmaleimide
BM	Bone Marrow
BSA	Bovine Serum Albumin
C-	Carboxyl-
C3G	Crk SH3-domain-binding Guanine-nucleotide-releasing factor
CAT	Catalytic
CD-	Cluster of Differentiation
CDK	Cyclin-Dependent Kinase
cDNA	Complementary DNA
CFU-MK	Colony-Forming Unit-Megakaryocyte
CLP	Common Lymphoid Progenitor
CML	Chronic Myelogenous Leukemia
CMP	Common Myeloid Progenitor
CT	Control
Cy3	Cyanine 3
Cy5	Cyanine 5
DAPI	4´, 6-Diamino-2-Phenilindol
DIC	Differential Interference Contrast Microscopy
DMEM	Dulbecco´s Modified Eagle´s Medium
DMS	Demarcation Membrane System
DMSO	Dimethyl Sulfoxide
dNTP	Deoxyribonucleotide triphosphate
DSB	Double Strand Breaks
dsDNA	Double Stranded DNA
DTT	Dithiothreitol
E. coli	Escherichia coli
ECL	Enhanced Chemiluminescence
EPO	Erythropoietin
ERK	Extracellular signal-Regulated Kinases
EryP	Erythroid Progenitor
FACS	Fluorescence-Activated Cell Sorting
FBS	Fetal Bovine Serum
FITC	Fluorescein
FSC	Forward Scatter
GAP	GTPase Activating Proteins
GAPDH	Glyceraldehyde 3-phosphate dehydrogenase
GDP	Guanosine Diphosphate
GEF	Guanine-nucleotide-Exchange Factor
GFP	Green Fluorescence Protein
GMP	Granulocyte-Macrophage Progenitor
GPA	Glycophorin A
gRNA	Guide RNA
GST	Glutathione S-transferase
GTP	Guanosine Triphosphate
HDR	Homology-Directed Repair
HIV-1	Human Immunodeficiency Virus-1
HPP-CFU	Highly Proliferative Potential-Colony-Forming Unit-Megakaryocyte

HRP	Horseradish Peroxidase
HSC	Hematopoietic Stem Cells
IFN	Interferon
IgG	Immunoglobulin G
IL-	Interleukin-
IMDM	Iscove´s Modified Dulbecco´s Medium
IMS	Invaginated Membrane System
Jak2	Janus Kinase 2
JNK	c-Jun N-terminal Kinase
KO	Knock-Out
LB agar	Luria-Broth agar
LMPP	Lymphoid-primed Multipotent Progenitor
LSK	Lin-Sca1+c-kit+
LT-HSC	Long-Term Hematopoietic Stem Cell
LTR	Long Terminal Repeat
MAPK	Mitogen-Activated Protein Kinase
MAPKK	Mitogen-Activated Protein Kinases Kinase
MCS	Multiple Cloning Sites
MEF	Mouse Embryonic Fibroblasts
MEK	MAPK/ERK Kinase
MEP	Megakaryocyte-Erythroid Progenitor
MK	Megakaryocytes/Megakaryocytic
MLB	Mg^{2+} Lysis/Wash Buffer
MOI	Multiplicity of Infection
MPP	Multipotent Progenitor
mRNA	Messenger RNA
N-	Amino-
NADPH	Nicotinamide Adenine Dinucleotide Phosphate
NES	Nuclear Export Signal
NK	Natural Killer
NLS	Nuclear Localization Signal
o/n	Over night
Oligo(dT)	Oligo (deoxythymine)
ORF	Open Reading Frame
p-	Phospho-
PBS	Phosphate Buffered Saline
PCR	Polymerase Chain Reaction
PE	Phycoerythrin
PEI	Polyethylenimine
PF4	Platelet factor 4
PFA	Paraformaldehyde
PI	Propidium Iodide
PI3K	Phosphoinositide 3-kinase
PKC	Protein Kinase C
PMA	Phorbol 12-Myristate 13-Acetate
PVDF	Polyvinylidene difluoride
qPCR	Quantitative-Polymerase Chain Reaction
RBC	Red Blood Cells
RBD	Rap-Binding Domain
REM	Ras-Exchange-Motif
RFP	Red Fluorescence Protein
ROS	Reactive Oxigene Species
RPMI	Roswell Park Memorial Institute
RT	Room Temperature

RT-PCR	Reverse Transcription PCR
SB	SB203580, inhibitor of p38 pathway
SCF	Stem Cell Factor
SDF1α	Stromal-Derived Factor 1α
SDS-PAGE	Sodium Dodecyl Sulfate-Polyacrylamide Gel Electrophoresis
SEM	Standard Error of the Mean
SH3b	SH3-binding
shRNA	Short Hairpin RNA
SSC	Side Scatter
STAT	Signal Transducer and Activator of Transcription
ST-HSC	Short-Term Hematopoietic Stem Cell
TAE	Tris-Acetic-EDTA
Tg-	Transgenic
TPO	Thrombopoietin
TTBS	Tween Tris-Buffered Saline
Tyr	Tyrosine
U0	U0126, ERK1/2 inhibitor
vWF	Von Willebrand Factor
W	Wortmannin, PI3K inhibitor
WT	Wild Type

Table of Contents

Introduction

1. C3G

1.1. Generalities

C3G (Crk SH3-domain-binding guanine-nucleotide-releasing factor) is a Guanine Nucleotide Exchange Factor (GEF) for several members of the Ras superfamily of GTPases, mainly Rap1 and R-Ras (Gotoh, T. et al. 1995, Gotoh, T. et al. 1997). C3G mediates functions associated with its catalytic domain, thus promoting the binding of GTP to the GTPases. In addition, C3G can behave as an adapter protein, performing functions based on protein-protein interactions, independently of its GEF domain (Guerrero, C. et al. 1998, Shivakrupa, R. et al. 2003, Guerrero, C. et al. 2004). The alternative names of C3G are RapGEF1, GRF2, and CRK SH3-binding GNRP (guanine nucleotide releasing protein).

C3G was initially isolated as a Crk SH3-binding protein (Knudsen, B.S. et al. 1994, Tanaka, S. et al. 1994) and later identified as the first Rap GEF described (Gotoh, T. et al. 1995). Although C3G is ubiquitously expressed in human adult and fetal tissues, high levels of C3G have been reported in specific tissues, such as placenta, heart and skeletal muscle, while it is poorly expressed in the liver (Guerrero, C. et al. 1998).

1.2. C3G structure

The human C3G gene comprises 3231 bp, distributed in 24 exons spanning 163 kb on chromosome 9q34.3 (Acc. Num. NM_005312) (Takai, S. et al. 1994, Radha, V. et al. 2011), although several isoforms have been described, as detailed below. The C3G ORF encodes a protein of 1077 amino acids, which has several functionally and structurally, well differentiated, domains (Tanaka, S. et al. 1994) (**Figure I-1**).

The C-terminal region of C3G contains a 224 aa sequence corresponding to the **Catalytic Domain,** responsible for the GEF function. This domain is also known as CDC25-H (*CDC25-homology*) for its homology to the CDC25 protein of *S. cerevisae* (Martegani, E. et al. 1992). Upstream the catalytic domain is the **REM** domain (Ras Exchange-Motif), which, collaborates with the catalytic domain in the exchange reaction (Bos, J.L. et al. 2007). The central region, called **SH3-binding Domain (SH3b),** contains five proline-rich sequences (amino acids 280 to 646) that follow the Pro-Pro-X-X-Pro-X-K/R consensus motif (Knudsen, B.S. et al. 1994). These motifs bind to SH3 domains of adaptor proteins, such as Crk (Matsuda, M. et al. 1992) and p130Cas (Kirsch, K.H. et al. 1998), as well as tyrosine kinases, such as c-Abl (Radha, V. et al. 2007) and Bcr-Abl (Gutierrez-Berzal, J. et al. 2006), among many others proteins (Maia, V. et al. 2013). The N-terminal region (amino acids 144 to 230)

includes an E-cadherin binding domain (Hogan, C. et al. 2004), which is involved in the recruitment of E-cadherin during the initial steps of junction formation (Hogan, C. et al. 2004, Pannekoek, W.J. et al. 2009). The N-terminal region also behaves as a cis-acting negative regulatory element, inhibiting the GEF activity of C3G. This negative effect is suppressed when C3G is phosphorylated in Tyr-504 (Ichiba, T. et al. 1999).

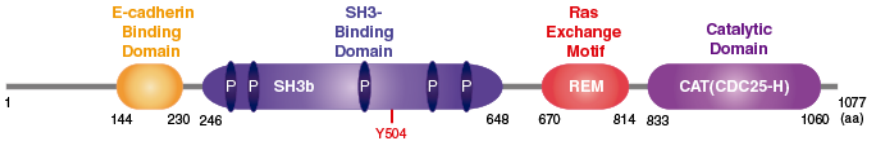

Figure I-1. Schematic representation of C3G structure, showing its domain organization. The illustration shows the C-terminal Catalytic domain (purple) homologous to CDC25 (CDC25-H), the Ras Exchange Motif or REM (red), the central SH3b domain, containing five proline-rich sequences (blue), and the N-terminal region containing the E-cadherin binding domain (orange). The numbers indicate the amino acids (aa) that approximately limit the start and end of each domain. The position of the tyrosine residue 504 is indicated in red (Y504).

In human, two isoforms of C3G, a and b, generated by alternative splicing, have been described. These isoforms differ in the N-terminal region, with isoform b having 18 more aa than isoform a (Figure I-2). Both C3G isoforms show ubiquitous expression in human tissues (Zhai, B. et al. 2001, Radha, V. et al. 2011).

A third isoform of 87 kDa (p87C3G) has been characterized in chronic myeloid leukemia (CML) cells. This isoform lacks the first 305 amino acids, corresponding to the E-cadherin binding domain and the two first proline-rich regions (Gutierrez-Berzal, J. et al. 2006) (Figure I-2). The p87C3G isoform is overexpressed in CML cell lines and also in primary bone marrow cells from CML patients. In addition, p87C3G is phosphorylated by Bcr-Abl, suggesting a role for C3G in CML (Gutierrez-Berzal, J. et al. 2006).

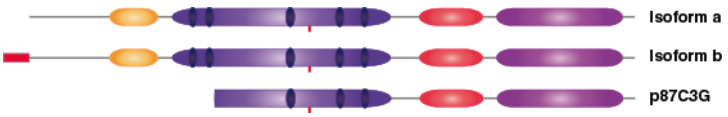

Figure I-2. Human isoforms of C3G. Schematic representation of the three isoforms of C3G described in human tissues. Isoforms a and b, arise due to alternate splicing and differ in the N-terminus. A truncated isoform, p87C3G, is expressed in CML cells and patients. For the legend of the different domains, see Figure I-1.

1.3. Activation of C3G

C3G is activated by multiple extracellular stimuli, which indicates its involvement in different signaling pathways. Among the stimuli that activate C3G signaling pathways are interferon-gamma (IFN-γ) (Alsayed, Y. et al. 2000), growth hormone (GH) (Zhu, T. et al. 1998,

Ling, L. et al. 2003), insulin (Okada, S. et al. 1997), platelet-derived growth factor (PDGF) (Yokote, K. et al. 1998), interleukin-3 (IL-3) (Nosaka, Y. et al. 1999) and integrin binding to extracellular matrix (ECM) components (Buensuceso, C.S. et al. 2000). In particular, it has been reported that hematopoietic cells stimulated with IL-3 cytokine, which is involved in the proliferation of megakaryocytes colonies, show an activation of gene transcription, mediated by Elk-1- and c-fos, through the CrkL-C3G complex (Nosaka, Y. et al. 1999).

The activation of C3G requires its recruitment to membranes through binding to Crk adapter proteins, CrkII, CrkI (an alternative spliced form of CrkII) and CrkL (Birge, R.B. et al. 2009). CrkII and CrkL are composed of a SH2 domain that interacts with tyrosine phosphorylated residues present in focal adhesion proteins, such as p130Cas, Cbl and paxillin, and two SH3 domains, which bind to proteins containing proline-rich sequences (Bhat, A. et al. 1997). The N-T-SH3 domain of Crk proteins has been found to interact with C3G, Sos, DOCK180, c-Abl and EPS15 (Feller, S.M. et al. 1994, Matsuda, M. et al. 1994, Ren, R. et al. 1994, Schumacher, C. et al. 1995, Hasegawa, H. et al. 1996). However, so far no binding-partners have been described for the C-T-SH3 domain (Birge, R.B. et al. 2009). In addition, it has shown that binding of the SH3 domain of p130Cas to Pro-267 and Pro-270 residues of C3G might be required for optimal activation of C3G, suggesting that Crk brings C3G to the vicinity of p130Cas to facilitate its interaction and subsequent phosphorylation and activation (Kirsch, K.H. et al. 1998). The phosphorylation of C3G can be performed by several tyrosine kinases, such as c-Src, Hck, Fyn. c-Abl and Bcr-Abl (Ling, L. et al. 2003, Shivakrupa, R. et al. 2003, Radha, V. et al. 2004, Gutierrez-Berzal, J. et al. 2006, Mitra, A. et al. 2010). It has been reported that C3G is completely active when is phosphorylated in Y504 (Ichiba, T. et al. 1999), although the implication of other phosphorylated residues in its activation is not excluded (Mitra, A. et al. 2010). Removal of the N-terminal region of C3G, including Tyr-504, generates a mutant that is fully active, in concordance with the negative regulation exerted by this region on the catalytic activity.

1.4. C3G as a GEF of small GTPases

C3G through its catalytic domain promotes guanine nucleotide exchange reactions for the Ras family members, Rap1, Rap2, R-Ras and TC21, and for the Rho family member, TC10 (Radha, V. et al. 2011). Ras proteins are small monomeric GTPases that cycle between a GTP-bound (active) conformation and a GDP-bound (inactive) one, leading to a quick on/off switch of the signaling pathways. In the active conformation, the GTPase interacts with effector proteins, thereby inducing downstream signaling events. The GDP-GTP cycle is regulated by GEFs, such as C3G, which induce the release of bound GDP to be replaced by

GTP, and by GAPs (GTPase Activating Proteins) that catalyze the hydrolysis of GTP to GDP (Figure I-3).

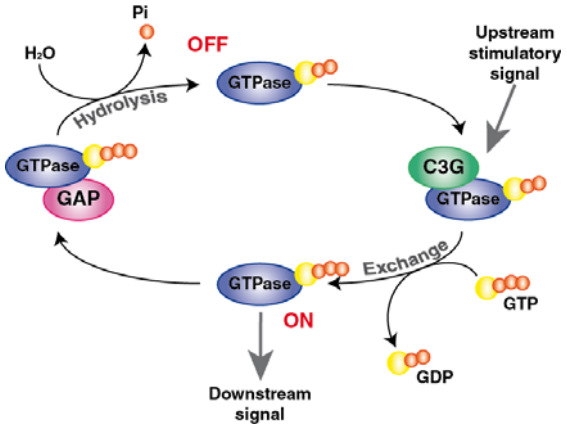

Figure I-3. GTPase activity cycle. C3G GEF activity, modulated by upstream signals, catalyzes the dissociation of GDP from the GTPase by modifying its affinity for the nucleotide-binding site. GDP is released and subsequently replaced by GTP, 10 times more abundant than GDP in the cells, allowing the activation of downstream signaling pathways. GTP-bound GTPases (active) associates with GAPs, which accelerate the hydrolysis of GTP, releasing an inorganic phosphate. GEF: Guanine-nucleotide exchange factor; GAP: GTPase-activating protein; GTP: guanosine triphosphate; GDP: guanosine diphosphate; Pi: inorganic phosphate.

1.5. C3G as an adapter protein

C3G is able to modulate several cellular functions independently of its catalytic, GEF, domain. Its central region contains several poly-proline tracts that can interact directly with proteins that contain SH3 domains, such as Crk, Abl, Hck and p130Cas (Knudsen, B.S. et al. 1994, Tanaka, S. et al. 1994, Kirsch, K.H. et al. 1998, Shivakrupa, R. et al. 2003), among many others (Maia, V. et al. 2013). In addition, it has been described that through its N-terminal region C3G is also able to interact with E-cadherin (Hogan, C. et al. 2004).

The interaction with Crk is especially relevant, since the formation of Crk-C3G complexes is essential for the subsequent activation of C3G-mediated Rap1 signaling pathways (Ichiba, T. et al. 1997, Radha, V. et al. 2011).

1.6. Functions of C3G

C3G plays a crucial role in several cellular processes. As mentioned, some of these functions are mediated by its GEF activity, while others are established by protein-protein interactions through its SH3-binding region. The main functions and interactions of C3G are summarized in Figure I-4.

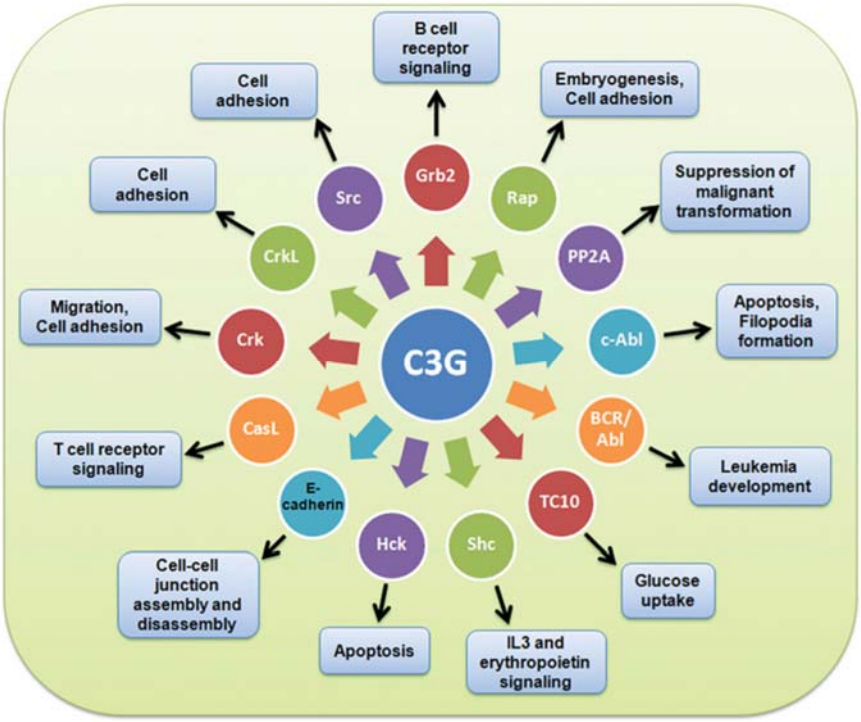

Figure I-4. Interacting partners of C3G and the specific functions in which they are involved (Radha, V. et al. 2011). Except for E-cadherin and Rap, all these interactions are established through the proline-rich region of C3G and SH3 domains present in the indicated proteins. A direct interaction has been characterized between C3G and Crk, CasL (p130Cas-related protein), Hck and Abl.

C3G is involved in the following functions:

Embryonic development

C3G is essential for mouse embryonic development, since C3G −/− homozygous mice die before embryonic day 7.5 (Ohba, Y. et al. 2001). C3G-knock-out mice show defects in the nervous system, due to lack of cortical neuron migration (Voss, A.K. et al. 2006), and in blood vessel maturation, caused by inappropriate development of vascular supporting cells (Ohba, Y. et al. 2001, Voss, A.K. et al. 2003). Embryonic fibroblasts from these mice show impaired cell adhesion, delayed cell spreading and accelerated migration. These defects were rescued by the expression of active Rap1 or R-Ras, suggesting the importance of the GEF function of C3G in cell adhesion, spreading and embryogenesis. The fact that other GEFs do not compensate for embryonic lethality highlights the relevance of the C3G-Rap1 pathway in adhesion during the early stages of embryogenesis (Ohba, Y. et al. 2001).

Cell adhesion and migration. Role of integrins

Integrins play a role in the control of proliferation, apoptosis, migration and mobilization of hematopoietic cells in the bone marrow. Specifically, integrins α5β1 and αIIbβ3 are especially important in the adhesion of megakaryocytes to fibronectin (Schick, P.K. et al. 1998). In mouse embryonic fibroblasts, recruitment of C3G to the p130Cas-Crk complex is related to the activation of inside-out integrin signaling pathways through Rap1 (Ohba, Y. et al. 2001). Similarly, in hematopoietic cells the formation of the CrkL-C3G complexes induces the activation of the inside-out β1 and β2 integrin signaling, and consequent adhesion of hematopoietic cell to fibronectin, by activation of R-Ras and Rap1 pathways (Arai, A. et al. 1999, Arai, A. et al. 2001). Additionally, in Ba/F3 hematopoietic cells, overexpression of C3G enhances CrkL-dependent migration through the formation of Cbl-CrkL-C3G complexes (Uemura, N. et al. 1999). Finally, the CrkL-C3G complex induces sustained activation of the Ras/Raf/ERK signaling pathway in hematopoietic cells upon stimulation with EPO and IL-3 (Nosaka, Y. et al. 1999).

Platelet aggregation and activation

Rap1 GTPases (mainly the Rap1b isoform) play an essential role in most platelet functions, including aggregation, coagulation, adhesion and spreading, through activation of the platelet integrin αIIbβ3 (Franke, B. et al. 2000, Chrzanowska-Wodnicka, M. et al. 2005). Rap1b also modulates the interaction of integrin αIIbβ3 with the actin cytoskeleton in murine megakaryocytes, which exhibit inside-out signaling similar to platelets (Bertoni, A. et al. 2002). Although it had been described that platelet Rap1b was mainly activated by CalDAG-GEFI (Crittenden, J.R. et al. 2004, Bergmeier, W. et al. 2007), CalDAG-GEF KO platelets showed Rap1 activation and platelet aggregation in response to thrombin and PMA (Crittenden, J.R. et al. 2004), indicating the existence of Rap1b-GEFs other than CalDAG-GEF, involved in platelet function.

In this line, using transgenic mouse models, our group has established that C3G increases platelet activation and aggregation, both *in vitro* and *in vivo* (Gutierrez-Herrero, S. et al. 2012). C3G mediates platelet functions triggered by thrombin, ADP, PMA and collagen through the activation of Rap1b. In particular, C3G is a mediator of Rap1 activation induced by thrombin and PMA via PKC pathways (Gutierrez-Herrero, S. et al. 2012). This new role of C3G in platelets has been supported by other investigators, who have proposed the formation of a ternary CrkL-C3G-VASP complex regulating Rap1b (Benz, P.M. et al. 2016).

Cell differentiation and cell cycle arrest

Numerous evidences indicate a central role of C3G in differentiation of multiple cell types. C3G levels are upregulated during differentiation of monocytes to macrophages (Radha, V. et al. 2011). In addition, C3G overexpression in mouse mesenchymal cells enhances myotube formation and myogenic differentiation through Akt activation. During this process, there is an increase in tyrosine phosphorylated C3G (pY504), indicating the participation of its catalytic activity (Sasi Kumar, K. et al. 2015). Additionally, association between Crk and C3G is required for adipocyte differentiation (Jin, S. et al. 2000). Finally, C3G induces the differentiation of human neuroblastoma cells, independently of its catalytic domain, while simultaneously repressing cell cycle progression through the induction of the cell cycle inhibitor p21 (Radha, V. et al. 2008).

It has been speculated that C3G could be involved in megakaryocytic differentiation (hereafter referred as MK differentiation) induced by TPO through interaction of the CrkL-C3G complex with Mpl receptor (Oda, A. et al. 1996, Stork, P.J. et al. 2005). The proposed TPO-induced megakaryocytic differentiation model has two components; initially a Sos-1-Ras-dependent transient ERK activation is required for the proliferation of MK progenitors, which is replaced later by a sustained activation of ERK dependent on Rap1 (Stork, P.J. et al. 2005). However, the Rap1-GEF involved in this process remains unknown.

Nuclear functions of C3G

The first evidence of a putative role of C3G in the nuclear compartment came from the observation that C3G is highly expressed in the nuclei of differentiated myotubes, suggesting that C3G could contribute to skeletal muscle differentiation, which involves the formation of multinucleated cells, by modulating specific nuclear functions (Sasi Kumar, K. et al. 2015). In addition, a recent study showed that C3G has functional NES (Nuclear Export Signal) and NLS (Nuclear Localization Signal) sequences located in the central domain, and that these sites, along with the N-terminal region, are responsible for the translocation of C3G into the nucleus, where C3G is associated with chromatin and nuclear matrix fractions (Shakyawar, D.K. et al. 2017). These authors suggest a role for C3G in the nuclear compartment, through the regulation of chromatin dynamics in response to physiological stimuli.

Cell-cell junction assembly and disassembly

There are two main types of junctions that mediate adhesion in epithelial cells, adherens junctions and focal adhesions. Adherens junctions facilitate cell-cell adhesion through hemophilic interactions between two E-cadherin molecules in adjacent cells. C3G

participates in the early stages of adherens junctions formation, through direct interaction between its N-terminal domain and the cytoplasmic tail of E-cadherin (Hogan, C. et al. 2004). Moreover, there is evidence of a c-Src-Crk-C3G-Rap1 signaling pathway, which regulates the formation of adherens junctions in keratinocytes (Fukuyama, T. et al. 2005).

C3G is also involved in the formation of focal adhesion complexes, submembrane structures that connect integrins to the actin cytoskeleton. Our group has described a role for C3G in the regulation of CML cell adhesion, through its interaction with p38α MAPK and focal adhesion proteins, such as Cbl, p130Cas, paxillin and FAK (Maia, V. et al. 2013).

Filopodia formation

C3G is required for c-Abl-induced filopodia formation during cell spreading on fibronectin. In epithelial cells, C3G expression induces the reorganization of the actin cytoskeleton and promotes filopodia formation by the activation of the Crk-C3G pathway (Radha, V. et al. 2007).

Role in tumor growth

Our group has described that overexpression of C3G blocks the focus-forming activity of co-transfected, activated, *sis*, *ras*, v-*raf*, *dbl* and R-*ras* oncogenes in NIH/3T3 cells (Guerrero, C. et al. 1998, Guerrero, C. et al. 2004). This transformation suppressor function of C3G is independent of its GEF activity, but dependent on its SH3-binding domain (Guerrero, C. et al. 2004). The mechanism of suppression involves PP2A-mediated inhibition of ERK phosphorylation, and the consequent reduction in cyclin A expression, resulting in loss of the anchorage-independent growth ability of the oncogenic cells (Guerrero, C. et al. 2004, Martin-Encabo, S. et al. 2007). However, in v-Crk transformed cells, C3G, through its GEF activity, enhances growth rate and anchorage-independent growth via R-Ras and JNK (Tanaka, S. et al. 1997, Mochizuki, N. et al. 2000).

In fact, the function of C3G in cancer is quite controversial as it can act as either a tumor suppressor or promoter. As a tumor suppressor, C3G expression was shown to be reduced in cervical squamous cell carcinoma (Okino, K. et al. 2006). In contrast, an increased C3G expression was found in human non-small-cell lung cancer (Hirata, T. et al. 2004). Crk-C3G-Rap1 pathway, downstream RET, has also been implicated in the process of transformation produced in papillary thyroid carcinoma (De Falco, V. et al. 2007). The expression of p87C3G isoform in CML cells is also associated with the development of this type of cancer (Gutierrez-Berzal, J. et al. 2006). Recent data also suggest that C3G, acting

through Rap1, would promote invasion of epithelial ovarian cancer cells through increasing MMP2 and MMP9 secretion (Che, Y.L. et al. 2015). Finally, somatic demethylation of C3G intronic sequences, suggestive of C3G expression, is frequently found in colorectal, cervical and ovarian cancers (Samuelsson, J. et al. 2011).

Cell survival and apoptosis

C3G has been shown to modulate apoptosis in several cell types and in response to multiple stimuli. For example, C3G, independently of its GEF activity, interact with Hck and collaborates with this kinase in inducing apoptosis in primary hematopoietic cells (Shivakrupa, R. et al. 2003). In addition, a dual regulatory role for C3G in CML cells has been described; on one hand C3G modulates imatinib-induced apoptosis, via a Rap1-p38α MAPK-dependent pathway, and on the other hand, C3G induces ERK and Akt survival pathways, through Rap1-independent mechanisms (Maia, V. et al. 2009). C3G also plays a dual role in regulating cell death in mouse embryonic fibroblasts (MEFs), depending on the stimuli. Thus, upon serum deprivation, C3G induces survival, but in response to oxidative stress, C3G acts as a pro-apoptotic/anti-proliferative molecule. In both cases, C3G acts through the inhibition of p38α MAPK activity and in a Rap1-independent manner (Gutierrez-Uzquiza, A. et al. 2010). Finally, phosphorylation of C3G in Y504 by c-Abl is essential for the regulation of the apoptosis induced by oxidative stress in Cos-1 cells (Mitra, A. et al. 2010).

2. Hematopoiesis

Hematopoiesis is the process by which the cellular components of the blood are formed. Primary sites of blood cell production change throughout the development of most vertebrates. In mice and humans, blood cells first emerge in the extraembryonic yolk sac, which generates transitory hematopoietic cell populations, such as primitive erythrocytes, megakaryocytes and macrophages. With the onset of the vascular system, the liver becomes the predominant site of blood cell production and the spleen and marrow also become producers. In both mice and humans, hematopoiesis in the bone marrow is maintained throughout adult life, being the main blood-forming organ. In adults, all hematopoietic blood lineages (erythroid, myeloid and lymphoid) are continuously produced from a pool of progenitors cells that derive from hematopoietic stem cells (HSCs) (Yoder, M.C. 2002, Kauts, M.L. et al. 2016).

2.1. HSCs and models of the hematopoietic hierarchy

HSCs undergo successive lineage commitment steps to generate mature blood cells. Each HSC is programmed to allow the efficient production of the cellular blood components and is defined by its pluripotentiality. The capacity of a single HSC to generate any type of mature hematopoietic cells is based on its ability to undergo asymmetric cell divisions; one of the daughter cells remains as a stem cell (self-renewal), to maintain the pool of immature HSCs in the bone marrow, while the other is committed to a specific lineage (Seita, J. et al. 2010).

In the classical model of hematopoiesis (**Figure I-5**), HSCs give rise to increasingly committed progenitors with a progressively decrease in their self-renewal capacity and a more restricted lineage potential. Initially, pluripotent HSCs commit to either myeloid or lymphoid lineages, called Common Myeloid Progenitors (CMP) and Common Lymphoid Progenitors (CLP), respectively. The first isolation of CLPs determined that these progenitors can develop T and B Lymphocyte and Natural Killer (NK) cells but not myeloid cells (Kondo, M. et al. 1997). In the same way, CMPs exclusively produce the granulocyte/macrophage (neutrophils, eosinophils, basophils and monocytes-macrophages) and the megakaryocyte/erythroid (platelets and erythrocytes) lineages (Akashi, K. et al. 2000).

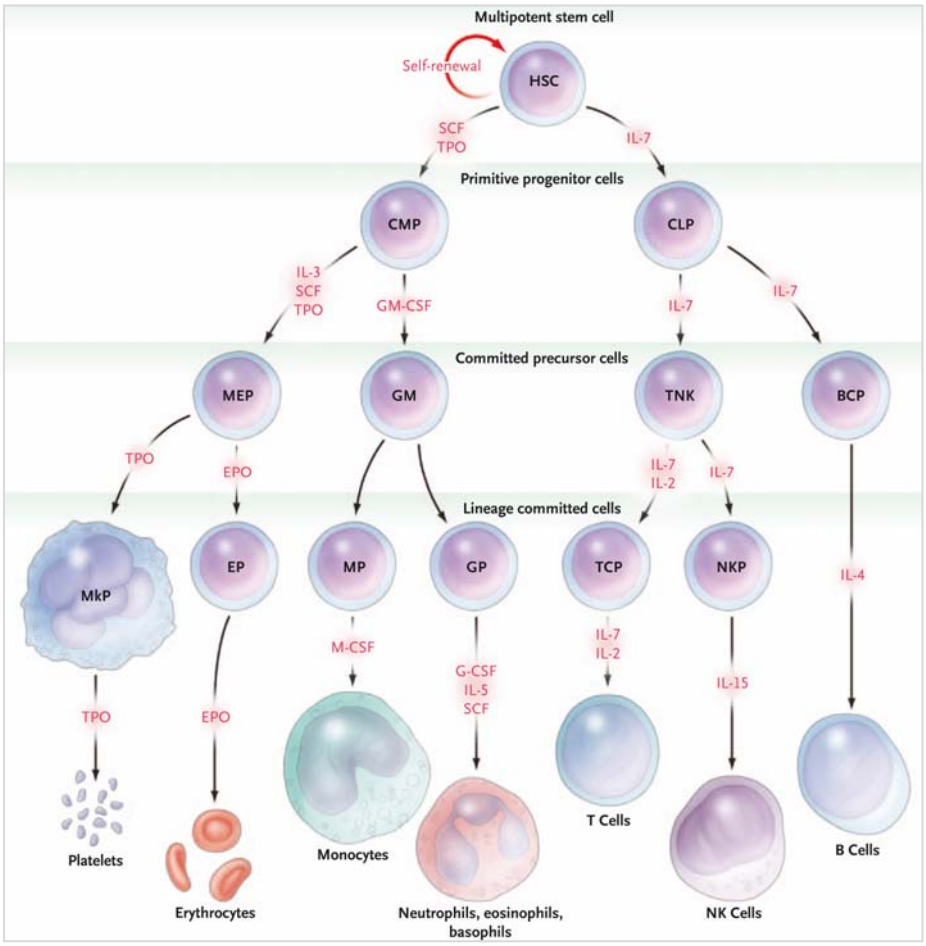

Figure I-5. Classical model of hematopoiesis. The figure shows the development of the different blood cells, from HSC to mature cells, and the major cytokines that stimulate the development of the different lineages. Figure from (Kaushansky, K. 2006).

However, this model has been changed with the study of the origin of the megakaryocyte precursors. In fact, the identification of the different precursors following the Multipotent Progenitors is very controversial. Recent studies suggest a new, non-classical, megakaryocytic differentiation model in which the megakaryocytes (MKs) can be generated from multiple pathways, some of which do not require transit through the megakaryocyte-erythroid progenitor (MEP) stage (**Figure I-6**). According to this new model, there is heterogeneity within the HSC population, including a megakaryocytic-biased HSC that would give rise directly to MK progenitors, thus bypassing the intermediate MEP stage (Woolthuis, C.M. et al. 2016).

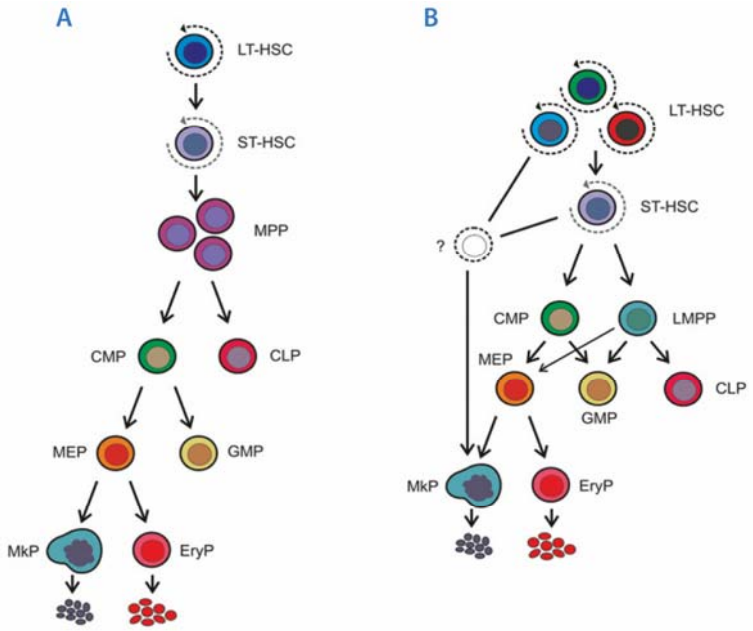

Figure I-6. Models of the hematopoietic hierarchy. A) Classical model with a strict separation between the myeloid and lymphoid lineages as the first step in lineage commitment downstream of the HSCs. **B)** Recently published model proposing an immediate committed progenitor with restricted megakaryocytic potential. LT-HSC (long-term-HSC), ST-HSC (short-term-HSC), MPP (multipotent progenitor), CMP (common myeloid progenitor), CLP (common lymphoid progenitor), MEP (megakaryocyte-erythrocyte progenitor), GMP (granulocyte-macrophage progenitor), MkP (megakaryocytic progenitor), EryP (erythroid progenitor) and LMPP (lymphoid-primed multipotent progenitor). Figure modified from (Woolthuis, C.M. et al. 2016).

3. Megakaryopoiesis

Megakaryopoiesis is the process by which mature megakaryocytes (MKs) develop from HSCs. This is a complex process that involves the commitment of HSCs to the megakaryocyte lineage, proliferation of progenitors, MK maturation and terminal differentiation to produce platelets (thrombopoiesis) (Yu, M. et al. 2012). Platelets are small anucleated cell fragments (1-3 μm of diameter) that, apart from their main role in hemostasis, participate in many other processes, such as angiogenesis, inflammation and innate immunity, among others (Blair, P. et al. 2009). Platelets are formed from the cytoplasm of MKs, large (50-100 μm), multilobulated and polyploid cells that are located in the bone marrow in a low proportion (0.01% of nucleated bone marrow cells).

In response to cytokines and environmental factors, the bipotential MEP sequentially develops into the highly proliferative potential-colony-forming unit-megakaryocytes (HPP-

CFU-MK), the burst-forming unit-megakaryocytes (BFU-MK) and the colony-forming unit-megakaryocytes (CFU-MK), being CFU-MK the most differentiated MK progenitor and the first in the MK lineage that have been identified by its surface markers-based phenotype (Deutsch, V.R. et al. 2006, Szalai, G. et al. 2006). CFU-MKs then give rise to immature MKs or megakaryoblasts, which undergo endomitosis to increase in size and in DNA content. In addition to undergoing endomitosis, immature MKs increase their reservoir of granules and cytoskeletal proteins and form the Invaginated Membrane System (IMS), also known as Demarcation Membrane System o DMS (Behnke, O. 1968, Radley, J.M. et al. 1982). Megakaryoblasts are transition cells to mature MKs, which are polyploid and no longer proliferates. Mature MKs then begin the process of shedding their cytoplasm to produce platelets, which is a complex process that requires the formation of elongated structures called proplatelets. Platelet formation and release is a terminal process for mature MKs, which leads to their apoptosis and subsequent phagocytosis by macrophages (Radley, J.M. et al. 1983, Severin, S. et al. 2010). (Figure I-7).

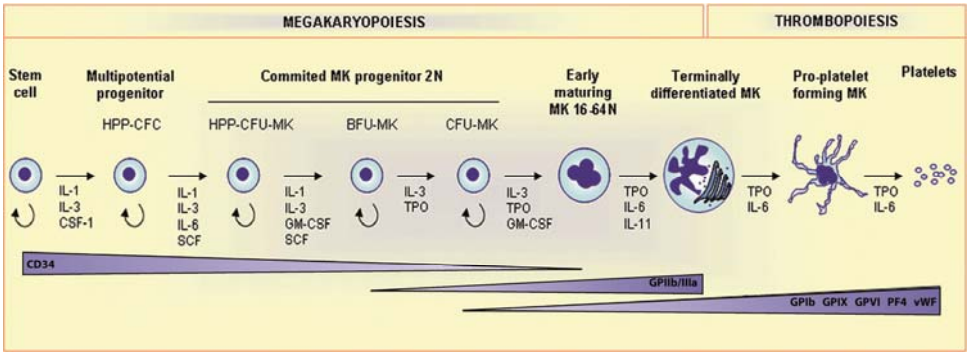

Figure I-7. Megakaryocyte differentiation and maturation, and platelet formation. The figure illustrates the development of mature MKs (megakaryopoiesis) and platelets (thrombopoiesis) from HSC. Associated surface markers are shown to indicate the MK stage at which they are expressed. Growth factors and cytokines involved in the process are depicted between each cell type. Figure modified from (Pendaries, C. et al. 2007).

3.1. Cytokines involved in megakaryopoiesis and thrombopoiesis

Megakaryocyte development and platelet formation are regulated at multiple levels by many different cytokines and environmental factors. Thrombopoietin (TPO) is produced in the liver, and is the main regulator of megakaryopoiesis and thrombopoiesis, modulating all stages of MK development, from HSC proliferation to cytoplasmic maturation. TPO alone through its receptor, c-Mpl, is able to increase MK size, ploidy and expression of lineage-specific markers, such as glycoproteins GPIb and GPIIb/IIIa (Kaushansky, K. et al. 1994). Additionally, although *in vitro* TPO is sufficient to produce MK colonies from CFU-MKs, it has

been observed that in combination with other cytokines, such as IL-3, IL-11 and Stem Cell Factor (SCF), it is able to increase the size of the colonies (Kaushansky, K. et al. 1995). Furthermore, *in vitro* studies have shown that TPO increases the survival of hematopoietic progenitor cells (CD34+), especially in combination with IL-3 and SCF, suggesting the importance of TPO, not only in the MK lineage, but also in HSC proliferation and survival (Ku, H. et al. 1996). Despite the great effects that TPO seems to have on MK differentiation and maturation, it appears to have little effect during platelet release.

Concerning other cytokines involved in this process, we focused our attention on SCF, IL-3, IL-6 and IL-11. IL-3 produces an additive effect to that of TPO and may play a role primarily as a proliferation factor, but does not participate in terminal differentiation into polyploid cells. On the other hand, SCF and IL-11 synergize with TPO to increase the number and maturation of megakaryocytes, although its main effect is on the proliferation of MKs progenitors (Broudy, V.C. et al. 1995). Finally, IL-6 stimulates the megakaryopoiesis, being important at the end of this process, modulating MK maturation and the increase in the number of platelets (**Figure I-7**).

3.2. TPO-mediated signaling pathways implicated in MK differentiation and maturation

The TPO receptor, c-Mpl, is a member of the hematopoietic cytokine receptor superfamily and is expressed on the surface of platelets, megakaryocytes and MK progenitors (Li, J. et al. 1999). The extracellular domain of c-Mpl is composed of two repeating modules, which form a dimer upon binding of TPO (Kaushansky, K. et al. 1995). c-Mpl has no intrinsic kinase activity, but is associated with the cytoplasmic tyrosine kinase, Janus kinase 2 (Jak2), so that TPO-mediated signaling is dependent on the activation of Jak2. The activation of Jak2 occurs when the domains of the receptor dimerize, so that two Jak2 molecules are close enough to be activated by trans-autophosphorylation (Witthuhn, B.A. et al. 1993). The phosphorylation of Jak2 and c-Mpl result in the recruitment of a variety of adapter protein that contain SH2 domains, leading to the activation of several signaling pathway that regulate cellular proliferation and differentiation. The signaling pathways activated in response to TPO are JAK-STAT, mitogen-activated protein kinase (MAPK) and phosphoinositol-3-kinase (PI3K) pathways (**Figure I-8**).

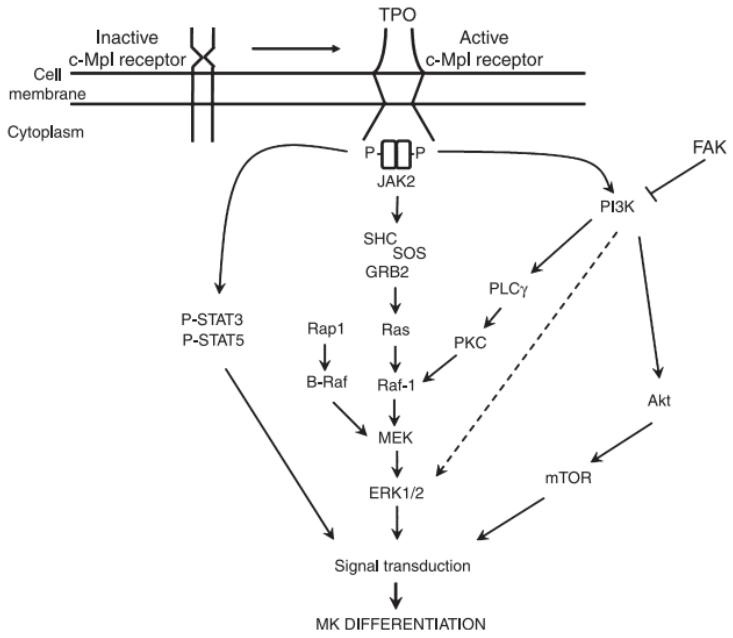

Figure I-8. Signaling pathways induced by TPO through the c-Mpl receptor. TPO binds to its receptor (c-Mpl) and initiates the downstream signaling pathways including STAT, ERK and PI3K. Figure from (Severin, S. et al. 2010).

Even though TPO is the most physiological signal promoting MK differentiation, it is well established that, *in vitro,* phorbol esters, such as PMA (phorbol 12-myristate 13-acetate), are able to mimic the physiological MK differentiation through activation of Protein Kinase C (PKC), as reported in the erythroleukemic cells lines K562 and HEL (Long, M.W. et al. 1990, Jacquel, A. et al. 2006, Conde, I. et al. 2010, Sardina, J.L. et al. 2010).

3.2.1. MAPK signaling

Multiple studies have demonstrated the importance of the TPO-induced MAPK/ERK1/2 signaling in megakaryocytic differentiation. However, there is no functional evidence for a role of p38 MAPK in MK differentiation of primary bone marrow cells. In contrast, in cell lines p38 MAPK seems to modulate differentiation, although the mechanism and significance are unclear. Similarly, the role of JNK in MK differentiation is poorly defined.

MAPKs are a family of serine/threonine kinases that control the major cellular processes and contribute to proliferation, migration, differentiation and apoptosis. MAPKs comprise several subfamilies: extracellular signal-regulated kinases 1 and 2 (ERKs 1/2 or p44/p42), p38 MAPK (p38α, p38β, p38γ, p38δ) and c-Jun N-terminal kinases (JNKs) (Severin, S. et al. 2010). The members of the different MAPK subfamilies are regulated by upstream

dual kinases called MAPK kinases (MEKs and MKKs), which are capable of phosphorylating MAPKs in both threonine and tyrosine residues and exhibit relative specificity for each MAPK subfamily. The MEK/ERK pathway is preferentially activated by mitogens, such as serum or growth factors, whereas p38 and JNK pathways are mainly regulated by stress stimuli (Roux, P.P. et al. 2004).

The strength and duration of MAPK activation plays an important role in the regulation of hematopoietic cell functions. Transient MAPK activation (minutes/hours) is sufficient for cell cycle progression and proliferation, whereas sustained activation (several days) is required during cell cycle arrest and differentiation (Marshall, C.J. 1995).

In general, studies using ERK1/2 inhibitors have demonstrated a positive and negative role of ERK1/2 and p38 pathways, respectively, in the acquisition of MK surface markers, polyploidization, hematopoietic progenitors commitment, and even in MK migration and proplatelet formation (Miyazaki, R. et al. 2001, Mazharian, A. et al. 2009).

MEK/ERK signaling pathway

The Ras/Raf/MEK/ERK is a very conserved pathway that is involved in the control of several main cell processes, such as cell proliferation, survival, differentiation, motility and metabolism (Fernandez-Medarde, A. et al. 2011). The role of this pathway in MK differentiation was described in PMA-stimulated cell lines, and then confirmed in TPO-induced murine bone marrow MKs (Herrera, R. et al. 1998, Rojnuckarin, P. et al. 1999).

Numerous evidences point to a positive role of ERK1/2 pathway in MK differentiation in K562 and HEL cell lines (Herrera, R. et al. 1998, Jacquel, A. et al. 2006, Conde, I. et al. 2010, Sardina, J.L. et al. 2010). ERK1/2 is rapidly activated in response to PMA, which results in cell cycle arrest, increase in cell size and DNA content and increased adhesion. This is accompanied by an increased expression of cell surface markers associated with MK differentiation, such as CD41 (also called glycoprotein IIb, GPIIb or integrin αIIβ) and CD61 (glycoprotein IIIa, GPIIIa or integrin β3), as well as a reduction of erythroid markers such as GPA (glycophorin A) (Long, M.W. et al. 1990, Herrera, R. et al. 1998, Sardina, J.L. et al. 2010). In agreement, the ERK inhibitor, PD98059, was found to block all these effects (Melemed, A.S. et al. 1997, Sardina, J.L. et al. 2010). Phospho-ERK1/2 levels are modulated by a NADPH oxidase-dependent ROS production, during MK differentiation (Sardina, J.L. et al. 2010). Additionally, constitutive ERK expression has been shown to induce MK characteristics as does PMA (Whalen, A.M. et al. 1997). Therefore, sustained activation of the ERK pathway is required to initiate the MK differentiation program in K562 cell lines, while transient ERK

activation causes cell proliferation (Melemed, A.S. et al. 1997, Racke, F.K. et al. 1997, Whalen, A.M. et al. 1997, Herrera, R. et al. 1998, Uchida, M. et al. 2001). However, other authors have demonstrated, in PMA-stimulated K562 cells, that a sustained activation of ERK is not required for the expression of megakaryocytic markers and that ERK is not involved in endomitosis (Conde, I. et al. 2010), so the role of ERK in MK differentiation remains controversial.

In contrast, in murine bone marrow MKs, treated with TPO, ERK1/2 is rapidly but transiently activated, with a decrease over 1-2h probably due to longer exposure to TPO (Rojnuckarin, P. et al. 1999). It has been reported that the Shc/SOS/Ras/Raf-1 signaling pathway is the responsible of the transient activation of ERK by TPO (Avruch, J. et al. 2001). However, subsequent sustained activation of ERK, which is necessary for proper MK differentiation, could be mediated by the Rap1-B-Raf signaling pathway (Garcia, J. et al. 2001, Geddis, A.E. 2010).

p38 MAPK pathway

The role of p38 MAPK in MK differentiation is not clear. Some studies suggest a negative role of p38 MAPK in MK differentiation, through the inhibition of the ERK pathway. In contrast, other authors have proposed a regulatory role of p38 MAPK in MK differentiation, depending on its levels. Thus, low doses of SB202190 (1-10 μM), a p38 MAPK inhibitor, would favor the acquisition of MK surface markers in K562 cells stimulated with PMA. On the other hand, high SB202190 concentration (20-40 μM) would result in inhibition of MK differentiation and induction of death cell (Jacquel, A. et al. 2006). Based on this data, downregulation of p38 activity could be important to stimulate the early expression of MK markers, whereas, a transient activation of p38 MAPK may induce cell cycle arrest and modulate the increase of DNA content (Conde, I. et al. 2010). On the other hand, p38 MAPK pathway is not involved in MK migration and proplatelet formation (Mazharian, A. et al. 2009).

It has been reported that p38 and ERK can differentially regulate the same cellular events, in which p38 could negatively regulate ERK signaling under various stimulation conditions and in several cell types (Ding, B.C. et al. 2001, Li, S.P. et al. 2003, Liu, Q. et al. 2004). Additionally, this antagonistic role of ERK and p38 MAPK was observed in platelet physiology (Mazharian, A. et al. 2005) and in K562 cells, where cyclin D1, which is involved in the acquisition of ploidy features, is up-regulated during PMA-induced MK differentiation via ERK pathway, (Lee, C.H. et al. 1999) presumably through a negative regulation of p38 (Chang, Y.I. et al. 2010).

Additionally, it has been described that inhibition of ERK, together with the activation of p38 MAPK, promotes the acquisition of erythroid markers, suggestive of a positive role of p38 in erythroid differentiation (Miyazaki, R. et al. 2001, Uddin, S. et al. 2004, Moosavi, M.A. et al. 2007), which could be considered an antagonist process to that of MK differentiation.

JNK pathway

The implication of JNK signaling pathway in MK differentiation and maturation is less studied. Some reports have described a modest role of JNK in this process. In one study, full acquisition of MK phenotype induced by PMA in K562 cells required the activation of JNK, ERK and the inhibition of p38 MAPK (Jacquel, A. et al. 2006). Additionally, inhibition of JNK produced a significant increase in all MK markers, but had little effect on other MK features, such as cell morphology or cell size (Sardina, J.L. et al. 2010). These results would suggest that, as in the case of p38 MAPK, moderate levels of JNK may be required for the normal acquisition of MK markers in K562, but excessively high levels may have a negative effect on differentiation.

3.2.2. Jak2/STAT signaling

Signal transducer and activator of transcription (STAT) proteins are important signal regulatory proteins activated by TPO and other cytokines involved in megakaryopoiesis such as IL-6 or IL-11. Once TPO binds to its receptor, c-Mpl, Jak2 is activated and phosphorylates STAT3 and STAT5, which dimerize and translocate into the nucleus, where they act to promote gene transcription (Drachman, J.G. et al. 1997). Jak2 protein expression progressively increases along normal human megakaryopoiesis, where its levels regulate megakaryocytic proliferation versus differentiation (Besancenot, R. et al. 2014). STAT5 is required for the normal MK development, since STAT5-deficient mice showed reduced platelet production. This effect is probably due to impaired survival and proliferation of HSCs (Snow, J.W. et al. 2002). In contrast, STAT3 deficiency in mice showed no effect on the number of megakaryocytes and platelets, although a role in the early stages of megakaryopoiesis is not discarded (Kirito, K. et al. 2002).

3.2.3. PI3K/Akt signaling

TPO and PMA activate PI3K, which leads to the phosphorylation and activation of its effector, Akt. Activation of this pathway has been shown to be involved in the expression of MK markers CD41, CD61 and CD42b (GPIbα) (Conde, I. et al. 2010). In addition, it modulates the expression of the cell cycle inhibitor p27, which is required for the cell cycle progression of MK progenitors leading to polyploidy, but its constitutive activation is not sufficient to drive

proliferation in the absence of TPO (Geddis, A.E. et al. 2001, Nakao, T. et al. 2008). Moreover, in primary murine megakaryocytes stimulated by TPO, activation of PI3K and PKC, specifically PKCζ, contributes to ERK phosphorylation through activation of MEK or Raf-1, suggesting a Shc-Ras-independent ERK activation, with an important role in megakaryopoiesis (Rojnuckarin, P. et al. 2001). Other studies have described a role for p-Akt in MK differentiation independently of PI3K, whose levels are modulated through ROS production by NADPH oxidases (Sardina, J.L. et al. 2010).

3.3. Expression of glycoproteins during megakaryocyte differentiation and maturation

Like all blood cells, MKs derive from HSCs and during differentiation into mature cells, they undergo changes in their cell surface markers. Through the use of flow cytometry techniques, it has been possible to identify the hierarchical relationship between different cell populations during hematopoiesis, since each population produced along hematopoiesis is associated with specific markers on the cell surface.

Murine HSCs are highly enriched in a population of Lin-Sca1+c-Kit+ (LSK) cells (Ikuta, K. et al. 1992, Okada, S. et al. 1992). A subpopulation of HSC is the so called LT-HSC (Long-term Hematopoietic Stem Cell). These cells can reconstitute a lethally irradiated animal and provide multilineage hematopoiesis for the lifetime of the animal. Through a process of asymmetric cell division, LT-HSC can self-renew, to maintain the stem cell pool, or differentiate into a second subpopulation defined as ST-HSC (Short-term HSC), which are only able to sustain hematopoiesis in the short term (see **Figure I-6**) (Uchida, N. et al. 1998). In mice, both populations, LT-HSC and ST-HSC are (LSK)CD34-Flt3- and (LSK)CD34+Flt3-, respectively, while in humans they are CD34+CD38-. ST-HSCs give rise to the multipotent progenitor (MPP), which is (LSK)CD34+Flt3+ (Yang, L. et al. 2005, Seita, J. et al. 2010). Then, MPP gives rise to the committed lymphoid progenitor (CLPs), which can form all cells of the lymphoid lineage, and the committed myeloid progenitor (CMP), which can differentiate into, either granulocyte/macrophage progenitors (GMPs), or megakaryocyte/erythroid progenitors (MEPs). These last progenitors have Lin-Sca1-cKit+CD34- cell surface marker phenotype (Akashi, K. et al. 2000).

One of the hallmarks of the MK lineage is the presence of the surface markers CD41 and CD61, two membrane glycoproteins that dimerize to form the integrin αIIbβ3. CD41 is present on about 3% of CD34+ cells and is enriched in megakaryoblasts. The expression of CD41 precedes the onset of CD42a (GPIX) and CD42b (GPIb); thus CD34+CD41+CD42- cells correspond to megakaryoblast, whereas CD34-CD41+CD42+ cells are

promegakaryocytes. Therefore, the expression of CD42 correlates with late differentiation stages. On the other hand, CD61 expression begins with the differentiation of MEP to megakaryoblast and finally, as cells mature, the expression of CD34 disappears (Debili, N. et al. 1992, Chang, Y. et al. 2007) (See **Table I-1**).

Table I-1. Expression of the most relevant surface markers during the different stages of mouse megakaryopoiesis**.**

	MEP	Megakaryoblast	Promegakaryocyte	Megakaryocyte
CD34	-	-/+	-	-
CD41	++	+	+	++
CD42	-	-	-/+	+
CD61	-	+	+	++
vWF	-	+	+	+
PF4	-	+	+	+

Additionally, mature megakaryocytes and platelets express on their surface: CD51 (integrin αV), platelet α-granules proteins, von Willebrand factor (vWF), platelet factor 4 (PF4), β-thromboglobulin (β-TG), fibrinogen, c-Mpl, coagulation factor VIII, and factor V (Tomer, A. 2004).

3.4. Endomitosis

Megakaryocytic differentiation is characterized by the development of progressive polyploidy and accumulation of large nuclear mass and cytoplasmic volume, presumably to execute more functions than diploid cells. During differentiation, diploid megakaryoblasts lose their proliferation capacity and undergo repeated incomplete cell cycles, in which mitosis is aborted in late anaphase with failure of both karyokinesis (division of the nucleus) and cytokinesis (division of the cytoplasm to form two separate daughter cells). This process by which cells do no longer divide but continue increasing the DNA content, is called endomitosis (Geddis, A.E. et al. 2006). MK progenitors undergo a proliferative 2n stage, in which their progression through the cell cycle is identical to that of other cells. Then, megakaryoblasts undergo endomitosis and accumulate a DNA content of 4n, 8n, 16n, 32n and 64n in mouse, and even 128n in humans, in a single polylobulated nucleus before proceeding with their final maturation and subsequent proplatelet formation (Zimmet, J. et al. 2000). An important thing to keep in mind is the difference between endomitosis and endocycle (**Figure I-9**). Endomitosis involves entry in mitosis, progression through metaphase, chromosome condensation, spindle formation and initiation of chromatid separation, but anaphase is not completed, due to defects in karyokinesis/cytokinesis, resulting in a polyploid cell with a polylobulated nucleus (Lordier, L. et al. 2012). However, in the endocycle, polyploidy is produced as a result of aberrant regulation, since DNA synthesis is initiated multiple times,

without ending in mitosis (successive DNA synthesis and gap phases). Both endocycles and endomitosis lead to duplication of the genome (Sher, N. et al. 2013). Another feature of MK maturation is that the expression of CD41 and CD61 correlates directly with the increase in cell size and ploidy, being the mean diameter of normal human bone marrow cells 14 ± 2 µm, while in MKs it ranges between 21 ± 4 µm, in 2n cells, and 56 ± 8 µm in 64n cells (Tomer, A. 2004).

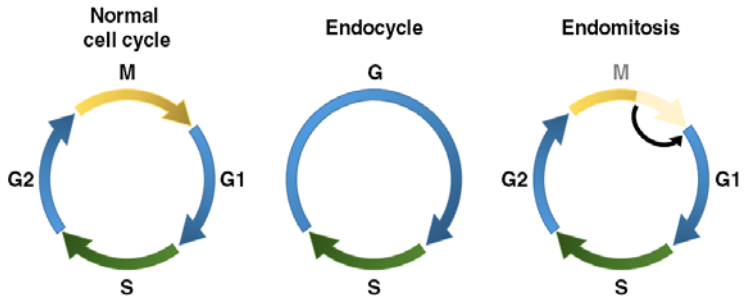

Figure I-9. Normal cell cycle, endocycle and endomitosis. Left: normal cell cycle responsible for cell proliferation, in which G1, S, G2 and M phases are well defined. Center: endocycle, in which mitosis is not produced, so the S phase is followed by the G phase. Right: endomitosis cycle, in which cells do not complete mitosis.

Progression through normal cell cycle is controlled by cyclins, whose expression is subjected to periodic synthesis and destruction cycles, in synchrony with the specific cell cycle phase they regulate, resulting in the partner kinase activity being turned on and off (Bertoli, C. et al. 2013). The regulation of the cell cycle during MK differentiation is mainly mediated by the action of cyclin D3, which expression is increased during endomitosis, leading to polyploidization (Zimmet, J.M. et al. 1997, Ravid, K. et al. 2002).

$p21^{WAF1/Cip1}$, is a potent CDK inhibitor, which is upregulated during MK differentiation induced in hematopoietic cell lines with a megakaryocytic phenotype, such as CMK, UT-7, MEG-01, Dami and K562 (Kikuchi, J. et al. 1997, Matsumura, I. et al. 1997). The expression of p21 is an early event in MK differentiation and precedes polyploidization, suggesting its implication in this process (Kikuchi, J. et al. 1997). TPO-induced overexpression of p21, which is mediated by the STAT5 signaling pathway, was sufficient to induce MK differentiation in CMK cells (Matsumura, I. et al. 1997). Other report suggests that the complex p21-cyclinD3-Cdk4 is crucial in the G1/S transition during the endomitotic cycle, acting when proliferation stops. In general, the role of p21 in normal MK differentiation leading to polyploidy is not critical, but it became crucial in conditions where the level of cyclin D3 is decreased (Raslova, H. et al. 2006). However, the expression of p21 needs to be transient to irreversibly inhibit mitosis but not DNA replication (Munoz-Alonso, M.J. et al. 2012).

3.5. Influence of the microenvironment on megakaryocyte maturation

HSCs reside in complex and dynamic microenvironments known as niches. This microenvironment is composed of supportive cells, extracellular growth factors, metabolic components and matrix factors, which actively regulate stem cell functions and enable a sustainable and responsive HSC pool. Two physiologically distinct HSC niches have been described in the BM (**Figure I-10**): the osteoblastic or endosteal niche at the BM interface and the vascular niche around the specialized vascular endothelium (Kiel, M.J. et al. 2008). Most HSCs are perivascular and are preferentially located in the endosteal regions in the bone marrow, consisting of a complex network of stromal cells that are involved in the maintenance of HSCs.

Megakaryopoiesis and thrombopoiesis occur within these niches, where the interactions between stem cells and the microenvironment are bidirectional; MKs require several cytokines that are present in the microenvironment, such as TPO and interleukins, whereas, MKs are able to maintain the quiescence and proliferation of HSCs under normal and injury conditions. In fact, osteoblast expansion and HSC engraftment after irradiation are promoted and regulated by TPO, and by the relocalization of MK to the endosteal surface proximal to this niche (Olson, T.S. et al. 2013).

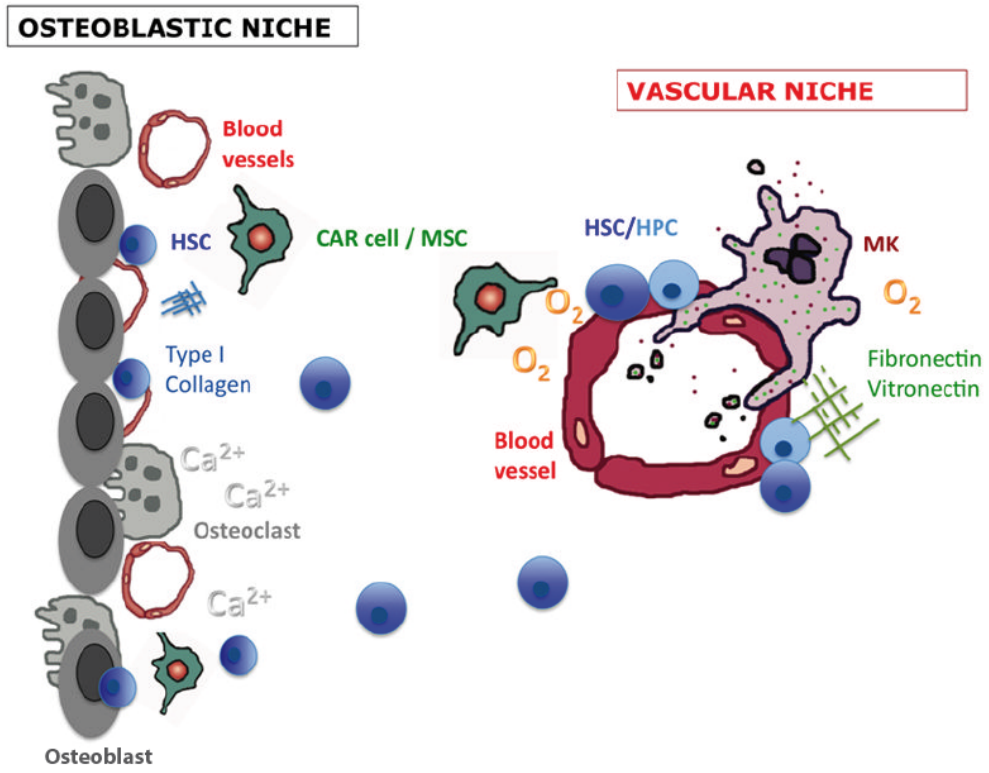

Figure I-10. Bone marrow niches. Figure modified from (Psaila, B. et al. 2012). **Osteoblastic niche.** Osteoblasts and osteoclasts maintain the HSCs (dark blue) in a quiescence state by secretion of numerous factors such as calcium. Type I collagen, which is very abundant in this niche, inhibit proplatelet formation. **Vascular niche.** Fibronectin, vitronectin and Type III and IV collagens are found around blood vessels, which enhance MK development and function. CAR cell / MSC: mesenchymal cell. HPC: hematopoietic progenitor cell (light blue).

3.5.1. Osteoblastic niche

The majority of LT-HSCs are found near the endosteal niche of the bone, where they are in close contact with osteoblasts and osteoclasts. Osteoblasts secrete several growth factors required for HSC maintenance, including TPO and stromal-derived factor-1 (SDF1), while osteoclasts retain HSCs close to the endosteum by releasing Ca^{2+} and stem cell factor (SCF) (Psaila, B. et al. 2012).

The dynamic interaction of MKs with the different component of the extracellular matrix in the endosteum regulates their differentiation, maturation and subsequent migration to the vascular niche before proplatelet formation and platelet release. The most abundant component of the osteoblastic niche is type I collagen, which binds to integrin α2β1 and GPVI of megakaryocytes (Zou, Z. et al. 2009). The interaction with integrin α2β1 activates a mechanism that negatively regulates proplatelet formation, presumably through the activation

of the Rho/ROCK signaling pathway (Sabri, S. et al. 2004), while type II and IV collagens, which are found around the bone marrow vessels, possibly support it (Balduini, A. et al. 2008). Additionally, using a co-culture model with osteoblasts, it has been demonstrated that cell-cell contacts promotes MK differentiation and inhibits MK maturation and proplatelet formation by a mechanism dependent on the interaction with Type I collagen (Pallotta, I. et al. 2009).

3.5.2. Vascular niche

The murine bone marrow is highly vascularized, with large central arteries branching into progressively smaller arterioles that eventually ramified to form venous sinusoids near the bone (osteoblastic niche).

The vascular niche supports thrombopoiesis, during which mature and polyploid MKs, primary located near the bone marrow cells, produce proplatelets and release the platelets through the endothelium into the bloodstream. Several studies have implicated chemokine stromal cell-derived factor-1α (SDF1α) signaling, via its receptor CXCR4, in the migration of MK to the vascular niche. SDF1 is produced locally by stromal cells, creating an increase gradient that promotes the migration and contact of the MKs with the vascular niche (Hamada, T. et al. 1998).

The vascular niche is composed by extracellular matrix proteins, such as type IV collagen, fibronectin, fibrinogen and von Willebrand factor. Interaction of the MKs with these components favor their migration to the vascular niche. In particular, integrin αIIbβ3, through outside-in signaling pathways, modulates proplatelet formation in response to fibrinogen (Larson, M.K. et al. 2006).

3.6. Demarcation membrane system

Following nuclear polyploidization, megakaryocytes undergo cytoplasmic maturation, consisting in the accumulation of granules, and a large quantity of protein and phospholipids, to create the demarcation membrane system (DMS, also called invaginated membrane system or IMS). The DMS is an extensive complex of cisternae and tubules distributed throughout the MK cytoplasm that is continuous with the plasma membrane of the cell, through which it is in contact with the external environment (**Figure I-11**) (Behnke, O. 1968, Nakao, K. et al. 1968). There is a great controversy about the events that give rise to DMS and the subsequent formation of platelets during thrombopoiesis. In the most accepted model, DMS would be formed by invagination of the plasma membrane to form long extensions that will form the future proplatelets. Therefore, DMS would acts as a reservoir for the plasma

membrane of future blood platelets and would partition at the edge of this structure to release the platelets (Radley, J.M. et al. 1982, Italiano, J.E., Jr. et al. 1999).

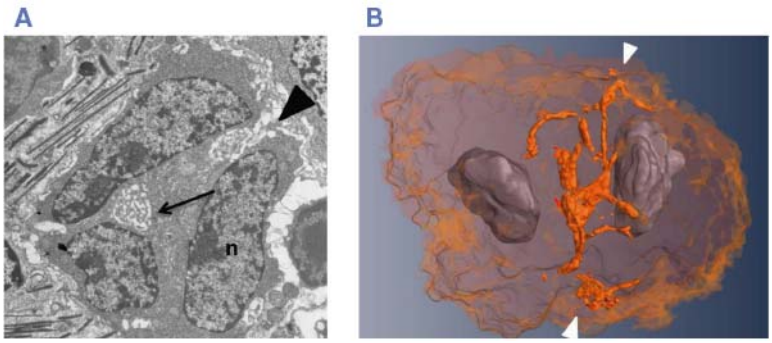

Figure I-11. Demarcation membrane system in bone marrow MKs. **A)** TEM image of the DMS and perinuclear region (arrow) and the connection with the cell surface (arrowhead). **B)** 3-D reconstruction of the DMS (orange) in a bilobulated MK. Figure modified from (Eckly, A. et al. 2014).

3.7. Platelet production

Two models have been proposed to explain platelet formation from mature MKs:

3.7.1. Proplatelet formation in the bone marrow

During the initial stages of proplatelet formation, MKs remodel their cytoplasm into pseudopodia by a process based on microtubules. Then, the pseudopodia elongate into proplatelets, which form constrictions along their length, in a structure reminiscent of “beads on a string” (Italiano, J.E., Jr. et al. 1999). More recently, it has been observed that the MKs extend the proplatelets into the lumen of sinusoids, where they are segmented by the flowing blood and thereby produce proplatelets that subsequently fragment into individual platelets (Junt, T. et al. 2007).

Dynamic reorganization of tubulin (specially β1-tubulin) in the cytoskeleton precedes, promotes and is essential for proplatelet formation, as it has been demonstrated using chemical inhibitors of polymerization and depolymerization (Italiano, J.E., Jr. et al. 1999). In addition, during proplatelet formation specific platelet membrane proteins, such as receptors, are synthetized and sent to the MK surface, while others are packaged into secretory granules, mainly α-granules (derived from the Golgi, which is close related to DMS formation) (Heijnen, H.F. et al. 1998).

Imaging studies supports this model: proplatelet production has been observed *in vivo* in sinusoidal blood vessels of the bone marrow (Junt, T. et al. 2007), and spontaneous proplatelet formation also occurs *in vitro* in MKs derived from murine fetal liver cells (Italiano, J.E., Jr. et al. 1999, Patel, S.R. et al. 2005) and in human MKs (Miyazaki, R. et al. 2000) (Figure I-12).

The MEK/ERK1/2 pathway plays an important role in the regulation of MK differentiation, promoting polyploidization in the later stages of the process. However, there is no consensus on the implication of this pathway in proplatelet formation, since it has been published that the inhibition of ERK1/2, increases, decrease or has no effect on this process (Minamiguchi, H. et al. 2001, Rojnuckarin, P. et al. 2001, Jiang, F. et al. 2002). A more recent study with murine bone marrow and fetal liver cells argues that ERK1/2 MAPKs, but not p38 MAPKs, play a role in proplatelet formation by the regulation of the phosphorylation state of microtubule-associated proteins, and subsequent organization of the microtubule networks (Mazharian, A. et al. 2009). Additionally, studies performed in human megakaryocytic cell lines demonstrated that activation of the MEK/ERK1/2 and PI3K pathways are required for proplatelet formation *in vitro,* through integrin β1 signaling (Kawaguchi, T. et al. 2012).

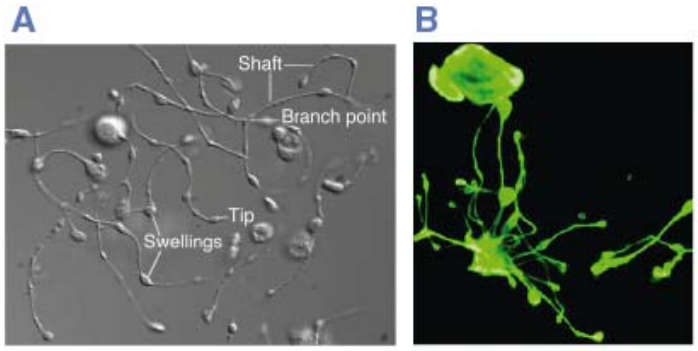

Figure I-12. Proplatelet images. A) Differential interference contrast images of proplatelets from mouse megakaryocytes, formed *in vitro*, indicating some of their features: tip, shafts, swellings and branch point. B) Immunofluorescence images of murine MKs grown in culture and labeled with β1–tubulin. Figure modified from (Patel, S.R. et al. 2005).

3.7.2. Proplatelet formation in the lungs

The presence of intravascular MKs in the lungs was first described by Aschoff in 1893 and the idea that lungs could be a new site of platelet production first appeared in 1937, based on the fact that blood leaving the lungs contained more platelets and less MKs than blood entering the lungs (Howell, W.H. et al. 1937). Additionally, it was observed in humans that 98% of MKs leaving the lungs were devoid of cytoplasm (Levine, R.F. et al. 1993), characteristic of post-platelet release MKs. Nowadays is accepted that MKs migrate from the

bone marrow to the lungs through circulation (Tavassoli, M. et al. 1981) and that they break up into platelets in the lung microvasculature.

Since all the evidences that platelets are released from MK into the pulmonary capillaries were indirect, this concept was not universally accepted. This changed with a recent report (Lefrancais, E. et al. 2017), demonstrating *in vivo* by video microscopy the release of platelet from megakaryocytes in mouse lungs. Therefore, it is now clear that, in adult mice, functional hematopoietic precursors are able to migrate to the lungs and produce platelets. Furthermore, lung hematopoietic progenitors can migrate out of the lungs, repopulate the BM and reconstitute blood platelet counts, in a situation of thrombocytopenia. Additionally, this study demonstrated that the contribution of the lungs to platelet biogenesis is around 50% of total platelet production (10 million platelet/hour).

3.8. Platelet release and terminal maturation

Once the mature MKs are in the vascular niche and produce proplatelets, their cytoskeleton takes on a leading role, providing a mechanism for deriving platelets into the bloodstream (Machlus, K.R. et al. 2013). Proplatelets are highly dynamic structures that extend through a microtubule-based system, repeatedly bifurcate to increase the number of ends, and deliver packets of platelets at these ends (Italiano, J.E., Jr. et al. 1999). *In vivo*, proplatelets extend into the vascular sinusoids, where they are released and enter the bloodstream. A study using multiphoton intravital microscopy showed real-time proplatelet formation in the murine bone marrow (Junt, T. et al. 2007). In this experiment it was observed that blood flow helps to separate the proplatelet fragments from MKs.

MKs release a heterogeneous proplatelet mixture into the blood, indicating that terminal platelet maturation can continue in the bloodstream. The presence of proplatelet-like structures in the blood could indicate that proplatelets are released as chains of platelet-sized particles called preplatelets (Schwertz, H. et al. 2010). Preplatelets are an intermediate stage in the platelet production. They have a diameter of 2-10 µm and can be reversibly converted into barbell-shaped proplatelets (**Figure I-13**). Preplatelets are able to mature into platelets both *in vitro* and, after transfusion in mice, *in vivo*, through an event in which the preplatelet split into two individual mature platelets (2 µm diameter) (Thon, J.N. et al. 2010).

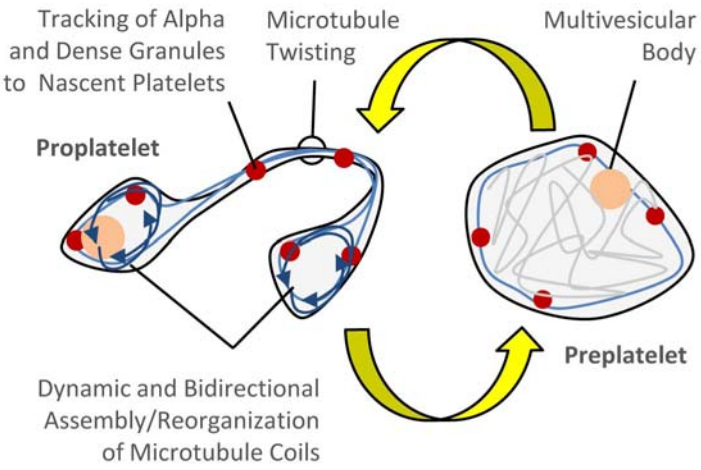

Figure I-13. Preplatelet model. During barbell proplatelet formation dynamic and bidirectional assembly and reorganization of microtubule coils mediate platelet cytoskeleton arrangement. Barbell proplatelets reversibly convert into preplatelets. Platelets release from proplatelet ends after the final fission event. Figure modified from (Thon, J.N. et al. 2010).

Objectives

Our group had previously demonstrated that C3G modulates most platelet functions, including activation, aggregation and spreading, through a signaling pathway involving Rap1 and PKC. Based on that, the overall scope of this work is to try to determine whether C3G is also involved in the differentiation processes that lead to platelet formation. To achieve this goal, the following specific objectives have been addressed:

1. To study whether C3G regulates the expression of surface markers, as well as changes in morphology and ploidy status leading to MK differentiation in K562 and HEL cell lines

2. To identify signaling pathways by which C3G regulates MK differentiation

3. To analyze MK differentiation, maturation and proplatelet formation *in vivo* and *ex vivo* in mouse models with transgenic expression of C3G or its mutant C3GΔCat

Materials & Methods

1. Cell Line culture

1.1. Cell lines

In this work we have used the following cell lines, which grow in suspension: K562 (Lozzio, C.B. et al. 1975) and HEL (Martin, P. et al. 1982). Both of them are derived from patients with different hematopoietic neoplasias (**Table M-1**). In addition, the adherent cell line, HEK-293T (Pear, W.S. et al. 1993) was used as a tool to produce lentiviral particles (**Section 8.2**).

Table M-1. Cell lines used in this work, indicating their origin, the cell type and ATCC reference.

Cell Line	ATCC Ref.	Organism	Tissue	Cell Type	Disease
K562	CCL-243	Human	Bone Marrow	Lymphoblast	CML
HEL	TIB-180	Human	Bone Marrow	Erythroblast	Erythroleukemia
HEK-293T	CRL-3216	Human	Embryonic Kidney	Epithelial	--

1.2. Cell culture conditions

- K562 and HEL cells were cultured in RPMI-1640 medium (Gibco) supplemented with 10% Fetal Bovine Serum (FBS, Gibco), 2 mM Glutamine (Gibco), 100 U/ml Penicillin (Gibco) and 100 µg/ml Streptomycin (Gibco), at a density of 1 x 10^5 to 1 x 10^6 cells/ml, using 75-cm^2 culture flasks (40 ml). To change media, cells were centrifuged at 445 x*g* for 5 min, washed with PBS and resuspended in fresh complete RPMI medium.

- HEK-293T cells were grown in DMEM medium (Sigma) containing 10% FBS, 2 mM Glutamine, 100 U/ml Penicillin and 100 µg/ml Streptomycin until confluence. Cells were dissociated by trypsinization with 0.25% Trypsin-EDTA (Gibco) and then reseeded into culture dishes.

- All cell cultures were maintained at 37ºC in a humidified 5%CO_2/95% air incubator.

1.3. Freezing, cryopreservation and thawing of cells

Cells were stored at -180ºC in freezing medium (complete media with 10% DMSO) into cryogenic storage vials. Cells suspensions were progressively frozen: at -80ºC for at least 4h (decrease of 1ºC/min) and finally at -180ºC into a liquid nitrogen freezer.

The cryogenic vials were quickly thawed in a 37ºC water bath and cells were placed in warmed complete media.

1.4. Differentiation of cell lines

K562 and HEL cells are erythroleukemic cell lines that serve as a model to study the molecular mechanisms associated with megakaryocytic differentiation. K562 and HEL cells function as pluripotent hematopoietic precursors, expressing, in undifferentiated conditions markers for both erythroid and megakaryocytic lineages. To stimulate megakaryocytic or erythroid differentiation and study the signaling pathways that are involved in this process, cells were treated with PMA alone or in combination with the inhibitors shown in **Table M-2**.

Table M-2. Reagents used in the treatment of cell lines, their concentrations and Suppliers.

Name	Description	Final concentration	Supplier and reference
Phorbol 12-Myristate 13-Acetate (PMA)	Protein Kinase C (PKC) activator	20 nM	Sigma (P1585)
U0126 (U0)	MEK1/2 inhibitor	10 μM	Selleckchem (S1102)
SB203580 (SB)	p38 MAPK inhibitor	10 μM	Calbiochem (559389)
Wortmannin (W)	PI3K inhibitor	10 μM	Calbiochem (681676)
Bisindolylmaleimide I, hydrochloride (Bis)	PKC inhibitor	10 μM	Calbiochem (133052)
Imatinib mesylate (STI-571)	Tyrosine Kinase inhibitor	0.5-2 μM	Sigma (SML1027)

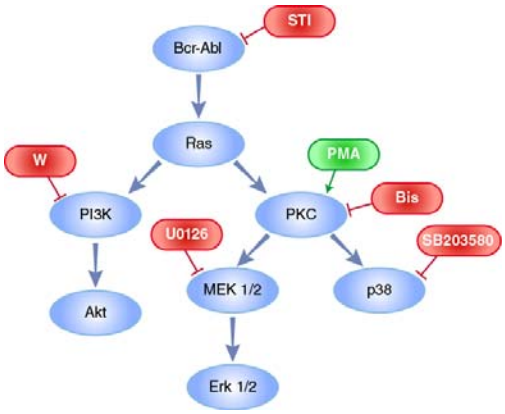

Figure M-1. Squematic representation of the main targets of the activator (green) and inhibitors (red) used in this work.

The signaling pathways involved in megakaryocytic differentiation were analyzed by Western Blot. Cells (~2 x 10^5 per/ml) were starved for at least 6h and then stimulated with PMA for 10 min in the presence of inhibitors of the different signaling pathways, that were added 1h before. After stimulation, cells were harvested and processed as indicated in **Section 4** (Protein analysis by Western Blot). **Figure M-1** represents the targets of the activator and the inhibitors used.

Expression analysis of megakaryocytic (CD41, CD61) or erythroid (Glycophorin A) surface markers was performed by flow cytometry. Cells were simultaneously incubated with the activator and inhibitors for 48h and then harvested and processed as described in **Section 9** (Analysis of cell surface markers by flow cytometry).

2. Primary cell culture

2.1. Mice

The transgenic mice used for this work are C57BL/6-derived mice generated in our laboratory, in collaboration with the company GenOway (Lyon, France), as described previously (Gutierrez-Herrero, S. et al. 2012). In these transgenic mice, human full-length C3G and mutant C3GΔCat (mutant lacking the last 439 bp of the gene, affecting the catalytic domain) are expressed under the control of the PF4 (platelet factor 4) gene promoter, specific of platelets and megakaryocytes. For transgenic full-length C3G, lines 2C1 and 6A6 were used and for transgenic C3GΔCat, 8A3 line was used. All mice used in these studies were 8 – 12 week-old.

All animal surgeries were performed under Isoflurane anesthesia, and all efforts were made to minimize suffering. This study was carried out in strict accordance with the EU Directive 2010/63/EU for the protection of animals used for experimentation and other scientific purposes.

2.2. Isolation of bone marrow cells from femurs and tibia of mice

The femurs and tibias were removed after mouse euthanasia by cervical dislocation under anesthesia. Bone marrow was isolated by flushing with PBS using a 25-gauge needle. All bone marrow is considered to have been expelled when the color of the bones changes from red to white. Washed cells were resuspended in IMDM (Iscove´s Modified Dulbecco´s Medium, Gibco) supplemented with 10% FBS, 100 U/ml penicillin and 100 µg/ml streptomycin. Primary bone marrow cells (BMC) were maintained at 37ºC, 5% CO_2/95% humidity in air incubator at a density of 1 x 10^6 cells/ml. The expected number of nucleated cells is detailed in **Table M-3**.

Table M-3. Expected cell recovery from mice bones.

Bones Flushed	Number of nucleated cells
1 femur	1 – 2 x 10^7
1 tibia	0.6 – 1.2 x 10^7

2.3. Isolation of cells from the bone matrix

After isolation of bone marrow cells (Section 2.2) the remaining bones were cut into 1 mm pieces and incubated with 1 mg/ml collagenase type I (Sigma) and 1 mg/ml dispase type II (Sigma) at 37ºC for 2h under vigorous stirring. To remove small pieces of bone, the released cells were filtered using a cell strainer (70 µm nylon, Falcon). Then, cells were stained for CD41/CD61 (Section 9, Analysis of cell surface markers by flow cytometry).

2.4. Red Blood Cell Lysis

For some experiments, the erythrocytes were eliminated from the isolated bone marrow cells by incubation, for 2 min on ice, with 2 ml of Red Blood Cell (RBC) lysis buffer (155 mM NH_4Cl, 10 mM $KHCO_3$, 0.1 mM EDTA pH 7.4). Lysis is completed when the color of the pellet changes from red to white. Erythrocyte-free BMCs were incubated in complete IMDM.

2.5. Megakaryocytic differentiation of bone marrow cells

Freshly isolated BMCs were incubated with recombinant mouse thrombopoietin (TPO) alone or in combination with Stem Cell Factor (SCF), Interleukin-3 (IL-3), IL-11 and IL-6 (Table M-4) to induce the differentiation and production of mature megakaryocytes. After 6 - 8 days mature megakaryocytes were harvested to perform the experiments.

Table M-4. Cytokines used for the differentiation of BMCs into megakaryocytes, indicating working concentration and Suppliers.

Name	Supplier and reference	Final concentration
Mouse TPO	Miltenyi Biotec (130-094-083)	50 ng/ml
Mouse SCF	Miltenyi Biotec (130-094-079)	10 ng/ml
Mouse IL-3	Invitrogen (PMC0034)	10 ng/ml
Mouse IL-6	Miltenyi Biotec (130-094-065)	10 ng/ml
Mouse IL-11	Miltenyi Biotec (130-093-950)	10 ng/ml

2.6. Blood collection and serum preparation

Blood from anesthetized mice was collected by cardiac puncture into a glass tube without anticoagulant and allowed to clot, first for 2h at 37ºC and then o/n at 4ºC. Serum was clarified by centrifugation at 2000 x*g* for 5 min and stored in small aliquots at -80ºC until use.

3. Determination of cell viability and cell counts

To determine the concentration and viability of the cell suspensions, we used two different methods:

3.1. Cell counting by Trypan blue exclusion

Cell concentration and viability were quantified by staining with 0.4% Trypan Blue (Sigma) for 5 min and visual counting with a Neubauer Chamber (Marienfeld). Trypan blue is a permeable staining for dead cells; therefore, non-viable cells will be blue, and viable cells will be uncolored. The concentration was calculated with the following formula:

$$\frac{\text{Cells}}{\text{ml}} = \frac{\text{Number of Cells}}{\text{Number of counted Squares}} \times \text{Dilution Factor} \times 10^4$$

3.2. Cell Counting by flow cytometry

For the cell counting by flow cytometry, we used the Muse® Count & Viability Kit (Merck Millipore). Cell suspension was stained with the Count & Viability reagent, containing two DNA binding dyes, for 5 min at RT. Samples were acquired with a Muse® Cytometer (Merck-Millipore), which generated the following data: i) Viable cell count (cells/ml), ii) Percentage of viability (%) and iii) Total cell count (cells/ml).

4. Protein Analysis by Western Blot

4.1. Protein sample preparation

Cell lines were lysed under nondenaturing conditions using Cell Lysis Buffer from Cell Signaling Technology (10X, #9803), which composition (1X) is: 20 mM Tris-HCl pH 7.5, 150 mM NaCl, 1 mM Na_2EDTA, 1 mM EGTA, 1% Triton X-100, 2.5 mM Sodium Pyrophosphate, 1 mM Na_3VO_4, 1 mM β-glycerophosphate, 1 µg/ml Leupeptin. This buffer was supplemented with 25 µM NaF and 1 mM PMSF.

Cultured cell lines were collected on ice, washed with cold PBS and resuspended in cold lysis buffer. Cells were maintained on ice for 30 min, shaking every 10 min. The lysates were cleared by centrifugation at 16000 x*g* for 10 min at 4ºC. Supernatant was transferred to a new tube and stored at -80ºC.

Bone marrow cell cultures were harvested on ice, PBS washed, resuspended in cold RIPA buffer and maintained on ice for 20 min. Suspended cells were sonicated (in a Sonics

Vibracell™ VCX750 Ultrasonic Cell Disrupter at 30% amplitude) by applying pulses of 5 seconds, with 30 second on ice between each pulse, until the lysate was not viscous (generally about 3 pulses). Cell lysates were cleared by centrifugation at 16000 x*g* for 10 min at 4ºC and the supernatant stored at -80ºC.

4.2. Protein quantification

Protein concentrations were determined with a Bradford assay (Bradford, M.M. 1976). Briefly, 200 µl of Bradford reagent (0.25 mg/ml Coomasie Brilliant Blue G-250, 25% Methanol, 42.5% orthophosphoric acid) were added to 800 µl of an aqueous solution containing 1-2 µl of lysate. After vortexing, the mixture was incubated for 5 min for color development from brown to blue and the absorbance was measured on a spectrophotometer at a wavelength of 595 nm. Different known concentration of bovine serum albumin (BSA, 0 to 5 µg/µl) were used to create a standard curve by plotting the 595 nm values (y-axis) versus their concentration in µg/ml (x-axis). The unknown sample concentration was determined using this standard curve.

4.3. Protein denaturation for SDS-PAGE

Prior electrophoresis, proteins were denatured in Laemmli buffer (240 mM Tris-HCl pH 6.8, 40% glycerol, 8% SDS, 0.04% Bromophenol Blue, 5% β-mercaptoethanol), by boiling at 95-100ºC for 5 min. For determination of phospho-proteins, lysates were boiled immediately to prevent protein dephosphorylation.

4.4. Western Blot

4.4.1. Electrophoresis

SDS-Polyacrylamide gel electrophoresis (SDS-PAGE) is used to separate proteins in an electric field based on their length and mass-to-charge ratio. Equal amount of denatured protein was loaded onto polyacrylamide gels. The concentration of polyacrylamide depends on the molecular weight of the protein of interest, being inversely proportional to the size of the protein (**Table M-5**). Prestained protein standards (PageRuler™ Plus Prestained Protein Ladder, ThermoFisher) were used for the identification of the size of the proteins. The electrophoresis was performed in running buffer (25 mM Tris-HCl pH 8.3, 250 mM Glycine, 0.1% SDS) at constant voltage.

Table M-5. SDS-PAGE gels composition.

	Stacking Gel	Separating Gel		
		7.5%	10%	12.5%
Upper Tris 4x (pH 6.8)	0.625 ml	-	-	-
Lower Tris 4x (pH 8.8)	-	2.5 ml	2.5 ml	2.5 ml
Acrilamide 30% / Bis 3.3%	0.29 ml	2.5 ml	3.325 ml	4.167 ml
H_2O	1.555 ml	5 ml	4.125 ml	3.325 ml
Ammonium Persulphate (APS) 10%	25 µl	70 µl	70 µl	70 µl
Temed	1.875 µl	5 µl	5 µl	5 µl

4.4.2. Transfer of proteins to PVDF membranes

After electrophoresis, proteins were transferred to methanol-pretreated Immobilon-P PVDF membranes (Merck Millipore) by wet transfer using Mini Trans-Blot® system (Bio-Rad). The transfer was performed in transfer buffer (66 mM Tris-HCl pH 8.3, 386 mM Glycine, 0.1% SDS, 20% methanol) at a constant amperage of 0.3 A for 3 hours.

After transfer, membranes were incubated in blocking buffer (5% non-fat dry milk in TTBS [10 mM Tris pH 7.3, 150 mM NaCl, 0.5% Tween-20]) for 1h at RT to reduce non-specific protein binding. For determination of phospho-proteins, membranes were blocked with 5% BSA in TTBS.

4.4.3. Immunodetection

Membranes were incubated with primary antibodies in 2% BSA in TTBS for 1h at RT or o/n at 4ºC in rotation. After that, membranes were washed 3 times with TTBS (5 min/each) and incubated with secondary antibodies in 5% milk in TTBS for 1h at RT in rotation. Finally, they were washed 3 times with TTBS (5 min/each), prior detection. The dilution of the primary and secondary antibodies is specified in **Table M-6**.

For the detection by chemiluminescence, membranes were incubated with HRP-conjugated secondary antibodies, and proteins were detected using the reagents from the commercial kit, Clarity™ Western ECL Blotting Substrates (Bio-Rad) following the manufacturer´s instructions. For the detection by immunofluorescence, using Odyssey Infrared Imaging System (LI-COR), membranes were incubated with fluorochrome-conjugated secondary antibodies. The primary and secondary antibodies are described in **Table M-6**.

Table M-6. Primary and secondary antibodies used in Western Blot

Primary antibodies

Antibody	Target	Host	Supplier	Molecular Weight	Dilution
C3G (C-19)	C-terminus of human C3G	Rabbit	Santa Cruz (sc-869)	121 kDa	1:1000
C3G (H-300)	N-terminus of human C3G	Rabbit	Santa Cruz (sc-15359)	121 kDa	1:1000
ERK (K-23)	Subdomain XI of ERK	Rabbit	Santa Cruz (sc-94)	44/42 kDa	1:1000
p21 Waf1/Cip1	C-terminus of human p21	Rabbit	Cell Signaling (2947)	21 kDa	1:1000
p38α (C-20)	C-terminus of mouse p38α	Rabbit	Santa Cruz (sc-535)	38 kDa	1:1000
p-C3G (Tyr 504)	Sequence containing Tyr 504 phosphorylated human C3G	Rabbit	Santa Cruz (sc-12926)	135 kDa	1:750
p-C3G (Tyr 504)	Sequence containing Tyr 504 phosphorylated human C3G	Mouse	Santa Cruz (sc-365994)	135 kDa	1:1000
p-ERK (E-4)	Sequence containing Tyr 204 phosphorylated human ERK	Mouse	Santa Cruz (sc-7383)	44/42 kDa	1:1000
p-p38	Sequence containing Thr 180 and Tyr 182 p-p38	Rabbit	Cell Signaling (9211)	43 kDa	1:1000
Rap1	Aa 1-184 human Rap1	Mouse	BD Biosciences (610196)	21 kDa	1:1000
Rap1 (121)	C-terminus of human Rap1	Rabbit	Santa Cruz (sc-65)	21/24 kDa	1:1000
β-tubulin	β-tubulin	Mouse	Sigma (T 5293)	50 kDa	1:1000
α-globin (H-80)	Amino acids 62-142 of human α-globin	Rabbit	Santa Cruz (sc-21005)	16 kDa	1:1000

Secondary Antibodies

Antibody	Target	Host	Detection	Supplier	Dilution
Anti-Mouse IgG HRP-linked	Anti-Mouse	Sheep	Chemiluminescence	GEHealthcare (NXA931)	1:5000
Anti-Rabbit IgG HRP-linked	Anti-Rabbit	Goat	Chemiluminescence	Santa Cruz (sc-2004)	1:10000
Goat Anti-Mouse IgG, Dylight 680	Anti-Mouse	Goat	Fluorescence	ThermoFisher (35518)	1:5000
Goat Anti-Mouse IgG, Dylight 800	Anti-Mouse	Goat	Fluorescence	ThermoFisher (35521)	1:5000
Goat Anti-Rabbit IgG, Dylight 680	Anti-Rabbit	Goat	Fluorescence	ThermoFisher (35568)	1:10000

4.4.4. Membrane stripping

To reuse the immunoblotted membranes, they were stripped by incubation in 62.5 mM Tris-HCl pH 6.8, 2% SDS, 0.74% β-mercaptoethanol, at 55ºC for 30-40 min, followed by 3

washes with TTBS. Thereafter, the membranes were blocked again prior to incubation with antibodies.

4.4.5. Quantification

Quantification of the Western Blot bands was performed by densitometry using the ImageJ software. Relative levels of protein were calculated using actin or tubulin levels as loading controls.

5. DNA/RNA analysis

5.1. Total RNA isolation

Purification of total RNA was performed using RNeasy Mini Kit (Qiagen) following the manufacturer´s instructions. The size, concentration and quality of the isolated RNA were measured using a LabChip (Agilent). RNA was stored at -80ºC until use.

5.2. cDNA synthesis

cDNA synthesis was performed by a reverse transcription (RT) reaction according to the manufacturer´s specifications of SuperScript™ III First-Strand Synthesis System (ThermoFisher). Essentially, 1.5 µg of RNA was denaturalized at 65ºC for 5 min in the presence 50 ng/µl of oligo(dT) and 1 mM of dNTP mix, and immediately put on ice. After a minute, a cDNA synthesis mix (1X RT buffer, 5 mM $MgCl_2$, 10 mM DTT, 2 U/µl RNaseOUT Recombinant) was added to each sample, incubating for 2 min at 42ºC. Then, 200 U of SuperScript III RT was added to each tube and reaction was continued for an additional 50 min to allow cDNA synthesis. The reaction was stopped by incubation at 70ºC for 15 min to inactivate the enzyme. Finally, the sample was treated with RNase H to degrade the RNA. The cDNA was stored at -80ºC.

5.3. Semi-quantitative PCR

The semi-quantitative PCR technique was used to evaluate the expression levels of C3G, p38α MAPK, CD61 and GPA genes, using the specific primers described in **Table M-7**. PCR was performed by mixing 2 µl of cDNA, 1X PCR buffer, 1.5 mM $MgCl_2$; 200 µM dNTPs; 0.03 units of BioTaq™ polymerase (Bioline) and 0.3 µM of each specific primers (forward and reverse).

Table M-7. Sequence of primers used in PCR and size of the generated amplicon. The primers used in qPCR are indicated with an asterisk. The nomenclature of the primers Ex3F-Ex5R and Ex22F-24R refers to the exons of C3G they amplify.

Gene	Forward Primer (5´-3´)	Reverse Primer (5´-3´)	Amplicon
C3G Ex3F-Ex5R*	GCAACAGACAGATTTCTACCAG	CTTCACTCCATCCAGCACA	446 bp
C3G Ex22F-Ex24R*	GGCCTGGCCGAGTACT	TGCTGGAAGCAGCGCATG	223 bp
p38α	GTGCCCGAGCGTTACCAGACC	CTGTAAGCTTCTGACATTTC	293 bp
GPA	GGAATTCCAGCTCATGATCTCAGGATG	TCCACATTTGGTTTGGTGAACAGATTC	497 bp
CD61	TATAGCATTGGACGGAAGGC	GACCTCATTGTTGAGGCAGG	372 bp
GAPDH *	TGCACCACCAACTGCTTAGC	TCTTCTGGGTGGCAGTGATG	105 bp

PCR results were verified by agarose gel electrophoresis in TAE buffer (1.6 M Tris, 8.8 M sodium acetate and 40 mM EDTA), using the GeneRuler 1Kb DNA ladder (ThermoFisher) as a marker.

5.4. Quantitative PCR

The quantitative PCR (qPCR) allows to measure the amount of the product synthesized during each PCR cycle, which is proportional to the fluorescence signal and can be correlated with the amount of starting product (Woo, T.H. et al. 1998). qPCR was performed using the SYBR Green master mix (Biotool), by mixing 1 µl of cDNA, 1X SYBR Green and 0.4 nM of each primer (forward and reverse). PCR reactions were performed in duplicate and the levels of gene expression were normalized against the housekeeping gene GAPDH.

The data were analyzed using the $2^{-\Delta\Delta CT}$ method (Livak, K.J. et al. 2001); the C_T values of the gene of interest and GAPDH control were provided by the real-time PCR equipment software (Bio-Rad iQ5). The C_T is the cycle number at which the fluorescence signal of the amplification curve crosses the threshold, and is inversely correlated with the initial template concentration (**Figure M-2**).

The data were analyzed using the next equation:

$$2^{-\Delta\Delta CT} = 2^{-(\Delta CT \text{ gene} - \Delta CT \text{ GAPDH})} =, \text{ where } \Delta C_T \text{ gene is:}$$

$$\Delta C_T \text{ gene} = C_T \text{ gene in problem sample} - C_T \text{ gene in control sample}$$

and ΔC_T GAPDH is:

$$\Delta C_T \text{ GAPDH} = C_T \text{ GAPDH in problem sample} - C_T \text{ GAPDH in control sample}$$

Therefore, $2^{-\Delta\Delta CT}$ represents the fold-change in expression of a given gene in the problem sample with respect to the control of sample.

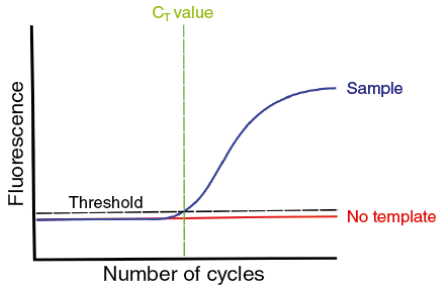

Figure M-2. Model of real time quantitative PCR plot. The threshold level and C_T value of a hypothetical curve sample are indicated.

6. General molecular biology techniques

6.1. Recombinant DNA maintenance and production

Recombinant plasmid DNA was maintained in the bacterial non-pathogenic strain of *Escherichia coli*, DH5α, easily transformable with high efficiency. Transformed bacteria (**Section 6.5**) were selected in LB agar plates (LB media supplemented with 15 g/l agar) or grown in liquid LB (5 g/l Tryptone, 5 g/l yeast extract and 5 g/l NaCl) or 2xYT media (16 g/l Tryptone, 10 g/l yeast extract and 5 g/l NaCl) with the antibiotic ampicillin (100 µg/ml). Plasmids were isolated from bacterial cultures using GeneJET™ Plasmid Miniprep and Maxiprep Kits (ThermoFisher) according to the manufacturer´s specifications.

6.2. Oligos designed for gene silencing

The shRNA oligonucleotides used to downregulate C3G and p38α MAPK expression were designed following the instruction indicated in the web site of GE Dharmacon (http://dharmacon.gelifesciences.com/) (**Table M-8**).

Table M-8. ShRNAs used to downregulate C3G and p38α MAPK expression, their position in the sequence and the name of the corresponding constructs.

Oligo	Sequence (5´-3´)	Position	Construct Name
C3G #3	CGGAGGAACGACGACATTATA	3178-3198 nt (C-T, RasGEF domain)	pSuper-C3Gi3
C3G #4	GCAAGGTGCTGGAGGCCAT	467-485 nt (N-T, Cadherin Domain)	pSuper-C3Gi4
C3G #7	CCACTATGATCCCGACTAT	1233-1251 nt (SH3b domain)	pLVTHM-C3Gi7
p38α	GCACATGCCTACTTTGCTC	909-927 nt	pSuper-p38αi

With these sequences two complementary oligonucleotides of 59-63 bp were designed with the structure:

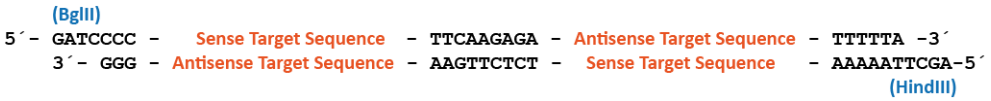

6.3. Annealing of shRNA oligos

The two shRNA oligos were annealed by mixing 1 µM of each primer in annealing buffer (10 mM Tris pH 7.5, 50 mM NaCl, 1 mM EDTA). The mix was heated for 5 min at 95ºC and then cooled down gradually to 15ºC. The resulting double strand DNA was cloned into the proper vector (**Sections 6.4** and **6.5**).

6.4. Digestion

To perform the digestion, 0.2-1.5 µg of DNA was incubated with BglII and HindIII restriction enzymes, in the presence of the proper 1x buffer, for 2-4h at 37ºC. The products of digestion were confirmed by electrophoresis.

After digestion, the vector was dephosphorylated by adding 1U FastAP Thermosensitive Alkaline Phosphatase (ThermoFisher), to prevent self-ligation.

Digested and dephosphorylated DNAs were purified from gel using GeneJET Gel Extraction Kit (ThermoFisher) according to the manufacturer´s specifications. Ligation was performed by incubating the purified insert and vector (molar ratio of 3:1) with 1x ligase reaction buffer and 1 U T4 DNA ligase (ThermoFisher) in a final volume of 10 µL, for 2h at RT. The ligation was transformed into *E. coli* DH5α competent bacteria.

6.5. Transformation of competent DH5α cells by heat-shock method

The ligated DNA was mixed with *E. coli* DH5α competent cells and maintained for 30 min on ice. The mixture was then heated at 42ºC for 45 secs (heat-shock) and placed immediately on ice for 1 min. After the addition of 4 volumes of 2xYT medium, the cells were allowed to recover at 37ºC for 45-60 min at 250 rpm. Finally, the transformed cells were spread onto LB agar plates containing ampicillin and incubated o/n at 37ºC to allow colony growth.

6.6. Screening of colonies by PCR

To identify bacterial colonies harboring the expected construct, we performed a screening by PCR. A small amount of the bacterial colony, used as template, was mixed with 1x PCR Buffer, 2 mM $MgCl_2$, 0.2 mM dNTPs, 0.1 µM each primer and 0.05 U/µl biotaq polymerase. The PCR conditions were: 94ºC, 30 secs; 51ºC, 45 secs and 72ºC, 45 secs/kb for 40 cycles. The results were confirmed by electrophoresis using agarose gels in TAE buffer.

6.7. Sequencing

When necessary, DNA constructs were sequenced using the ABI-3130 xl Genetic Analyzer (Applied Biosystems) in the Genomic Unit at CIC.

7. DNA constructs

Table M-9 summarizes the DNA constructs performed in this work.

Table M-9. C3G DNA constructs used in this work.

Vector	Plasmid type	DNA cloned	Construct name
pLTR2	Overexpression	Full-length C3G ΔN SH3b RemCat ΔCat	pLTR2-C3G pLTR2-ΔN pLTR2-SH3b pLTR2-RemCat pLTR2-ΔCat
pSuper.gfp/neo	shRNA	shRNA C3G shRNA p38α	pSuper-C3Gi pSuper-p38αi pSuper-C3Gi-p38αi
CRISPR	knock-out	gRNA C3G	CRISPR-C3G
pLVTHM	shRNA	shRNA C3G	pLVTHM-C3Gi
pWpI.PGK.neo	Overexpression	Full-length C3G	pWpI-C3Gi

The vectors used are described below:

7.1. pLTR2

pLTR2 is a mammalian expression vector highly efficient for overexpression based on resistance to xanthine, mycophenolic acid and HAT (**Table M-12**). It was used to clone full-length C3G, as well as several mutants (Guerrero, C. et al. 1998). pLTR2 constructs used in this work are represented in **Figure M-3**.

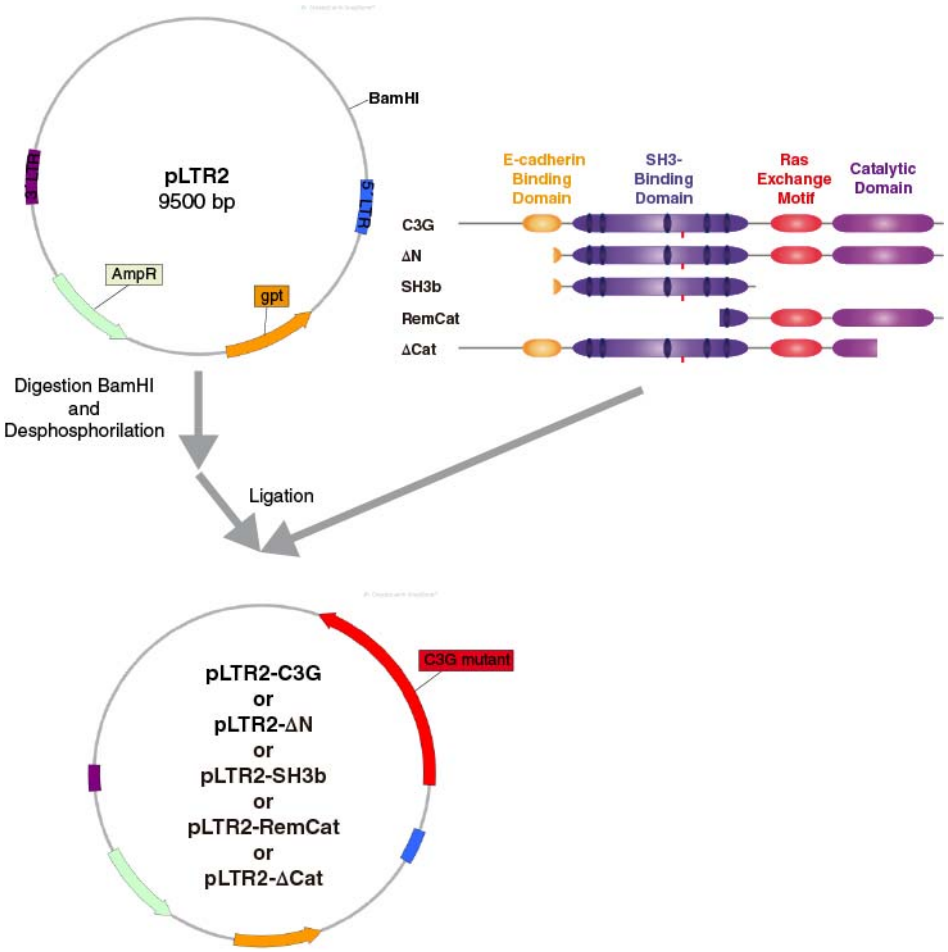

Figure M-3. Schematic representation of pLTR2 and pLTR2-C3G constructs. The structure of full-length C3G and C3G mutants is shown, indicating the different modular domains. LTR: long terminal repeats; AmpR: ampicillin-resistance gene; gpt: gene encoding xanthine phosphoribosyltransferase, which confers resistance to xhantine, mycophenolic acid and HAT salts.

7.2. pSuper

pSuper.GFP/neo constructs (hereafter referred as pSuper) were used to downregulate the expression of C3G and p38α MAPK in K562 cells. **Figure M-4** summarizes the steps followed to clone the aligned oligos into the vector (see 6.2).

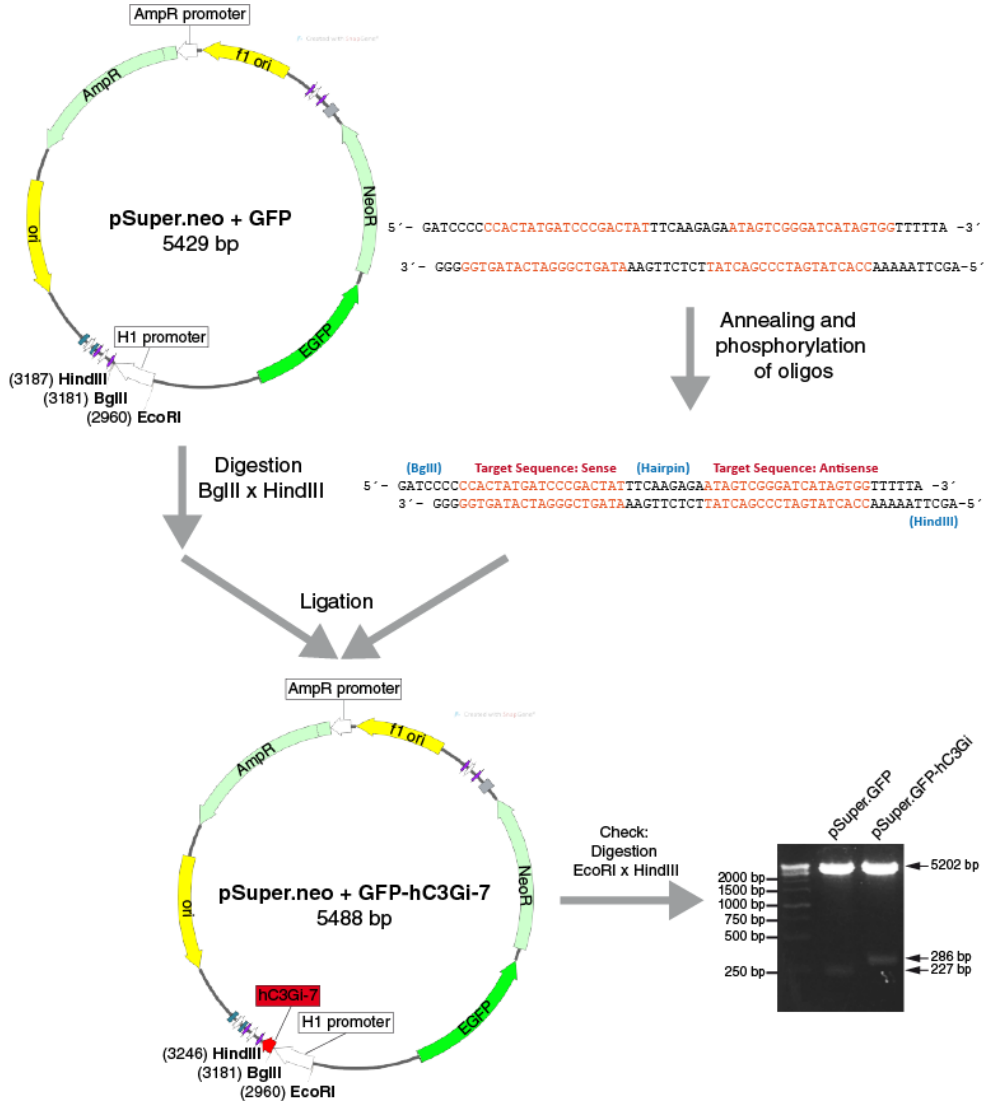

Figure M-4. Schematic representation of the cloning strategy of shRNA C3G #7 in pSuper.neo+GFP, indicating the sequence and structure of the annealed oligos. Cloning was confirmed by double EcoRI-HindIII digestion. Inserts of 227 bp or 286 bp were observed for pSuper and pSuper-hC3Gi, respectively. AmpR: ampicillin resistance gene; Neo: neomycin resistance gene; ori: replication origin; EGFP: enhanced green fluorescence protein; H1 promoter: H1 RNA polymerase III promoter, which drives the expression of the shRNA.

7.3. pWpI

pWpI.PGK.neo (hereafter referred as pWpI) is a lentiviral plasmid which was used to overexpress C3G in HEL cells. Full-length C3G was cloned by PCR with primers described in **Table M-10.** The cloning strategy, which includes the insertion of a PGK-neo cassette, is summarized in **Figures M-5** and **M-6**.

Table M-10. Primers used in the amplification of full-length C3G and PGK-neo cassette for their cloning into pWpI plasmid. Start and stop codons, as well as, PvuI and Pac1 restriction sites are indicated.

Primer	Sequence (5´-3´)
PvuI-C3G	GAG GAT CCG ATC GCC ATG TCC GGC AAG ATC GAG AAA PvuI Start
PacI-C3G	AGA CTA GTT AAT TAA CTA GGT CTT CTC TTC CCG GTC PacI Stop
PacI-PGKneo	AAA TTA ATT AAT TCT ACC GGG TAG GGG AGG PacI
PacI-PGKneo	AA ATT AAT TAA TCA GAA CTC GTC AAG GCG PacI Stop

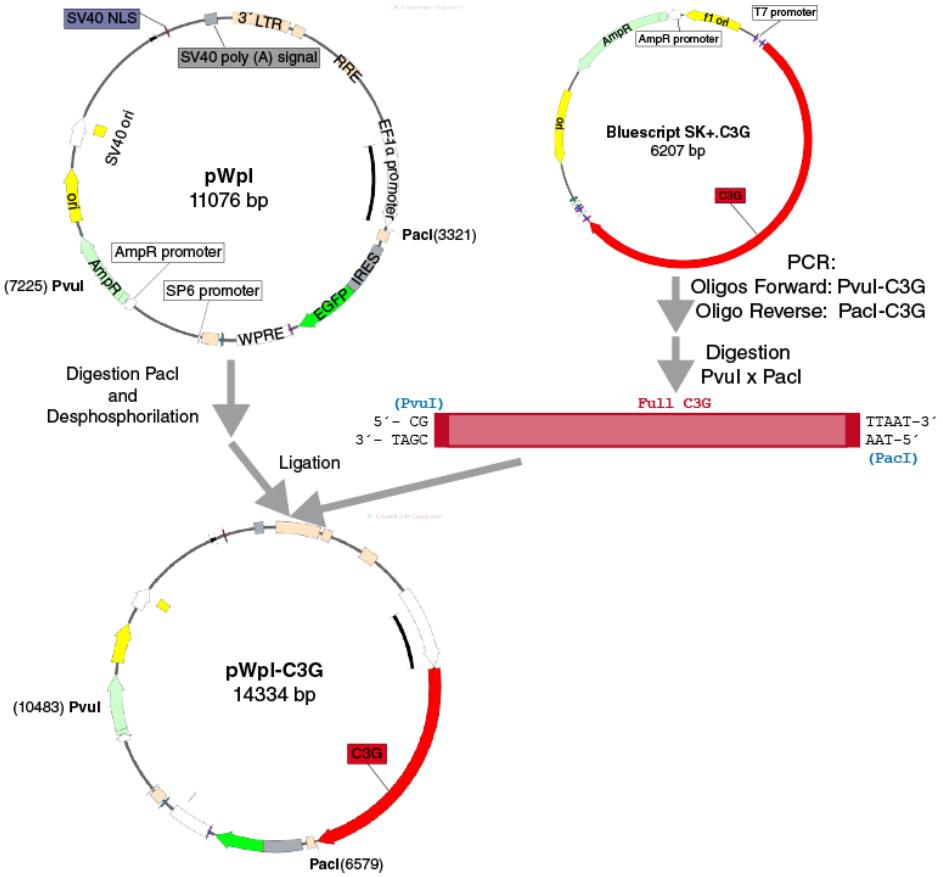

Figure M-5. Schematic representation of the strategy for cloning C3G into the pWpI lentiviral expression vector. AmpR: ampicillin resistance gene; ori: replication origin; EGFP: enhanced green fluorescence protein; SV40 NLS: nuclear localization sequence of SV40; LTR: long terminal repeats; RRE: Rev response elements; IRES: internal ribosome entry site; WPRE: Woodchuck hepatitis virus post-transcriptional regulatory element.

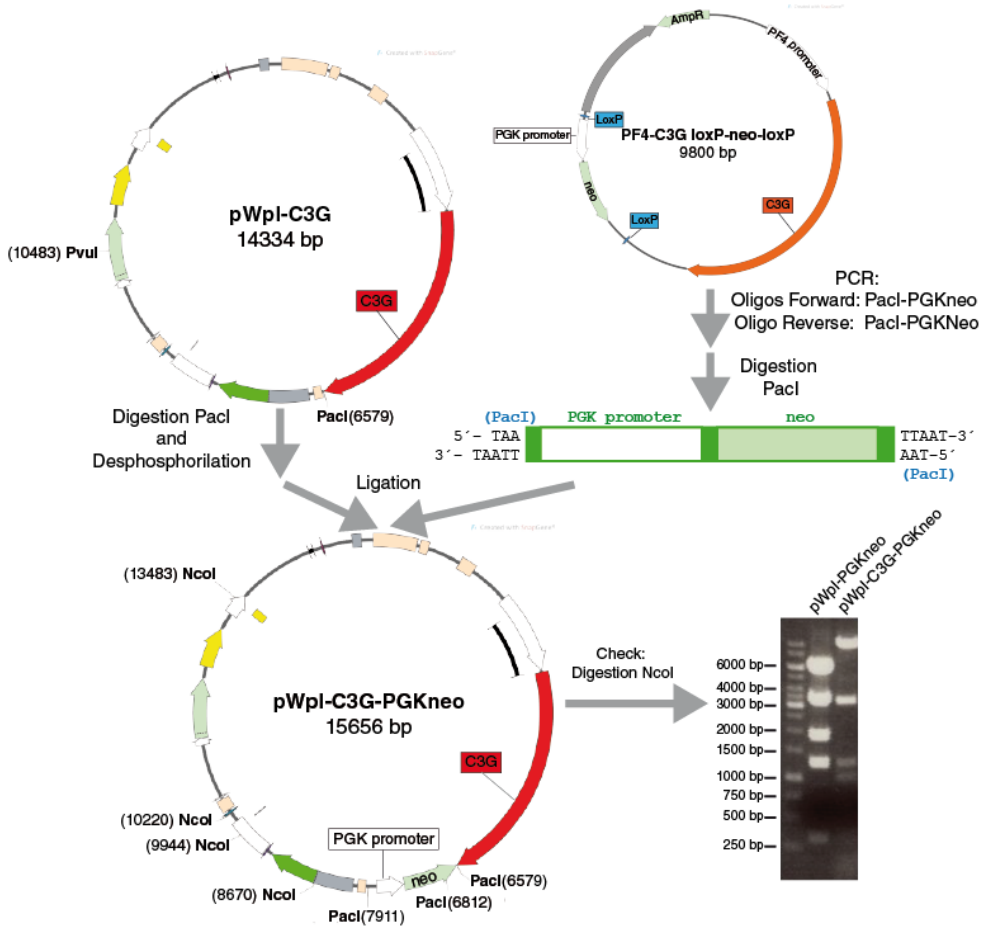

Figure M-6. Schematic representation of the cloning strategy of the PGK-neo cassette (PGK promoter + neomycin resistance gene) in the pWpI and pWpI-C3G vectors. Cloning was confirmed by NcoI digestion. Two different patterns of bands (6597 bp, 3263 bp, 1858 bp, 1234 bp, 316 bp) or (9855 bp, 3263 bp, 1234 bp, 988 bp, 316 bp) were observed for pWpI-PGKneo and pWpI-C3G-PGKneo, respectively. AmpR: ampicillin resistance gene; Neo: neomycin resistance gene.

7.4. pLVTHM

pLVTHM is a lentiviral vector which was used to downregulate the expression of C3G in HEL cells. **Figure M-7** summarizes the design followed to clone the shRNA oligo C3G #7 into this vector (**Table M-8**).

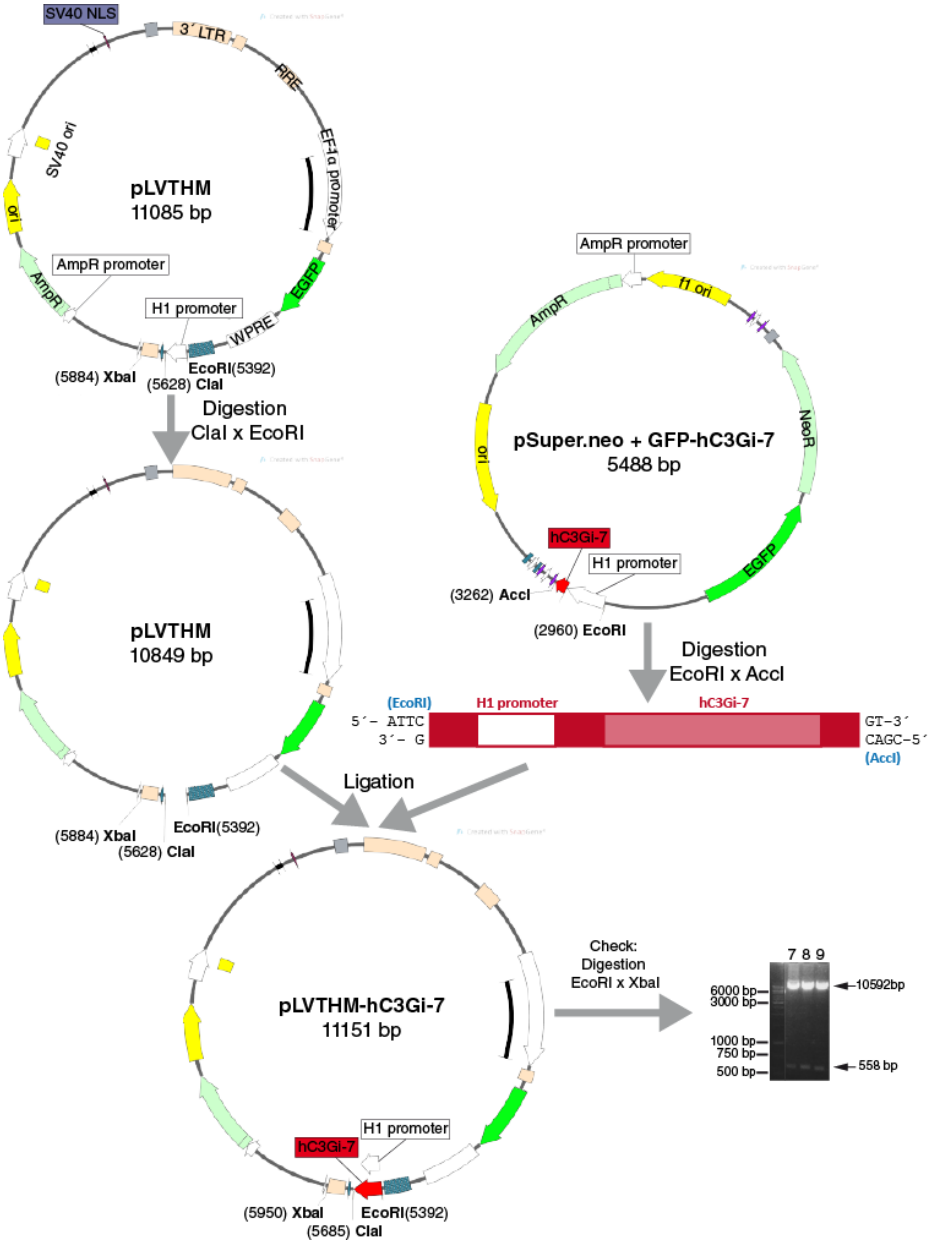

Figure M-7. Schematic representation of the cloning strategy of the shRNA oligo C3G #7 into pLVTHM plasmid. Cloning was confirmed by double EcoRI-XbaI digestion The pattern of bands observed for pLVTHM-hC3Gi was 10592 bp and 558 bp. AmpR: ampicillin resistance gene; NeoR: neomycin resistance gene; ori: replication origin; EGFP: enhanced green fluorescence protein; SV40 NLS: nuclear localization sequence of SV40; RRE: Rev response elements; WPRE: Woodchuck hepatitis virus post-transcriptional regulatory element.

7.5. CRISPR/Cas9

The plasmids used to knock-out C3G in K562 cells by the CRISPR/Cas9 system are from Santa Cruz Biotechnologies. K562 cells were co-transfected by electroporation with CRISPR/Cas9 KO and HDR plasmids (**Figure M-8**). The CRISPR/Cas9 KO plasmid harbors 3 guide sequences (gRNA) specific for C3G. The HDR plasmid contains sequences 5´arm and 3´arms that recognizes the target sequences (**Table M-11**). After the cells are transfected with the CRISPR and HDR plasmids, the sequences of Cas9 and the gRNAs are transcribed and form a complex capable of recognizing the target DNA. When gRNA-Cas9 complex binds to the target DNA, the Cas9 enzyme cleaves both DNA strands creating a Double-Strand Break (DSB) in the target DNA. Then, the DNA flanking the DSB is recognized by the homology arm sequences (5´arm and 3´arm) in the HDR plasmid, and the sequences of RFP (Red Fluorescent Protein) and puromycin resistance are inserted by homologous recombination. The insertion of the puromycin resistance and RFP fluorescence are the proofs of the successful gRNA-Cas9-induced DSBs.

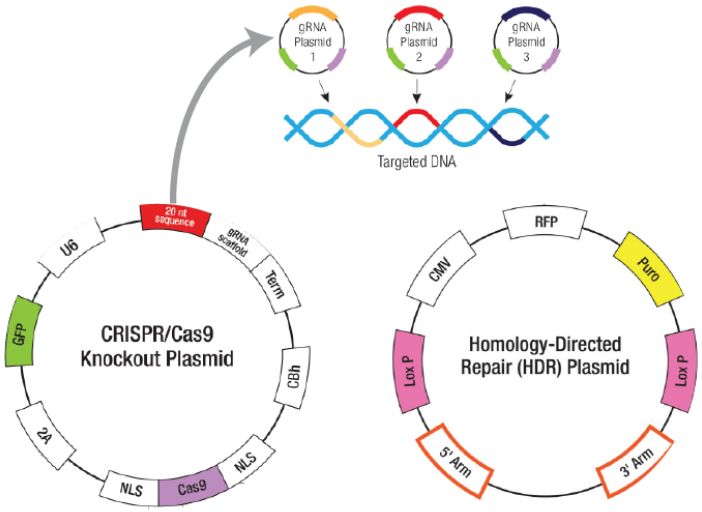

Figure M-8. CRISPR/Cas9 KO and HDR vector maps. The CRISPR system used 3 different gRNAs, (**Table M-11**) represented on the top, to increase the efficiency of the system.

Table M-11. Commercial C3G gRNA sequences cloned in the CRISPR/Cas9 knock-out plasmids

gRNA Name	Sequence	Recognition
sc-401616A1	GGGCGCGACCTCTTCATCCG	863-882 nt (SH3b domain)
sc-401616A2	TTATCAACCACCCGAATGCC	901-920 nt (SH3b domain)
sc-401616A3	GCCTCGCCAACCTCATTCGC	563-582 (N-T, Cadherin domain)

8. Transfection of mammalian cells

In this work we have used the following transfection techniques.

8.1. Electroporation

K562 cells were transfected with pLTR2, pSuper and CRISPR vectors by electroporation using Gene Pulser® Electroporation System with 0.4 cm electrode gap cuvettes (Bio-Rad). Exponentially growing cells (5-10 x 10^6) were collected and washed once with serum-free RPMI. Then, cells were resuspended in 400 µl of serum-free RPMI, place into the cuvette and mixed with 25 µg of plasmid DNA. Electroporation conditions were 260 V and 950 µFa for 10-12 msec. After electroporation, 800 µl of warmed complete RPMI medium was added to the cuvette to allow cell recovery for 5 min. Finally, cell suspension was transferred to a 25 cm^2 flask containing 10 ml of complete RPMI medium, and incubated under standard conditions for 48h prior to processing or addition of selection reagents (**Section 8.3**).

8.2. Production and purification of lentiviral particles

Lentiviral vectors are derived from the human immunodeficiency virus (HIV-1). To increase the safety during the handling of these viruses, the necessary components for their production are distributed in different plasmids. We have used a second generation lentiviral packaging system, whose components are:

- **Lentiviral transfer plasmid, encoding the insert** (pWpI for cDNA and pLVTHM for shRNA, **Figures M-5**, **M-6** and **M-7**). The transgenic sequence is flanked by LTR (Tat dependent) sequences, which facilitate integration of the cloned DNA into the host genome. The cloning was made as described in **Section 7.3** and **7.4**.
- **Packaging plasmid** (psPAX2, **Figure M-9**). This plasmid contains the genes encoding for Gag (polyprotein of retroviral core), Pol (reverse transcriptase), Rev and Tat (regulatory proteins).
- **VSV-G envelope expressing plasmid** (pMD2.G, **Figure M-9**). This plasmid contains the VSV-G gene (G glycoprotein, which facilitates the formation of the viral particles).

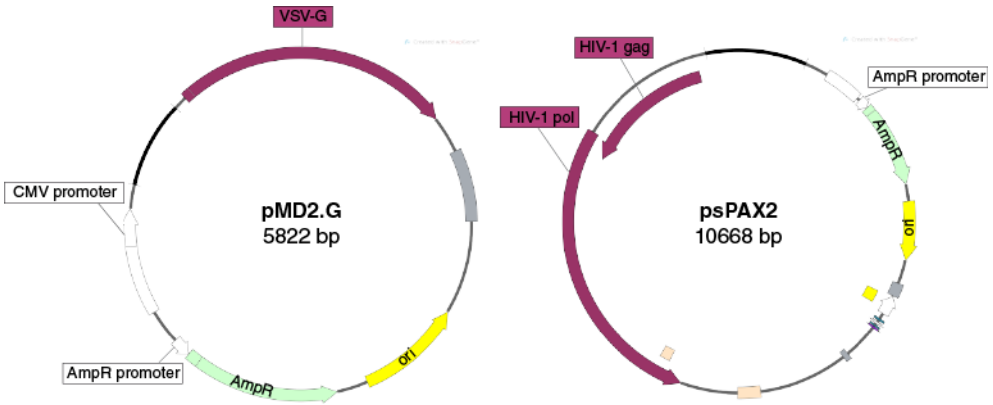

Figure M-9. Maps of pMD2.G and psPAX2 vectors indicating the packaging genes (HIV-1 gag and HIV-1 pol) and envelope genes (VSV-G). AmpR: ampicillin resistance gene. CMV: cytomegalovirus.

8.2.1. Transient transfection of HEK-293T cells

The HEK-293T cell line is a highly transfectable derivative of HEK-293 cells, containing the SV40-T antigen, which makes them competent to replicate vectors carrying the SV40 region of replication. So we used them to produce the lentiviral particles. For that, HEK-293T cells were simultaneously transfected with the 3 viral plasmids described above using a PEI (Polyethylenimine linear, Polysciences Inc.) transfection protocol. HEK-293T cells in complete DMEM medium were seeded on 100-mm culture dishes, coated with collagen (100 µg/ml Rat Tail Collagen, BD Sciences), until a confluence of ~100%. The transfection mix [1.2 ml NaCl (150 mM), 6 µg pLVTHM or pWpI, 6 µg psPAX2, 4.5 µg pMD2.G and 60 µl PEI (1 mg/ml, pH 7)] was incubated for 20 min at RT, to promote the formation of the DNA:PEI complexes, and then added to the cultures. Then, the medium was replaced with fresh DMEM + transfection mixture, followed by incubation o/n at 37ºC. The next day (day 2), medium was replaced by fresh complete DMEM medium, which was maintained for a further 24 h. The efficiency of the transfection was verified by the fluorescence emitted by the GFP protein encoded by the Lentiviral transfer plasmid.

8.2.2. Harvesting and concentration of lentivirus by ultracentrifugation

The medium, containing the lentiviral particles, was collected into a 50 ml centrifuge tube 48h after transfection and stored at 4ºC. Fresh complete DMEM medium was added to the culture to continue producing lentiviral particles for an additional ~12h.

On day 4, lentiviral particles were concentrated by ultracentrifugation at 20000 *rpm* for 2h at 16ºC using an Optima^{TM} Le-80K Ultracentrifuge (Beckman). Then, the virus was

resuspended in 200 µl of serum-free DMEM for 4h at 4ºC and finally stored in small aliquots at -80ºC.

8.2.3. Titration of infectious particles

To titrate the above lentiviral suspensions, HEK-293T cells (~10^5) were infected with different amounts of viral suspensions (1-10 µl from a 1:10 dilution) and the number of infected cells was quantified by flow cytometry. Incubation was performed in the presence of 8 µg/ml Polybrene (Hexadimethrine bromide, Sigma) to increase the efficiency of the infection. Additionally, the plate was centrifuged at 1000 x*g* for 90 min and 30ºC to promote the infection. Medium was refreshed after 24h.

After 3 days of infection, GFP positive (GFP^+) cells were analyzed by flow cytometry. The number of Transforming Units per ml (TU/ml) was calculated with the following formula:

$$\text{HEK}-293\text{T}\ \frac{\text{TU}}{\text{ml}} = \text{number of plated cells x}\ \frac{\%\ \text{GFP cells}/100}{\text{amount of viral suspension (ml)}}$$

Percentages of GFP^+ cells greater than 20% increase the probability of cells being infected by 2 viral particles, while below 5% cytometer measurement is not reliable.

8.2.4. Infection of HEL cells

The Multiplicity of Infection (MOI) is the ratio of the number of viral particles to the number of target cells, and it is dependent on the cell line. The MOI for HEL cells is between 25-50, and the amount of viral suspension needed to obtain a percentage of GFP^+ cells around 100% is calculated with the following formula:

$$\text{Amount of virus (µl)} = \frac{\text{Number of plated cells x MOI}}{\text{TU/ml}}\ \text{x}\ 1000$$

HEL cells at, a density of 4 x 10^5 cells/ml, were starved (RPMI + 1% FBS) 16h before infection. Then, 8 x 10^4 cells were plated in 96 well plates in 1% FBS RPMI with the proper amount of viral particles in a final volume of 200 µl. The plate was centrifuged at 1000 x*g* for 90 min at 30ºC and cultured under standard conditions until confluence.

8.3. Selection of stable-transfected cells

Transfection of a plasmid containing antibiotic resistance genes confers the cells the ability to grow in the presence of selective medium, such as Killer HAT medium or neomycin containing medium (**Table M-12**).

Table M-12. Plasmids used in transfection, indicating the method of transfection and the selective medium.

Cell Line	Method of Transfection	Vector	Selective medium
K562	Electroporation	pLTR2	Killer Hat Solution (1:20): - 12,5 µg/ml Xanthine Sodium Salt - 1,25 µg/ml Mycophenolic acid - 0,05x HAT Solution (20 nM aminopterine, 5 µM hypoxanthine and 0,8 µM thymidine)
		pSuper.gfp/neo	250 µg/ml neomycin (G418)
		CRISPR + HDR	-
HEL	Lentivirus	pLVTHM	-
		pWpI	250 µg/ml neomycin (G418)

Selection medium was added 48h post-transfection and refreshed every 2-3 days until all cells were resistant (typically 15 days). The appropriate concentration of the antibiotic was calculated by a kill curve, which determines the lowest antibiotic concentration at which all untransfected-cells are dead after a week.

Cells transfected with the CRISPR/Cas9 plasmids or with the pLVTHM plasmid were selected by single-cell isolation and clonal expansion. Single cells, expressing GFP or RFP, were isolated by Fluorescence-Activated Cell Sorting (FACS) into 96 well/plates and expanded. Clones with the lower levels of C3G were selected by Western Blot and qPCR (**Section 4** and **5**, respectively).

The proliferative capacity of single cell cultures was increased by adding a 1:1 mixture of fresh medium and conditioned medium from a culture of the same cell type. The conditioned medium provides growth factors and cytokines released from the cells in culture, which improves the growth of low density cultures. The concentration of the conditioned media was gradually reduced as the density of the culture increased.

9. Analysis of cell surface markers by flow cytometry

K562 or HEL cells, differentiated to megakaryocytes, as well as bone marrow cells, from the transgenic mice, were harvested by centrifugation at 445 x*g*, for 5 min and washed once with cold PBS. Then, 10^5 cells were resuspended in 100 µl of PBS and incubated with 0.5-1 µg of fluorochrome-conjugated antibodies (**Table M-13**) for 20 min on ice and protected from light. After the incubation, the excess antibody was washed out with 500 µl of PBS, and

cells were resuspended in 200 µl of PBS for acquisition using FACSCalibur™ or BD Accuri™ cytometers.

Table M-13. Fluorochrome-conjugated antibodies for flow cytometry

Antibody	Target	Host	Supplier
FITC Anti-Human GPA	Human CD235a (Glycophorin A)	Mouse	Immunostep (235AF-100T)
PE Anti-Human GPA	Human CD235a (Glycophorin A)	Mouse	Immunostep (235APE-100T)
PE Anti-Human CD41	Human integrin αIIb	Mouse	Immunostep (41PE-100T)
APC Anti-Human CD61	Human Integrin β3	Mouse	Immunostep (61A-100T)
APC Anti-Mouse CD41	Mouse Integrin αIIb	Rat	eBioscience (17-0411)
FITC Anti-Mouse CD41	Mouse Integrin αIIb	Rat	BD Pharmigen (553848)
PE Anti-Mouse CD41	Mouse Integrin αIIb	Rat	BD Pharmigen (558040)
PE Anti-Mouse/Rat CD61	Mouse/Rat Integrin β3	Armenian Hamster	eBioscience (12-0611)

10. Analysis of DNA ploidy by flow cytometry

After 6-10 days of differentiation, cultures of cell lines and bone marrow cells were harvested, washed and fixed with 70% ethanol. The cells were resuspended in 50 µl of PBS, and 100 µl EtOH was slowly added dropwise to the cell suspension, while vortexing to avoid aggregates. The fixed cell suspension was stored at 4ºC o/n prior the staining. Then, cells were washed twice with PBS by centrifuging at 200-500 x*g* for 10 min at 4ºC. Washed cells were stained with fluorochrome-conjugated CD41 antibody (primary cells only), as described in **Section 9**, and subsequently incubated with a mixture of 100 µg/ml RNase (Promega) and 50 µg/ml Propidium Iodide (PI, Sigma) in PBS for at least 40 min at RT in the dark. The ploidy distribution of the $CD41^+$ populations was determined using a BD Accuri™ cytometer.

For the analysis, we first gated the CD41+ cell population. Cell doublets were excluded based on pulse-width *vs* pulse-area. These gates (CD41+ and single cells) were combined and the PI histogram plot (Cell count *vs* PI intensities) applied. The histogram plot is composed of several peaks (**Figure M-10**), where each peak represents a population of CD41+ single cells having equal DNA content. The first peak corresponds to the population of diploid cells, the second correspond to tetraploid cells, and so up to the seventh peak (128n).

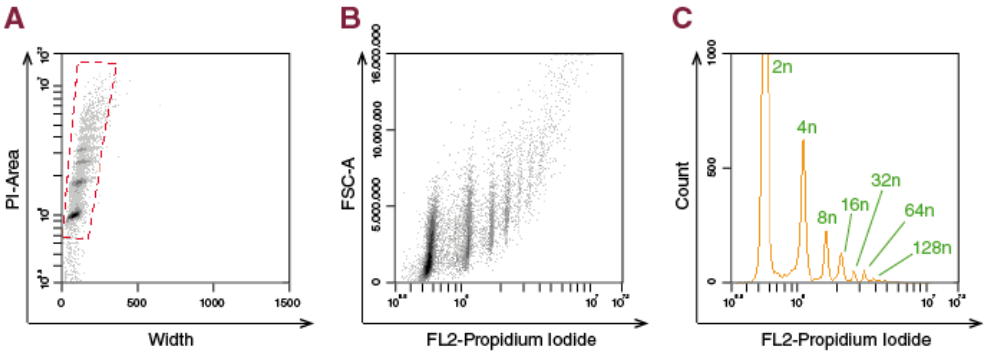

Figure M-10. Representative flow cytometry plots showing polyploid cells. A) PI-Area *vs* Width plot with a gate that represents the single cell populations **B)** Representative dot plot, FSC-A vs PI, that reflects the cell size and the DNA content. Note that cell size increases with increasing ploidy. **C)** Representative histogram plot of ploidy distribution, where each peak represents a population. This is an ideal plot in which all 7 possible populations (2n, 4n, 8n, 16, 32n, 64n and 128n) are identified.

11. Immunofluorescence

Cells were seeded at a concentration of 2 x 10^6 cell/ml onto 6 cm plates containing glass coverslips pre-coated with 5 µg/ml of fibronectin (Sigma). Cells were incubated with serum-free media for 48h, which allowed for enhanced cell attachment, and then the coverslips were washed with PBS to remove excess medium, and fixed with 3.7% paraformaldehyde (PFA, Sigma) for 15 min. The fixed cells were washed twice with PBS, permeabilized with 0.1% Triton™ X-100 (Sigma), and washed again with PBS. Coverslips were blocked with 2% BSA for 1h, incubated with primary antibodies for 1h, washed three times with PBS, and incubated with secondary antibodies for 1h, each step at room temperature. Nuclei were stained with DAPI for 10 min. After staining, coverslips were washed three times with PBS and once with H_2O, and finally were mounted with Mowiol® (Calbiochem). All antibodies used for immunofluorescence are described in **Table M-14**. Images were obtained at the same exposure time with a Leica TCS SP5 confocal microscope and pictures were processed using LSM Image Browser, ImageJ Software and ZEN lite Imaging Software.

Table M-14. Primary and secondary antibodies used for immunofluorescence

Primary Antibodies				
Antibody	**Target**	**Host**	**Supplier**	**Dilution**
C3G 1008	SH3b-RemCat domains from human C3G	Rabbit	C.Guerrero et al, 1998	1:50
GST (B-14)	Specific domain of GST	Mouse	Santa Cruz (sc-138)	1:30
Phospho-C3G (Tyr 504)	Fragment containing phosphorylated Tyr 504 from hC3G	Rabbit	Santa Cruz (sc-12926)	1:50
Rap1 (121)	C-terminus of human Rap1	Rabbit	Santa Cruz (sc-65)	1:30
Secondary Fluorochrome-conjugated Antibodies				
Antibody	**Target**	**Host**	**Supplier**	**Dilution**
Cy3-AffinityPure IgG (H+L)	Mouse	Goat	Jackson immunoresearch (115-165-146)	1:100
Cy3-AffinityPure IgG (H+L)	Rabbit	Goat	Jackson immunoresearch (111-165-144)	1:100
Cy5-AffinityPure IgG (H+L)	Mouse	Goat	Jackson immunoresearch (115-175-146)	1:100
Cy5-AffinityPure IgG (H+L)	Rabbit	Goat	Jackson immunoresearch (111-175-144)	1:100

12. Rap1 pull-down activity assay

To analyze the activation state of Rap1 we performed a pull-down assay based on the specific interaction between the active, GTP-bound, Rap1 form and the Rap-binding domain (RBD) of its target RalGDS fused to GST (glutathione S-transferase). The complexes are recovered by incubation with glutathione-Sepharose beads, with high affinity for GST.

12.1. Binding of GST-RalGDS-RBD to Glutathione-Sepharose beads

The first step of this assay was the pre-incubation of 20 µg of purified GST-RalGDS-RBD (a gift from Jose Maria de Pereda) with Glutathione-Sepharose 4 fast flow (GE Healthcare) in PBST buffer (2 mM EDTA, 0.1% β-mercaptoethanol, 0.2 mM PMSF in PBS) for 1-2h at 4ºC in rotation. After incubation, beads were washed 4 times with PBST, resuspended in MLB 1x (25 mM HEPES pH 7.5, 150 mM NaCl, 1% Igepal CA-630, 10 mM $MgCl_2$, 1 mM EDTA, 2% Glycerol, 0.4 µg/ml Leupeptin, 1 mM PMSF, 25 mM NaF, 1 mM Na_3VO_4) and kept on ice. All centrifugations with the beads were made at 300 x*g* and at 4ºC.

12.2. Cell lysis and pull-down

Confluent K562 cells (~4 x 10^6) were serum-deprived o/n. Starved cells were stimulated with PMA for 1-5 min to induce the activation of Rap1. Then, cells were collected, washed with PBS and lysed with 500 µl of 1x MLB by keeping them 10 min on ice. 0.5-1 mg of total cell lysate was incubated with GST-RalGDS-RBD bound beads (see above) for 30 min at 4ºC with gentle rotation. After incubation, the Beads-GST-RalGDS-RBD-Rap1-GTP complexes were washed twice with 1x MLB by centrifugation and then boiled with Laemmli buffer 2x to denature and separate the proteins from the beads.

12.3. Detection of Rap1-GTP

Samples were separated by 12.5% SDS-PAGE and activated Rap1-GTP was detected by Western Blot using an anti-Rap1 antibody (**Section 4.4**).

13. Rap1 activity assay by immunofluorescence

Cells were seeded at a concentration of 1 x 10^6 cell/ml (4 ml) onto 6 cm plates containing glass coverslips. Cells were incubated with serum-free media o/n at 37ºC, to allow cell attachment. Next day, cells were treated with 20 nM PMA at indicated times and then cells were fixed adding 4 ml of 8% paraformaldehyde (PFA, Sigma) for 15 min. Fixed cells were washed twice with PBS, permeabilized with 0.2% Triton™ X-100 (Sigma) in PBS containing 1% BSA for 5 min, and washed again with PBS. Coverslips were incubated with 0.3 mg/ml GST-RalGDS-RBD purified protein for 45 min, washed three times with PBS and incubated with primary antibodies for 1h (**Table M-14**). Then, cells were washed three times with PBS, and incubated with secondary antibodies for 1h (**Table M-14**), each step at room temperature. Nuclei were stained with DAPI for 10 min. After staining, coverslips were washed three times with PBS and once with H_2O, and finally were mounted with Mowiol® (Calbiochem). Two negative controls were performed as follows: (1) without the GST-RalGDS-RBD protein, as control of the specificity of the anti-GST primary antibody; (2) without anti-GST primary antibody, to detect any non-specific staining by the secondary antibody. Images were obtained at the same exposure time with a Leica TCS SP5 confocal microscope and pictures were processed using LSM Image Browser and ImageJ.

14. Bone marrow explants

The bone marrow explants are used to evaluate the formation of proplatelets. In this model, the environment and the interaction with the matrix are preserved in a more

physiological context. Small pieces of fresh bone marrow (explants) are maintained in a physiological buffer and monitored for 6h by time-lapse microscopy. After 30 min, megakaryocytes, which are visible at the periphery of the explants, begin to change their morphology, from round cells to cells with long extensions called proplatelets.

Mouse euthanasia and femur and tibia harvesting were performed as described in **Sections 2.1** and **2.2**. Once the bones were completely clean, the marrow was obtained intact by flushing it into a tube with Tyrode´s buffer (134 mM NaCl, 0.34 mM $NaHPO_4$, 2.9 mM KCl, 12 mM $NaHCO_3$, 20 mM HEPES, 5 mM Glucose, 0.35% Albumin, 1 mM $MgCl_2$, 2 mM $CaCl_2$ and 10 U/ml Penicillin/Streptomicin) using a 21-gauge needle (Behnke, O. 1968). The marrow was cut into 0.5-1 mm thick transverse sections with a surgical blade, under a binocular microscope. The explants were placed in an incubation chamber (µ-Slide 8 well IbiTreat, Ibidi) with Tyrode´s buffer containing 5% mouse serum (**Section 2.6**) and were maintained at 37ºC for 6h. Megakaryocytes at the periphery of the explant were monitored under an inverted microscope (Nikon Eclipse TE2000-E) coupled to a video camera (Hamamatsu Orca-er) and processed using Metamorph® software.

14.1. Quantification of Proplatelet-forming cells

To better identify the megakaryocytes in the periphery of the explant, anti-mouse CD41-APC antibody (eBiosciences) was added to the Tyrode´s buffer prior to placing the explants in the incubation chamber. Megakaryocytes were quantified using ImageJ. Megakaryocytes were classified according to the morphology: i) spherical megakaryocytes, ii) megakaryocytes with protrusion and iii) megakaryocytes with proplatelets.

14.2. Time-course acquisition

The images were sequentially acquired at 10 min intervals for 6h and then mounted and processed using ImageJ software. The video was used to determine the velocity and the mobility of each megakaryocyte from the explant, using ImageJ software.

15. Platelet counts in peripheral blood

Peripheral blood samples were collected from the submandibular plexus of 6-months-old mice into 1.6 mg/ml EDTA-containing tubes (Sarstedt). Platelet count was determined from 30 µl EDTA-anticoagulated blood using a hemocytometer (Hemavet Counter HV950FS).

16. Statistical Analysis

Data have been represented as the mean ± SEM (Standard Error of the Mean) or the median ± SEM values of at least 3 independent experiments from each genotype. The Kolmogorov-Smirnov test was performed to determine if the data fit into a normal distribution. To compare between two experimental groups, unpaired Student´s t-test was computed, when the data were normally distributed. The Mann Whitney´s U-test was computed as a non-parametric procedure when our data were not normally distributed.

In fluorescence measurements in cell lines cultures, due to high variability in fluorescence intensities between independent experiments, the data were normalized against the control values. To calculate the significance between the different experimental conditions, a two-way ANOVA test was performed. Then, Holm-Sidak post-hoc pairwise analysis was calculated to determine the significant differences in groups two to two.

17. Software Programs

17.1. Plasmid design

- Serial Cloner
- SnapGene Viewer

17.2. Imaging

- ImageJ Software
- LSM Image Browser
- Metamorph® Software
- ZEN lite 2.3 SP1 Digital Imaging Software

17.3. Cytometry

- FlowJo
- BD Accuri C6 Software
- Muse Software

17.4. Graphs and statistics

- Excel
- SigmaPlot

Results

1. Analysis of the implication of C3G in megakaryocytic differentiation using transgenic cell lines

The most widely used cellular models for studying megakaryocytic differentiation are the hematopoietic cell lines, K562 and HEL. As mentioned in the Introduction, K562 cell line behaves as a pluripotent hematopoietic precursor that expresses, under undifferentiated conditions, markers for both erythroid and megakaryocytic lineages. These cells could differentiate into one lineage or another depending on the stimulus. Thus, TPO or phorbol esters, such as PMA, induce MK differentiation, whereas Imatinib induces erythroid differentiation. PMA-induced differentiation is accompanied by changes in cell morphology, cell growth arrest, endomitosis and acquisition of specific megakaryocyte markers, in part mimicking the physiological process that takes place in the bone marrow.

The first evidence of the implication of C3G in MK differentiation was the observation of a high proportion of K562 cells, stably transfected with the plasmids pLTR2-C3G and pSuper.GFP/neo and thus overexpressing high levels of C3G and GFP, with an aberrant morphology. K562 cells are non-adherent, rounded and small blasts, whereas some of the cells overexpressing C3G were larger, vacuolated and with several extensions in the membrane, features which resemble that of megakaryocytes (Figure R-1).

K562 pLTR2-C3G/pSuper.GFP/neo

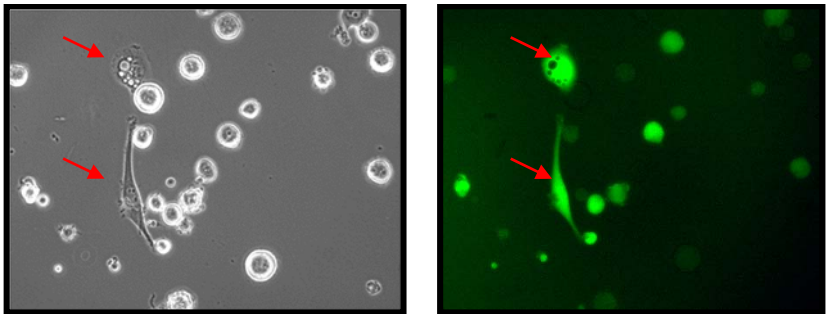

Figure R-1. **Representative images of K562 cells transfected with the plasmids pLTR2-C3G and pSuper.GFP/neo.** pSuper.GFP/neo harbors a gene encoding for the Green Fluorescence Protein (GFP). The arrows indicate cells with megakaryocyte-like features: large vacuolated cells and cells with long extensions. Left image: Differential Interference Contrast Microscopy (DIC). Right image: Fluorescence microscopy.

As mentioned before, PMA is a good inducer of MK differentiation in our two cellular models, K562 and HEL cells. Therefore, we analyzed whether C3G expression was increased along the PMA-induced MK differentiation in non-transfected K562 and HEL cells. For this

purpose, cells were cultured in the presence of 20 nM PMA for 3 days and harvested every 24 hours to determine C3G levels by Western Blot. **Figure R-2A** shows a clear increase in C3G protein levels over time in HEL cells, that correlates with the acquisition of a megakaryocytic morphology (**Figure R-2B**), indicating that C3G might be involved in this process. Although to a lesser extent, C3G levels also increased in PMA-treated K562 cells.

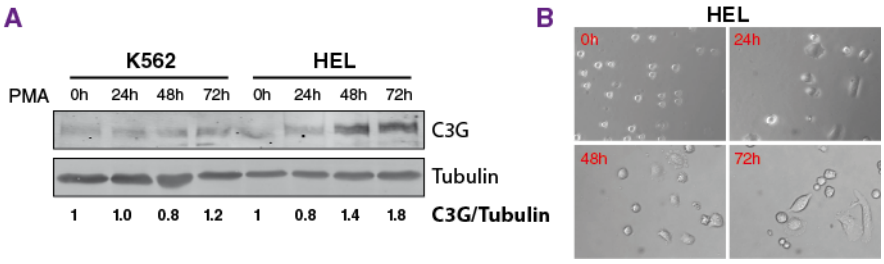

Figure R-2. Analysis of C3G expression in K562 and HEL cells. K562 and HEL cells were stimulated with 20 nM PMA for 3 days. **A)** The cultures were harvested at the indicated times and the expression of C3G was determined by Western blot. Tubulin was used as loading control. Relative C3G/Tubulin ratios are shown. All values are relative to non-treated cells. **B)** Representative images showing the morphology of HEL cells after 24, 48 and 72 hours of PMA treatment. Images were obtained using a Zeiss Axiovert 135 inverted microscope.

1. Establishment of transgenic, knock-down and knock-out C3G cell lines

In order to deep inside the involvement of C3G in the differentiation process, we generated stable cell lines with modified C3G expression. C3G overexpression or downregulation was confirmed in all clones prior their characterization.

1.1.1. C3G expression models in K562 cells

K562 cells were transfected by electroporation with plasmid pLTR2-C3G to overexpress C3G or with pSuper-C3Gi to silence it. After electroporation, the transgenic clones were selected by resistance to Killer Hat medium or G418 antibody respectively, as detailed in Materials and Methods (**Figure R-3A**). The expression of C3G was measured by RT-PCR and Western Blot, using specific oligonucleotides and antibodies. As shown in **Figure R-3B** C3G expression was increased by 11-fold in pLTR2-C3G-expressing cells, compared to cells expressing empty pLTR2 vector (pLTR2-CT). Similarly, **Figure R-3C** showed a 2-fold decrease in C3G expression in the pSuper-C3Gi clone, compared to its control (pSuper-CT).

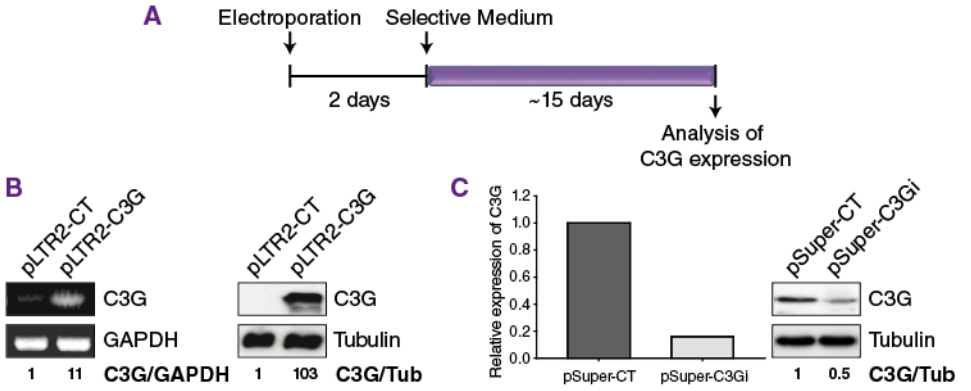

Figure R-3. Analysis of the expression of C3G in K562 transgenic cell lines. A) Temporal scheme of electroporation and subsequent selection of stable clones. **B)** Left panel: Representative semiquantitative RT-PCR analysis of C3G mRNA expression in K562 cells transfected with pLTR2-CT and pLTR2-C3G, using primers Ex3F-Ex5R and normalized against GAPDH. Right panel: Representative Western Blot showing C3G expression detected with anti C3G H-300 antibody. **C)** Expression of C3G in K562 cells transfected with pSuper-C3Gi or empty pSuper-CT plasmids. The histograms show the relative mRNA expression of C3G measured by qPCR. The right panel is a representative Western Blot showing the expression of C3G with anti-C3G H-300 antibody. The expression of tubulin was used as loading control in the Western Blots. Relative C3G/Tubulin ratios are shown. Values are relative to non-transfected cells.

Additionally, the expression of C3G in K562 cells was downregulated using the CRISPR/Cas9 system. In this case, the transfected cells were selected by single-cell isolation and clonal expansion. Once the clonal populations were established, a total of 3 clones for each genotype were selected to analyze C3G expression. The efficacy in C3G ablation was analyzed by qPCR using the oligonucleotides Ex3F-Ex5R and Ex22F-Ex24R, and confirmed by Western Blot using anti-C3G C-19 antibody (**Figures R-4A and R-4B**). We selected H11 as the C3G KO clone (CRISPR-C3G), and G5 as the control clone (CRISPR-CT) to perform the experiments of MK differentiation.

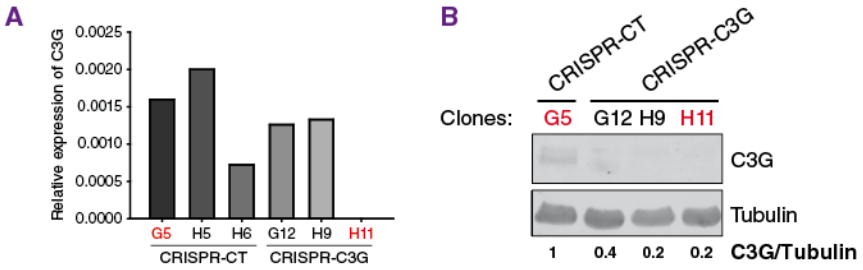

Figure R-4. Identification of CRISPR/Cas9 knock-out clones by Western Blot and qPCR. A) Relative C3G mRNA expression by qPCR in a representative subset of CRISPR-CT and CRISPR-C3G clones. GAPDH was used as housekeeping gene. **B)** C3G protein expression in a representative subset of CRISPR-CT and CRISPR-C3G clones. The clones selected to perform the experiments are shown in red. The expression of tubulin was used as loading control. Relative C3G/Tubulin ratios are shown.

1.1.2. C3G expression models in HEL cells

HEL is a cell line very sensitive to transfection by electroporation. Therefore, we used lentiviral particles as an alternative for the transfection of this type of cells. Lentiviral production, HEL infection and subsequent selection of transfected cells were performed following the scheme in **Figure R-5**.

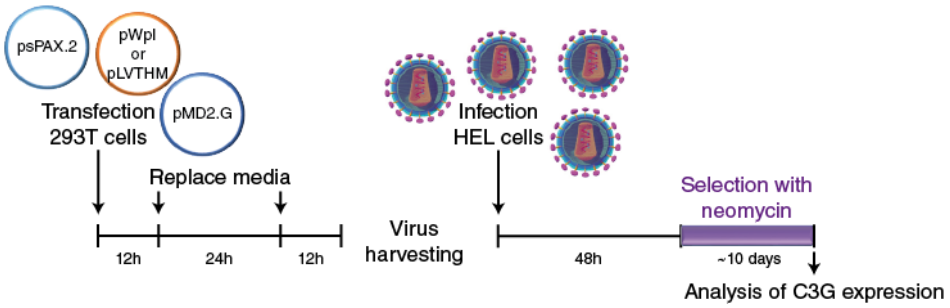

Figure R-5. Schematic representation of lentiviral particle production and HEL cell infection. The selection of stable cell lines by addition of neomycin was only performed with the pWpI clones.

After infection, we checked whether HEL cells had incorporated the lentiviral plasmid (pWpI or pLVTHM). As these plasmids contain the Green Fluorescence Protein gene, the percentage of transfected cells could be measured by flow cytometry. As shown in **Figure R-6A**, the percentage of GFP+ cells exceeded 90% in both clones. Then, the GFP+ cells were purified by FACS (Fluorescence-Activated Cell Sorting) and their genotype validated by PCR and by Western Blot. **Images R-6B** and **R-6C** show the increase and silencing of C3G expression in the HEL-pWpI and HEL-pLVTHM clones, respectively.

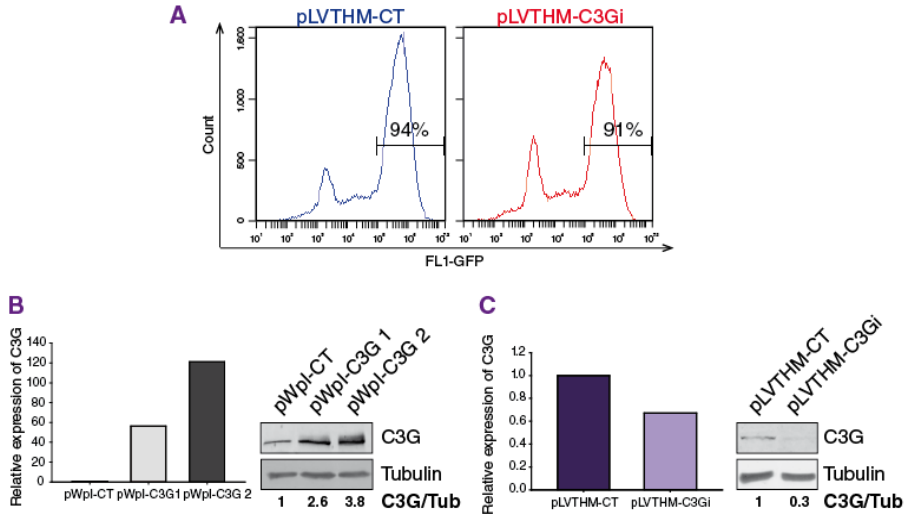

Figure R-6. Analysis of C3G expression in HEL transgenic cells. **A)** Representative plots showing the expression of GFP in HEL cells infected with lentiviral particles harboring the shRNA plasmids, pLVTHM-CT and pLVTHM-C3Gi. Numbers represent the percentage of GFP+ cells. Expression of C3G in HEL cells transfected with pWpI-CT (empty vector) and pWpI-C3G (two clones) **(B),** or containing the shRNA plasmids pLVTHM-C3Gi (two clones) and pLVTHM-CT (empty vector) **(C)** by qPCR, using oligonucleotides Ex22F-Ex24R (left histogram), and by Western Blot, using the antibody anti-C3G H-300 (right panels). GAPDH was used as housekeeping gene in the qPCR and the expression of tubulin was used as loading control in the Western Blots. Relative C3G/Tubulin ratios are shown. All values are relative to control cells.

1.2. C3G modulates the expression of megakaryocytic surface markers

As mentioned above, exposure of K562 and HEL cells to PMA induces MK differentiation. One of the changes that these cells undergo during this process is the modification of their surface markers. Megakaryocytes are identified by the increased expression of glycoproteins GPIIb (CD41) and GPIIIa (CD61), whereas cells differentiating into erythrocytes can be identified by the expression of glycophorin A (GPA) on their surface membrane. In this way, we can study the development of MK differentiation by measuring the levels of these surface markers by flow cytometry.

Based on the idea that C3G might be involved in MK differentiation, we decided to characterize the expression of megakaryocytic (CD41 and CD61) and erythroid (GPA) markers in our C3G-modified K562 and HEL clones in response to PMA.

1.2.1. Impact of C3G overexpression on the expression of CD41, CD61 and GPA on the surface. Effect of PMA

In a first approach, we measured in untreated C3G-transgenic K562 cells the expression of CD61 and GPA by semiquantitative RT-PCR. pLTR2-C3G transgenic cells showed two-fold higher CD61 levels, compared to cells transfected with pLTR2-CT, whereas GPA levels remained almost unchanged (**Figure R-7**).

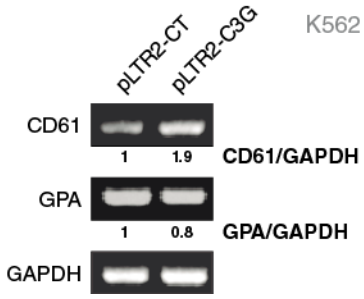

Figure R-7. Expression of megakaryocytic and erythroid markers in pLTR2-C3G K562 cells. Analysis of CD61 and GPA mRNA expression in untreated K562 clones, pLTR2-CT and pLTR2-C3G, by RT-PCR using oligonucleotides that amplify CD61 and GPA. Numbers represent values of expression, relative to control cells, pLTR2-CT. GAPDH was used as housekeeping gene.

To deeply characterize the effect of C3G in the expression of these markers, we analyzed them in two different C3G-overexpressing K562 clones: pLTR2-C3G and pLTR2-C3G/pSuper, as well as in their corresponding controls (K562 cells transfected with pLTR2 and pLTR2/pSuper respectively). Cells were cultured with PMA (20 nM) for 48h and the expression of CD41, CD61 and GPA was analyzed by flow cytometry (**Figures R-8A and R-8B**). C3G overexpression significantly increased CD41 and CD61 levels in both untreated clones, compared to their controls, although the increase in CD61 only reached significance in the pLTR2-C3G clone. On the other hand, GPA levels remained unchanged in both clones, although with a downward trend in the C3G clones. These results support the idea that C3G overexpression *per se* may induce the acquisition of MK markers.

On the other hand, PMA treatment induced a significant increase in the levels of both CD41 and CD61 markers in K562 cells expressing the empty vector, compared to untreated cells, especially in the case of CD61. These results support a role for PMA in the MK differentiation of K562 cells, as previously described (Jacquel, A. et al. 2006, Sardina, J.L. et al. 2010). However, overexpression of C3G did not further modify the increased levels of these MK markers induced by PMA, indicating that C3G could participate in the PMA-induced differentiation pathway.

It should be highlighted that, in most cases, the overexpression of C3G induced CD41 and CD61 expression levels similar to, or greater than, those induced by PMA in clones with endogenous expression of C3G (see red points in **Figure R-8B**), indicating an important contribution of C3G overexpression to this effect. On the other hand, and contrarily to the published, neither C3G overexpression nor PMA treatment produced a significant decrease in the levels of GPA (Jacquel, A. et al. 2006). This is probably due to the low levels of expression of this marker on the surface of our cells, making it very difficult to detect any additional decrease.

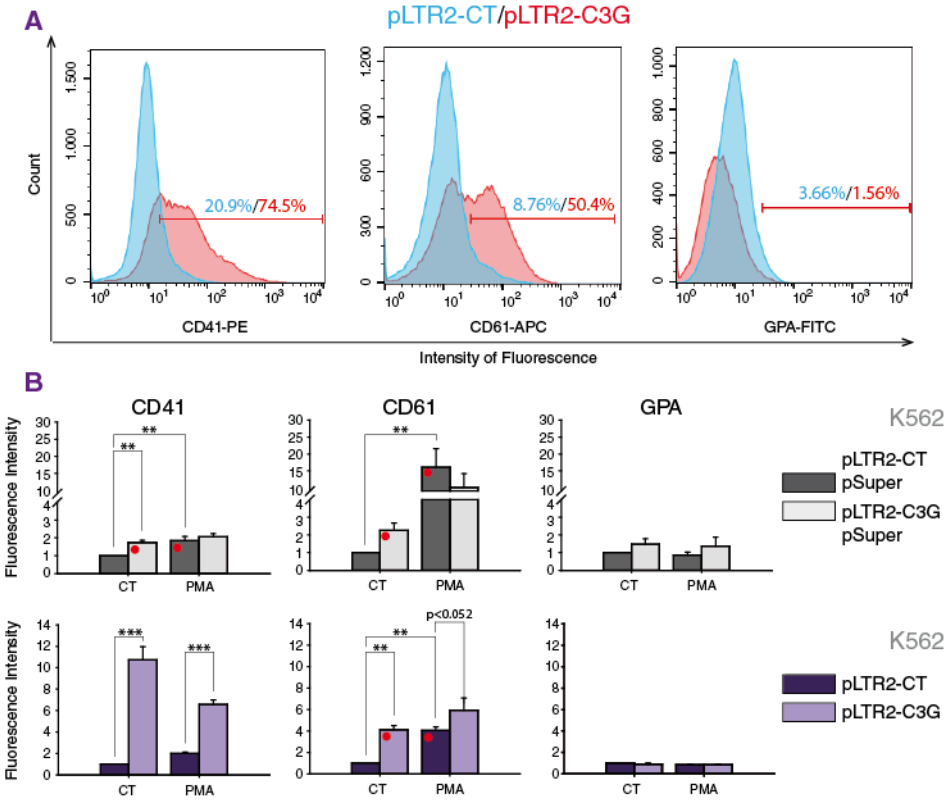

Figure R-8. Overexpression of C3G in K562 clones increases megakaryocytic markers. A) Expression of CD41, CD61 and GPA markers was analyzed by flow cytometry using specific fluorochrome-conjugated antibodies (CD41-APC, CD61-PE and GPA-FITC). Representative flow cytometry plots are shown. **B)** Histograms represent the mean ± SEM of the fluorescence intensity (relative units) of CD41, CD61 and GPA from at least 4 independent experiments with each clone, treated as indicated. 2-way ANOVA and Holm-Sidak method were done. **p<0.01, ***p<0.001.

1.2.2. Impact of C3G ablation on the expression of CD41, CD61 and GPA on the surface. Effect of PMA

To verify that the results obtained with overexpressing C3G clones were due to an increase in C3G protein levels and not to others factors, the same experiments were performed on K562 cells, in which the expression of C3G was silenced by a shRNA (pSuper-C3Gi) or eliminated using CRISPR/Cas technology. The results were confirmed in another human erythroleukemia cell line, HEL, in which the expression of C3G was also downregulated.

First, we determined the mRNA expression of CD61 and GPA by semiquantitative RT-PCR in cultures of untreated K562 cells with silenced C3G expression. As shown in **Figure R-9**, CD61 levels slightly decreased in pSuper-C3Gi cells, compared to control (pSuper-CT)

cells, whereas expression of the erythroid marker GPA clearly increased, indicating that C3G modulates the acquisition of megakaryocytic markers against erythroid.

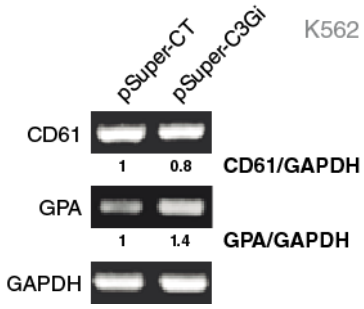

Figure R-9. Expression of megakaryocytic and erythroid markers in a K562 cell line with silenced C3G expression. **A)** Analysis of CD61 and GPA mRNA expression by RT-PCR in untreated K562 clones, pSuper-CT and pSuper-C3Gi, using oligonucleotides to amplify CD61 and GPA. Numbers represent values of expression relative to control cells. GAPDH was used as housekeeping gene.

Then, we determined by flow cytometry, whether C3G silencing or knock-out also modulates the expression of megakaryocytic markers on the cell surface. As shown in **Figures R-10A** and **R-10B**, and contrarily to the expected, C3G ablation did not modify the expression levels of CD41 and CD61, measured in untreated cells of the indicated clones. These results are in contrast to the clear increase in these markers observed in the C3G-overexpressing cells (**Figure R-8B**). The fact that the C3G silencing or knock-out does not reduce the levels of these MK markers below the control levels, but that the overexpression of C3G increases them, could indicate that C3G would contribute to the appearance of megakaryocytic markers but is not essential.

In addition, no differences were observed in the expression of CD41, CD61 and GPA between C3G silenced/knock-out cells and their controls following treatment with PMA. This suggests that the pathway activated via PMA is still induced despite the lack of C3G. It is possible that the cells compensate for the absence of C3G by the parallel activation of C3G-independent signaling pathways.

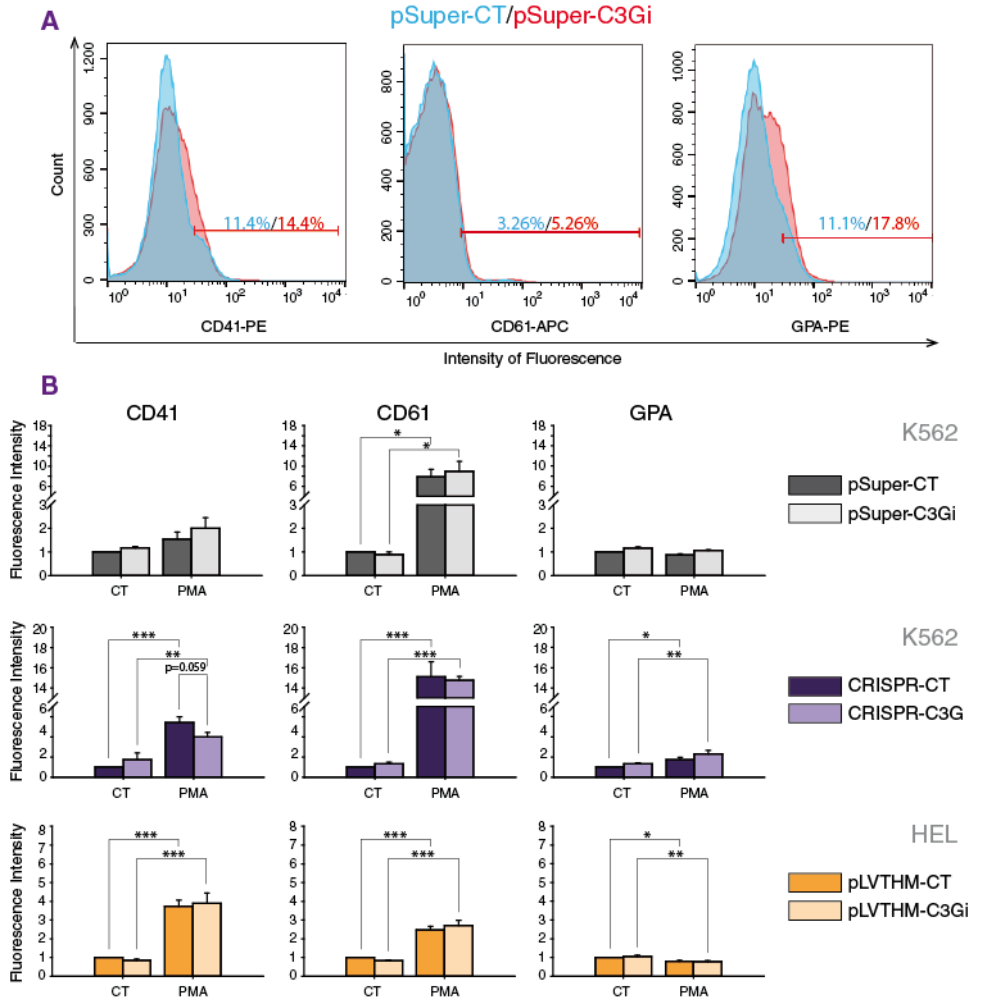

Figure R-10. Stable C3G silencing and knock-out in K562 and HEL cell lines did not modify the expression of megakaryocytic and erythroid markers. **A)** The expression of CD41, CD61 and GPA markers was analyzed by flow cytometry using specific fluorochrome-conjugated antibodies (CD41-APC, CD61-PE and GPA-PE). Representative flow cytometry plots are shown. **B)** Histograms represent the mean ± SEM of the fluorescence intensity (relative units) of CD41, CD61 and GPA from at least 4 independent experiments of each clone. 2-way ANOVA and Holm-Sidak method were done. *p<0.05, **p<0.01, ***p<0.001.

1.2.3. Effect of C3G on the erythroid differentiation induced by Imatinib

The erythroleukemia cell line K562 can be differentiated into erythroid cells by treatment with Imatinib mesylate (STI-571 or Gleevec®). STI-571 acts by blocking the Tyr-kinase activity of Bcr-Abl and it has been shown to induce the expression of erythroid markers, such as GPA and α-globin. Since the role of C3G in the expression of the erythroid marker

GPA was not clarified by the flow cytometry analysis, we studied the expression of α-globin by a different approach.

Thus, K562 cells with C3G overexpression and its control were cultured and treated with a low concentration of STI-571 (2 μM) for 24 hours and then, α-globin expression was analyzed by Western Blot (**Figure R-11**). The results show that the STI-571 treatment strongly increased α-globin levels, suggesting that STI-571 induces erythroid differentiation, in agreement with the literature (Jacquel, A. et al. 2007). In contrast, α-globin expression was virtually undetectable in the pLTR2-C3G clone. The effect of C3G on α-globin expression was reverted by STI-571, but without reaching the levels observed in pLTR2-CT cells.

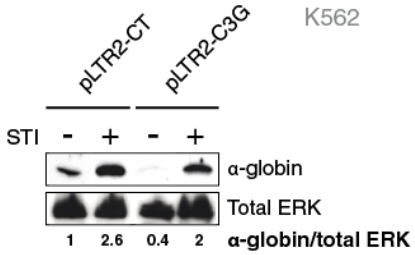

Figure R-11. Expression of the erythroid marker α-globin in C3G-overexpressing K562 clones. Expression of α-globin was analyzed by Western Blot in the indicated clones, treated or not with 2 μM STI-571. The expression of total ERK was used as loading control. Relative α-globin/ERK ratios are shown. All values are relative to control, non-treated cells.

Altogether, these results suggest a role for C3G in the regulation of the expression of differentiation markers in K562 and HEL cells, thus contributing to the commitment of these cells to the megakaryocytic lineage.

1.3. Overexpression of C3G induces MK morphological features

To analyze whether C3G is involved in the acquisition of the morphological features that characterize megakaryocytic cells, we analyzed by immunofluorescence confocal microscopy the morphology of K562 clones transfected with pLTR2-C3G/pSuper (C3G overexpression), pSuper-C3Gi (C3G silencing) and their controls. For that, cells were stained with a specific antibody for C3G (anti-C3G antiserum #1008, (Guerrero, C. et al. 1998)) and with the DNA marker, DAPI. The images shown in **Figure R-12** corroborated the increased expression of C3G in the pLTR2-C3G/pSuper clone, and the decreased expression of C3G in the pSuper-C3Gi clone, as compared to their control clones, pLTR2-CT/pSuper and pSuper-CT, respectively. Overexpression of C3G, which shows a membrane and cytoplasmic localization, induced an increase in cell size, as a result of a nuclear enlargement,

accompanied by an aberrant phenotype (see also **Figure R-1**), features that were not visible in cells with lower expression of C3G.

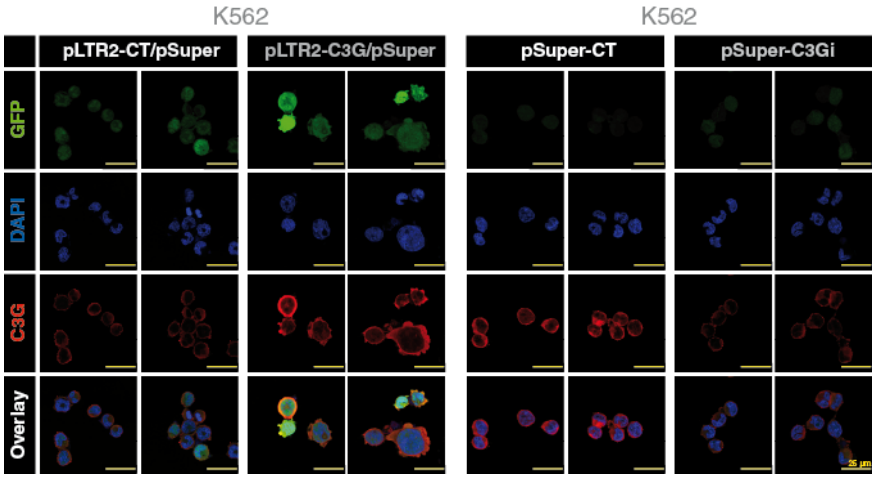

Figure R-12. The overexpression of C3G in K562 cells increased cell size an induced an aberrant phenotype. The indicated clones of K562 were plated on fibronectin-coated coverslips and stained with rabbit anti-C3G antiserum #1008 and DAPI. All clones express the GFP protein, encoded in the pSuper plasmid. Images were obtained using a Leica TCS SP5 confocal microscope. Scale bars: 25 μm.

After the observed differences in cell size between cells overexpressing C3G and control cells, we analyzed other morphological features using May-Grünwald-Giemsa staining. This staining allows to identify the structural changes associated with the MK differentiation, consisting of nuclear polylobulation, the marked expansion of the cytoplasm and the appearance of membranous vesicles.

C3G-overexpressing cells (pLTR2-C3G/pSuper) and their controls (pLTR2-CT/pSuper) were cultured in the presence of 20 nM PMA for 72h. Untreated control cells showed a round morphology, small size (approximately 4 μm), rounded nucleus at the center of the cell and a small cytoplasmic region, reflecting an undifferentiated morphology (**Figure R-13**). In the PMA-treated control cells we could distinguish 4 different morphologies: **i)** small rounded cells (the most abundant) similar to untreated control cells; **ii)** larger rounded cells (~7 μm) with abundant cytoplasm, large nucleus at the periphery and pseudopod-like structures in some of them; **iii)** fusiform cells with a large nucleus and abundant cytoplasm; **iv)** cells with a big nucleus with condensed chromatin and with microvesicles in the cytoplasm.

As expected, untreated C3G-overexpressing cells showed 3 of the phenotypes described in the PMA-treated control cells: **i)** small rounded cells; **ii)** large polynucleated cells (~10 μm) with some dense nucleoli and some cells with pseudopod-like structures; and **iii)**

fusiform cells. Finally, PMA-treated C3G-overexpressing cells showed the 4 described morphologies, with a smaller proportion of small rounded cells.

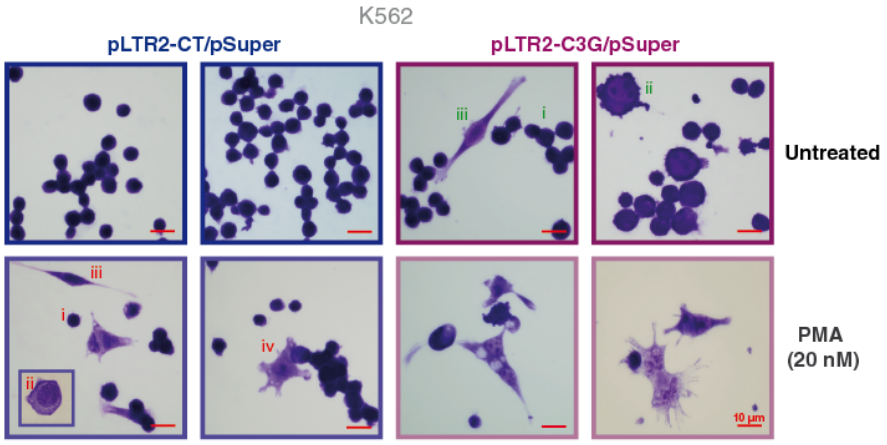

Figure R-13. K562 cells stably overexpressing C3G show megakaryocytic morphological features. May-Grünwald-Giemsa staining of the indicated K562 clones untreated or treated with 20 nM PMA for 72h. Scale bars: 10 µm.

These results indicate that, in K562 cells, the overexpression of C3G mimics PMA in the induction of the morphological features that characterize megakaryocytes.

1.4. Analysis of ploidy in K562 and HEL cells

At the end of the proliferation phase, megakaryocyte precursors exit the normal cell cycle and undergo endomitosis. These progenitors become polyploid through repeated cycles of DNA replication without karyokinesis and cytokinesis, resulting in cells with a unique polylobulated nucleus with a DNA content up to 128n. In order to establish the role of C3G in this phase of the differentiation of megakaryocytic progenitors, leading to polyploidy, we determined the ploidy status of our K562 and HEL clones, induced by PMA. For this purpose, our C3G-transgenic, or knock-down/knock-out, K562 and HEL clones were cultured in the presence of 20 nM PMA for 10 days. After fixation and permeabilization, the DNA was stained with Propidium Iodide (PI) and the DNA content measured by flow cytometry. Before performing the analysis, it is necessary to exclude cell doublets (pulse area *vs* pulse height) because PI staining increases cell aggregation, leading to false positives. **Figure M-10** (Materials & Methods), shows the DNA content distribution of a typical histogram plot (Cell count *vs* PI intensity), which is composed of different peaks, where each peak represents a population of cells having equal DNA content. The first peak corresponds to the population of diploid cells, the seconds correspond to tetraploid cells, and so on up to the seventh peak (128n).

1.4.1. Effect of decreased C3G expression on ploidy

First, we analyzed the ploidy status of K562 cells, in which the expression of C3G was depleted by the CRISPR/Cas9 system.

After the identification of 2n and 4n peaks, the percentage of cells with a DNA content equal to or greater than 8n (polyploidy) was estimated. As shown in **Figure R-14**, the percentage of polyploid cells decreased in C3G KO cells, compared to control cells. This was accompanied by an increase in the percentage of diploid cells.

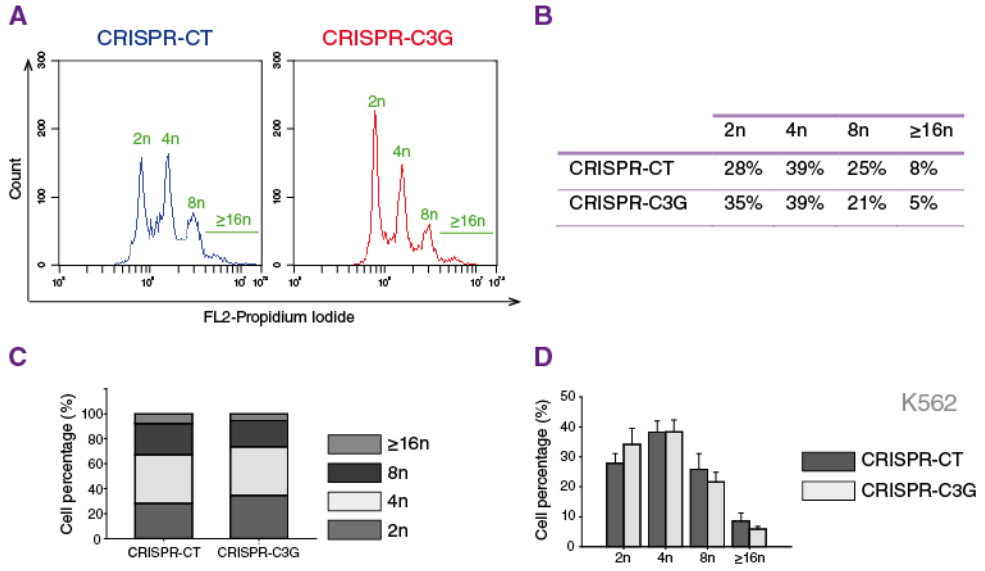

	2n	4n	8n	≥16n
CRISPR-CT	28%	39%	25%	8%
CRISPR-C3G	35%	39%	21%	5%

Figure R-14. C3G knock-out in K562 cells decreases polyploidization. The polyploidization state was identified by Propidium Iodide staining after 10 days of differentiation with 20 nM PMA. **A)** Two representative flow cytometry plots of ploidy distribution are shown. We identified 4 different populations: 2n, 4n, 8n and cells with a DNA content of 16n and higher (≥16n). **B)** Table indicating the percentage of cells of the different clones corresponding to each population. **C)** Stacked bar histograms represent the mean of the percentage of cells of each genotype belonging to the different ploidy populations (2n, 4n, 8n and ≥16n). **D)** Histograms represent the mean ± SEM of the quantification of the percentage of individual ploidy population of CRISPR-CT and CRISPR-C3G. Data from 3 independent experiments of each genotype are shown. Data were analyzed using the Mann Whitney U test, but no significant differences were observed between CRISPR-C3G and CRISPR-CT.

1.4.2. Effect of C3G overexpression on ploidy

To corroborate the above results, we performed a similar study in clones with C3G overexpression. Results, using pLTR2/pSuper (K562) and pWpI (HEL) clones, showed that the percentage of polyploid cells was higher in the C3G-overexpressing cells, in both cell lines, as compared to their controls (**Figure R-15**). As expected, this increase in the number of polyploid cells was accompanied, in general, by a decrease in diploid cells. Although only one experiment has been performed with each clone (one pLTR2-C3G and two pWpI-C3G), these

results are in concordance with those performed with the C3G KO clones (**Figure R-14**). Therefore, our results suggest a role for C3G in the modulation of endomitosis in K562 and HEL cells during MK differentiation.

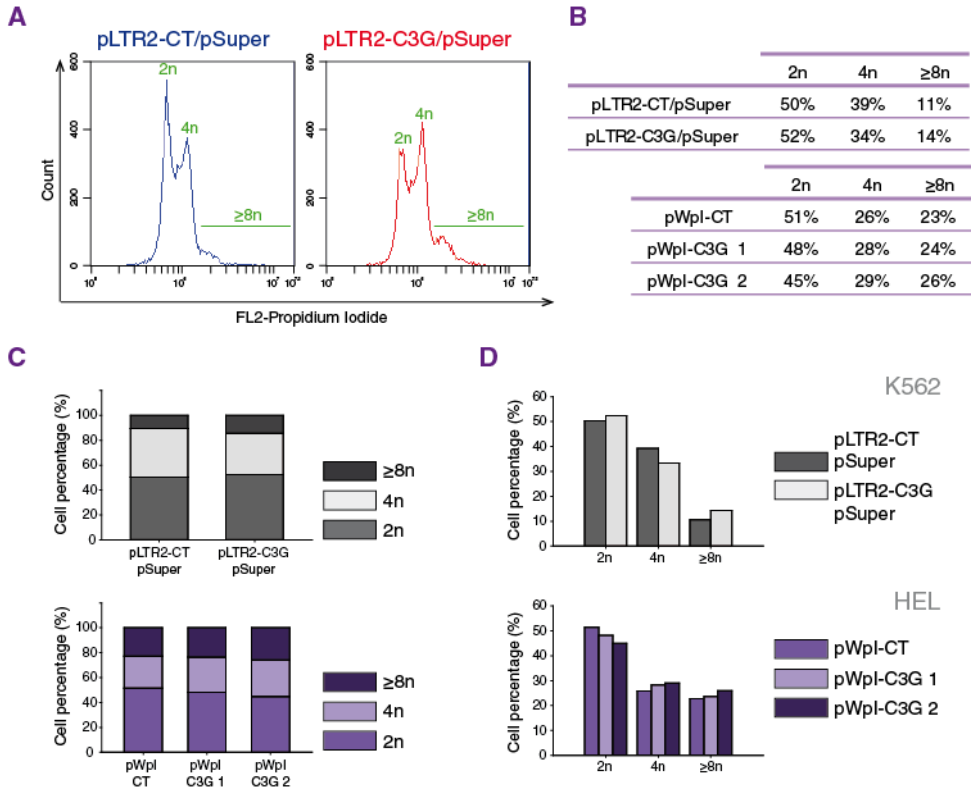

	2n	4n	≥8n
pLTR2-CT/pSuper	50%	39%	11%
pLTR2-C3G/pSuper	52%	34%	14%

	2n	4n	≥8n
pWpI-CT	51%	26%	23%
pWpI-C3G 1	48%	28%	24%
pWpI-C3G 2	45%	29%	26%

Figure R-15. Overexpression of C3G in K562 and HEL increases polyploidization. The polyploidization state was identified by Propidium Iodide staining after 10 days of differentiation with 20 nM PMA. **A)** Two representative flow cytometry plots of ploidy distribution are shown. We identified 3 different populations in K562 and HEL clones: diploid (2n), tetraploid (4n) and polyploidy cells (with a DNA content ≥8n). **B)** Table indicating the percentage of cells of the different clones corresponding to each population. **C)** Stacked bar histograms represent the percentage of cells of each genotype belonging to the different ploidy populations (2n, 4n and ≥8n) of pLTR2/pSuper (top panel) and pWpI clones (bottom panel). **D)** Histograms represent the quantification of the percentage of individual ploidy population of pLTR2/pSuper (top panel) and pWpI clones (bottom panel). An experiment of each genotype is shown.

1.4.3. Effect of C3G on cell cycle arrest

As mentioned in the Introduction, the polyploidization of early MK progenitors requires cell cycle arrest and entry into the endomitosis cycle (Baccini, V. et al. 2001, Trakala, M. et al. 2014). $p21^{Waf\text{-}1/Cip\text{-}1}$ (p21) is a potent inhibitor of cyclin-dependent kinases (CDKs) involved in cell cycle arrest of various cell types. It has been shown to be highly expressed in mature megakaryocytes, suggesting an important role of this protein in the proliferative arrest of cells during MK differentiation (Matsumura, I. et al. 1997). However, p21 is not essential for the

acquisition of the polyploid profile, since p21 knock-out does not rescue the mitotic arrest during differentiation. Nonetheless, the analysis of its expression is commonly used as a marker of mitotic arrest (Baccini, V. et al. 2001, Besancenot, R. et al. 2010). Additionally, it has been shown that C3G overexpression in neuroblastoma cell line induces the expression of p21 through activation of the ERK signaling pathway (Radha, V. et al. 2008). On the other hand, our data suggest that C3G might be involved in the regulation of endomitosis in K562 cells, triggered by PMA.

With all these considerations, we analyzed the expression of p21 in our K562 clones with C3G overexpression (pLTR2-C3G/pSuper) or downregulation (CRISPR-C3G). Cells were differentiated with 20 nM PMA for 3 days and harvested at the indicated time points to determine the expression of p21 by Western Blot. **Figure R-16** shows a clear increase in p21 expression throughout the treatment with PMA, that was maximum between 6 and 24h of stimulation. Interestingly, K562 cells overexpressing C3G showed a ten-fold increase in p21 expression under non-stimulation conditions, as compared to control cells. In addition, these pLTR2-C3G/pSuper cells maintained sustained levels of p21 throughout the time course. This result indicates that C3G could modulate the expression of p21, thus contributing to the arrest of cell cycle. In contrast, CRISPR-C3G expression hardly altered the levels of p21 throughout the time course, indicating that this function of C3G can be countervailed by other proteins.

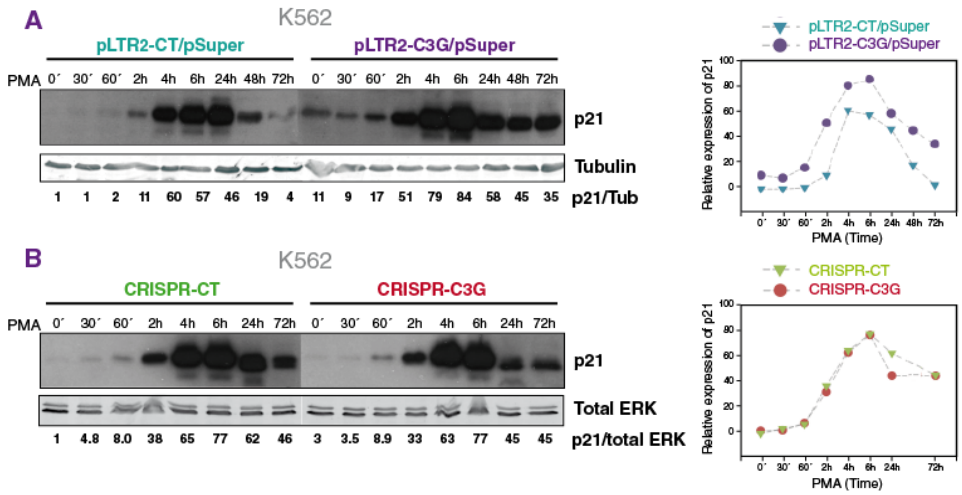

Figure R-16. Effect of C3G on p21 expression in K562 cells. Time course Western Blot analysis of the expression of p21 in K562 cells transfected with pLTR2/pSuper plasmids **(A)** or CRISPR plasmids **(B)** cultured with PMA (20 nM). Left panels: representative images of Western Blot. The numbers indicate expression of p21, relativized against tubulin (p21/Tub) or ERK (p21/ERK), which were used as loading controls. All values are relative to control, non-treated cells. Right panels: Line/scatter plots of the relativized p21 expression.

1.5. Determination of the C3G domain implicated in MK differentiation

The above results strongly suggest a role for C3G in some of the processes that occur during MK differentiation. C3G can perform functions dependent on its catalytic, GEF domain, but C3G actions often involve protein-protein interactions through its proline-rich sequences, or other N-terminal sequences, which is independent of its GEF function (Guerrero, C. et al. 1998, Hogan, C. et al. 2004). Therefore, we aimed at investigating which of the C3G domains were involved in the MK differentiation process.

K562 cells were transfected by electroporation with different C3G deletion mutants, cloned in pLTR2 (**Figure R-17A)** and transfected clones were selected by culturing in Killer Hat media. Expression of the mutants was checked by Western Blot using anti-C3G H-300 (against the N-terminus) and anti-C3G C-19 (against the C-terminus) antibodies (**Figure R-17B).** Therefore, C3G H-300 identified full-length C3G, ΔN, SH3b and the ΔCat mutant, whereas C3G C-19 detected full-length C3G, ΔN and RemCat mutants.

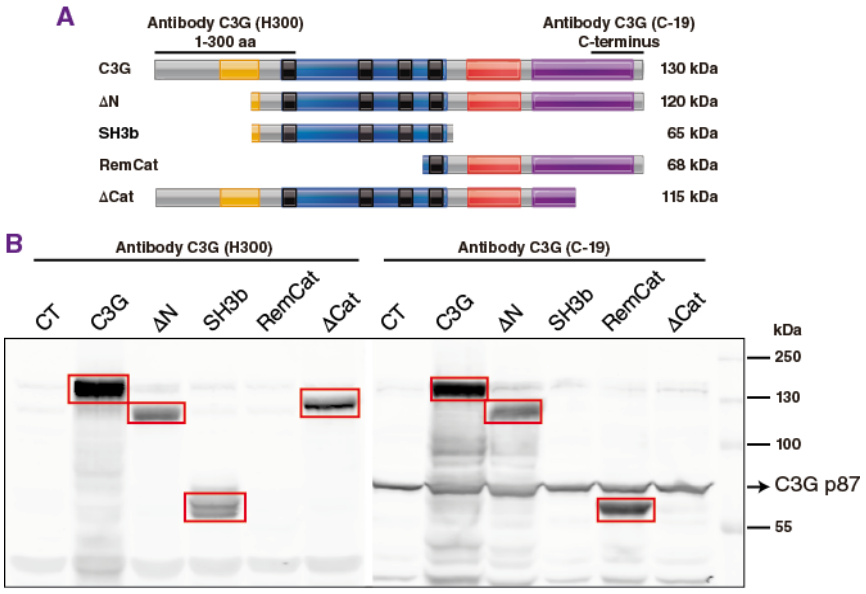

Figure R-17. Analysis of C3G expression in K562 transgenic cells. A) Structure of full-length C3G and the C3G mutants expressed in K562 cells, indicating its domains, its size (kDa) and the regions recognized by C3G H-300 and C3G C-19 antibodies (See **Figure I-1** of Introduction for description). **B)** Representative Western Blot using C3G H-300 (left panel) and C3G C-19 (right panel) antibodies, showing the expression of the different mutants (red boxes). C-19 antibody also recognizes endogenous C3G p87 isoform, abundantly expressed in K562 cells as described (Gutierrez-Berzal, J. et al. 2006).

To deeply characterize what is the domain of C3G involved in the acquisition of the megakaryocytic markers, C3G-mutant clones were cultured with PMA (20 nM) for 48h and the

expression of CD41, CD61 and GPA was analyzed by flow cytometry. Results in **Figure R-18** show that full-length C3G-overexpression increased CD41 levels, as previously shown. In contrast, all C3G deletion mutants reduced the expression of this marker to control levels or even below control, as in the case of the ΔN mutant. A similar tendency was observed when the expression of CD61 was analyzed, i.e., all deletion mutants induced CD61 levels similar to those of control, with the exception of the RemCat mutant, which induced CD61 levels similar to the full-length clone. These clones showed the same behavior under non-stimulation conditions, although in this case the differences were more difficult to appreciate. Our data indicate a relevant role for the catalytic (GEF) and N-terminal domains of C3G in regulating MK differentiation, although other domains may also play a role.

Additionally, the Anova analysis indicated that the CD41 expression results obtained with the ΔN mutant were significantly different, with respect to the other clones, independently of the treatment (p=0.017 ΔN mutant *vs* CT).

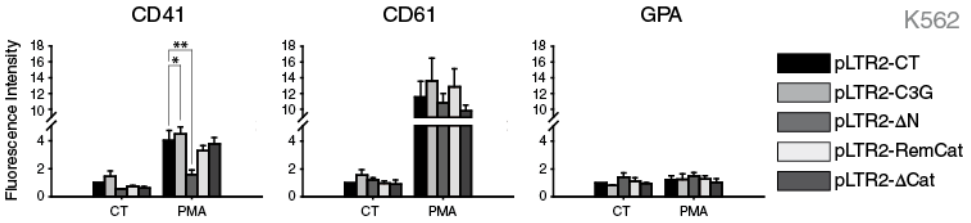

Figure R-18. Overexpression of C3G mutants in K562 cells affect the expression of megakaryocytic markers. K562 clones expressing the indicated C3G-mutants were maintained with PMA (20 nM) for 48h. Expression of the markers was analyzed by flow cytometry using specific fluorochrome-conjugated antibodies (CD41-APC, CD61-PE and GPA-FITC). Histograms represent the mean ± SEM of the fluorescence intensity (relative units) of CD41, CD61 and GPA from at least 3 independent experiments of each clone. 2-way ANOVA and Holm-Sidak method were done. *p<0.05, **p<0.01.

To further clarify which domain of C3G is involved in the regulation of the expression of megakaryocytic and erythroid markers, we analyzed the expression of α-globin in K562 cell, overexpressing different C3G mutants, that were untreated or treated with 2 μM STI-571 for 24 hours. Untreated K562 cells transfected with the empty vector (pLTR2-CT) showed high levels of α-globin (**Figure R-19**), in agreement with the erythroid nature of these cells. On the other hand, overexpression of full-length C3G and mutants ΔN and SH3b, greatly reduced α-globin expression. In contrast, expression of a mutant lacking the catalytic domain (ΔCat) did not affect the levels of α-globin. As expected, treatment with STI-571 further increased α-globin expression in control and ΔCat-expressing cells, and partially reverted the inhibitory effect of the other C3G mutants. These results suggest that the catalytic function of C3G could prevent the acquisition of erythroid markers under stimulation with Imatinib, or stimulate their

loss during MK differentiation. Results in **Figure R-19** also uncovered an essential role of the SH3b domain in the regulation of α-globin expression, probably acting as a dominant negative mutant, sequestering other regulators through protein-protein interactions.

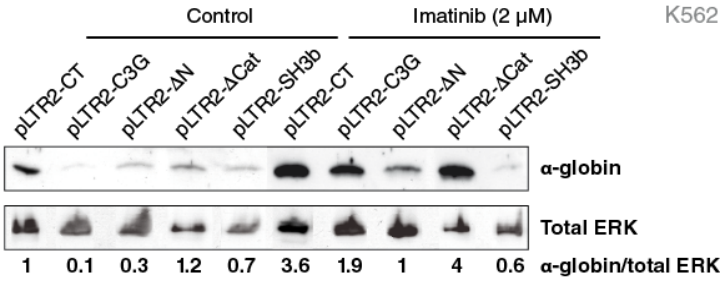

Figure R-19. Overexpression of C3G mutants in K562 cells affect the expression of α-globin. Analysis of α-globin by Western Blot in K562 cells overexpressing full-length C3G, ΔN, RemCat, ΔCat and SH3b mutants, untreated or treated with STI-571 for 24 hours. Total ERK was used as loading control. Relative α-globin/ERK ratios are shown. All values are relative to non-treated cells expressing the empty vector (pLTR2-CT).

Altogether these results indicate that C3G would modulate the expression of megakaryocytic and erythroid markers in K562 through its catalytic function, although other domains, such as the N-terminal region or the SH3b domain, could also contribute, probably through the modulation of the catalytic activity of C3G or by establishing interactions with other proteins.

1.6. Involvement of C3G in the megakaryocytic signaling pathways induced by PMA

Once we have demonstrated the involvement of C3G in the acquisition of megakaryocytic features in K562 and HEL cell lines treated with PMA, such as the expression of megakaryocyte markers and the increase in DNA content, we wanted to analyze the putative participation of C3G in the PMA-triggered signaling pathways involved in MK differentiation.

As previously commented, our model of study consisted in the stimulation of MK differentiation by PMA in K562 and HEL cells, whose phenotypic features classify them as erythroid cells. Several signaling pathways are involved in this process. It has been demonstrated that activation of the MEK/ERK1/2 transduction cascade is required for the MK differentiation, whereas the p38 MAPK signaling pathway contribute to the induction of erythroid differentiation (Jacquel, A. et al. 2006, Conde, I. et al. 2010). Based on this idea, we attempted to elucidate the signaling pathways in which C3G plays a role.

Since activation of C3G by phosphorylation on tyrosine 504 is required to carry out some of its functions (Ichiba, T. et al. 1999), we analyzed the phosphorylation status of C3G, in K562 and HEL cells treated with 20 nM PMA at several time points (10, 30 and 60 minutes), using a specific anti-phospho-Tyr 504 antibody. **Figure R-20** shows a gradual increase in the amount of the Tyr 504 phosphorylated form of C3G over time in both cell lines, indicating that activation of C3G is induced upon treatment with PMA.

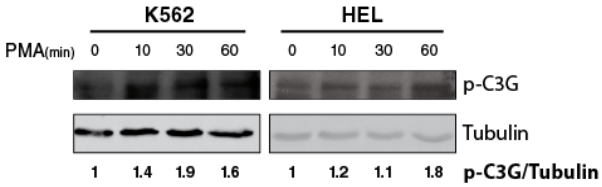

Figure R-20. PMA treatment induced C3G phosphorylation in K562 and HEL cells. Time course Western Blot analysis of phospho-C3G (p-C3G) expression in non-transfected K562 and HEL cells treated with 20 nM PMA for 10, 30 and 60 minutes, using a polyclonal antibody against phospho-Tyr-504. The expression of tubulin was used as a loading control. Relative p-C3G/Tubulin ratios are shown. All values are relative to control, non-treated cells.

1.6.1. Activation of Rap1 by C3G during PMA-induced MK differentiation

As mentioned in the Introduction, Rap1 is an ubiquitous Ras-related GTPase particularly abundant in blood platelets, which plays important functions in cell adhesion through the activation of integrins. In addition, it has been suggested that Rap1 may be involved in megakaryopoiesis and platelet production, as its levels increases during MKs differentiation (Balduini, A. et al. 2004). Activation of Rap1 by the PMA-PKC pathway has been described in murine myeloid leukemia cells (Dupuy, A.J. et al. 2001) and in platelets (Gutierrez-Herrero, S. et al. 2012). Taking into account that C3G is one of the main Rap1-GEFs and that C3G is phosphorylated during PMA-induced MK differentiation (see **Figure R-20**), we wanted to study whether PMA induces Rap1 activation via C3G. For that, we performed a Rap1 activity assay using our K562 clones expressing different C3G deletion mutants (**Figure R-17**).

Lysates from cells stimulated with 20 nM PMA for 5 min were incubated with RalGDS-RBD protein (RalGDS domain that specifically binds Rap1-GTP), fused to GST, as described in Materials & Methods. PMA treatment increased the activation of Rap1 in pLTR2-CT and in all C3G-mutants, compared to their respective untreated clones, with the exception of the RemCat mutant, which *per se*, was able to induce maximum levels of Rap1-GTP (**Figure R-21**). In addition, Rap1-GTP levels were increased in untreated clones expressing full-length C3G, as well as in mutants SH3b, ΔN and, especially RemCat, as compared to cell transfected with the empty vector. In contrast, and, as expected, Rap1 was poorly active in cells

expressing a C3G mutant lacking the GEF domain (ΔCat). The largest increase in Rap1-GTP levels induced by the expression of the RemCat mutant, as compared to full-length C3G, is in agreement with an inhibitory role played by the N-terminal domain of C3G on its catalytic activity (Ichiba, T. et al. 1999).

These results confirmed that C3G is involved in PMA-induced Rap1 activation, although we can not exclude the possibility that other Rap1 GEFs may contribute. Surprisingly, cells overexpressing the SH3b domain showed increased levels of Rap1-GTP, relative to control cells. One possibility is that this domain may act by sequestering negative regulators of the C3G-Rap1 pathway, through protein-protein interactions. These results, together with those in **Figure R-19**, are in favor of a role for the SH3b domain of C3G in the PMA pathway the regulates the expression of megakaryocytic and erythroid markers in K562 cells.

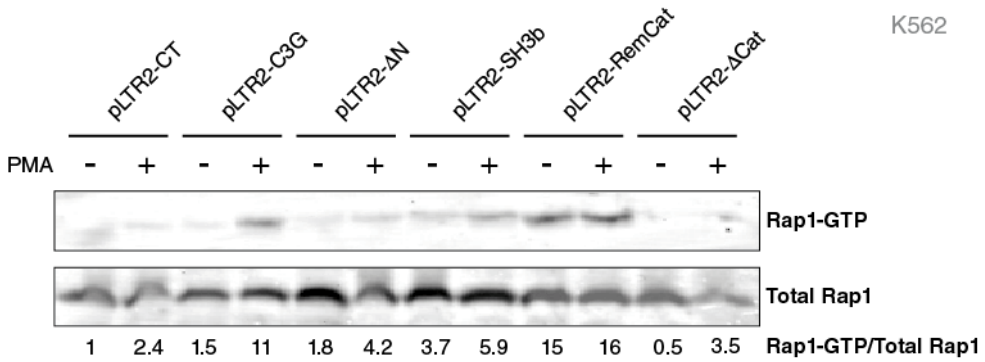

Figure R-21. Activation of Rap1 in K562 cells expressing C3G mutants. Representative pull-down assay to detect Rap1-GTP after treatment with 20 nM PMA for 5 min. Detection of total Rap1 in cell lysates was used as loading control. Relative Rap1-GTP/total Rap1 ratios are shown. All values are relative to EGF-treated cells (positive control of Rap1 activation).

To complement the data obtained from the Rap1 pull-down assay, we performed a Rap1 activity assay on intact cells by immunofluorescence confocal microscopy, as described (Balduini, A. et al. 2004). For that, C3G-overexpressing K562 cells and its control (pLTR2/pSuper clones) were stimulated with 20 nM PMA for 2 minutes. Next, the expression and subcellular localization of Rap1-GTP was examined by confocal microscopy using purified GST-RalGDS-RBD protein, in combination with anti-GST antibodies, as described in Materials & Methods. Total Rap1 was detected with anti-Rap1 antibodies. This experiment was complemented by several negative controls shown in **Figures R-22B** and **R-23B**.

Figure R-22 shows a cytoplasmic distribution of total Rap1 in both K562 clones, whereas active Rap1 was located mainly in the plasma membrane, indicating that following

activation Rap1 is translocated from the cytosol to membranous compartments. In addition, cells overexpressing C3G showed increased levels of Rap1-GTP, accompanied by increased levels of total Rap1, compared to control cells.

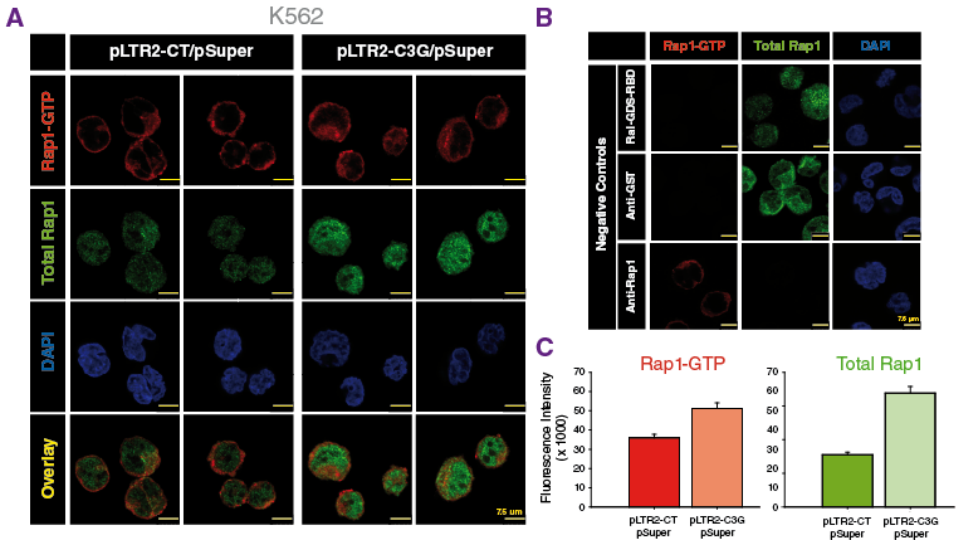

Figure R-22. Detection of Rap1-GTP and total Rap1 by immunofluorescence confocal microscopy in K562 cells with C3G overexpression. **A)** K562 cells were cultured on coverslip and starved o/n. Then cells were fixed, permeabilized and incubated with: anti-Rap1/anti-rabbit Cy3 antibodies (green), to mark total Rap1; purified GST-RalGDS-RBD and anti-GST/anti-mouse Cy5 antibodies (red) to detect Rap1-GTP; DAPI (Blue) to detect the nucleus. The overlay layers are made without DAPI channel. **B)** Negative controls of Rap1 activity assay by immunofluorescence. These controls were analyzed in parallel to the assay to interpret in a proper manner our microscopy images. The Ral-GDS-RBD negative control was made without the Ral-GDS-RBD purified protein; anti-GST and anti-Rap1 negative controls were made without primary antibodies anti-GST or anti-Rap1, respectively. **C)** Quantification of fluorescence intensity (relative values) of Rap1-GTP (left panel) and total Rap1 (right panel) in pLTR2-CT/pSuper and pLTR2-C3G/pSuper clones. Scale bars: 7.5 µm.

Next we wanted to analyze whether C3G overexpression modifies the activation of Rap1 induced by PMA, and whether the phosphorylation of C3G is involved. For that, starved pLTR2/pSuper clones were stimulated with PMA at different time points and the levels of Rap1-GTP, total Rap1 and phospho-C3G analyzed by immunofluorescence confocal microscopy as above.

Similarly to the results of the pull-down assay (**Figure R-21**), treatment with PMA induced an increase in the Rap1-GTP levels that was maximal between 2 and 5 min of stimulation and decreased after 10 min (**Figure R-23**), indicating that PMA promotes a transient activation of Rap1, as described by other authors (Franke, B. et al. 2000). In control cells, phospho-C3G levels clearly increased after 2 min of treatment with PMA, validating results shown in **Figure R-20**. On the other hand, C3G-overexpressing cells showed

increased basal levels of phospho-C3G that peaked at 2 min of PMA stimulation and lasted throughout the time course. Moreover, overexpression of C3G induced a more sustained Rap1 activation, in correlation with the sustained C3G phosphorylation. Overall, these results indicate that overexpression of C3G increases PMA-induced Rap1 activation and that phosphorylation of C3G is important in this effect. However, we can not exclude the participation of other Rap1GEFs in the activation of Rap1 induced by PMA.

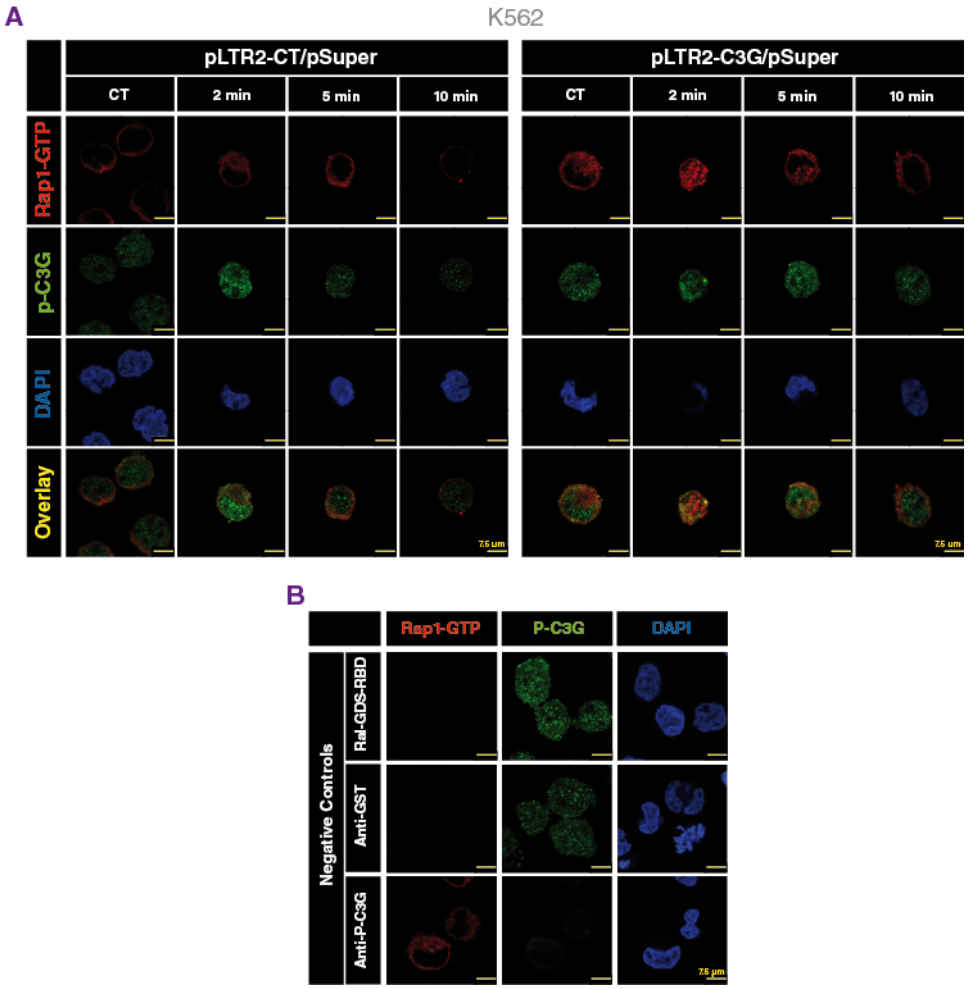

Figure R-23. Effect of C3G on PMA-induced Rap1 activation, using immunofluorescence confocal microscopy. **A)** K562 cells were cultured on coverslip and starved o/n. Then cells were treated with 20 nM PMA for 2, 5 and 10 min, fixed, permeabilized and incubated with: anti-phospho-C3G/anti-rabbit Cy3 antibodies (green); purified GST-RalGDS-RBD and anti-GST/anti-mouse Cy5 antibodies (red) to detect the Rap1-GTP, and DAPI (blue) to detect the nucleus. The overlay images are made without DAPI channel. **B)** Negative controls of Rap1 activity assay by immunofluorescence. The staining of Ral-GDS-RBD negative control was made without the Ral-GDS-RBD purified protein, anti-GST and anti-p-C3G negative controls were made without the corresponding primary antibodies. Scale bars: 7.5 µm

1.6.2. Role of PKC in the effect of C3G on MK differentiation

As previously mentioned, PMA induces MK differentiation in K562 and HEL cells through activation of protein kinase C (PKC). Bisindolylmaleimide (Bis), a highly selective inhibitor of all PKC isoforms, has been used to demonstrate the role of this protein in PMA-induced MK differentiation in K562 and HEL cells, as it completely inhibits PMA responses (Hong, Y. et al. 1996).

Results in **Figure R-8** corroborated that C3G is able to induce the appearance of megakaryocytic features *per se* without external stimulation, such as PMA. However, as demonstrated in **Figures R-20** and **R-23**, PMA activates C3G, which suggests a putative role of C3G in PMA-triggered pathways. In addition, we have demonstrated the involvement of C3G in the PKC-Rap1 pathway induced by thrombin in platelets (Gutierrez-Herrero, S. et al. 2012). Therefore, the participation of C3G in the acquisition of megakaryocytic features induced by PMA was further investigated by analyzing, in our K562 clones, the expression of megakaryocytic and erythroid markers, in the presence or absence of Bis (1 μM).

As shown in **Figure R-24,** Bis completely abrogated the increase in CD61 expression induced by PMA in the pLTR2-CT/pSuper clone, and partially the increase in CD41, demonstrating the inhibitory effect of Bis on the effects of PMA. However, expression of CD61 and, especially that of CD41 were poorly affected by this inhibitor in cells overexpressing C3G. This suggests the participation of C3G downstream of PKC in the PMA-triggered pathway. Additionally, Bis induced a slight increase in GPA expression, mainly in cells with C3G overexpression, indicating a role for C3G in the negative regulatory effect of PMA-PKC on the expression of this marker.

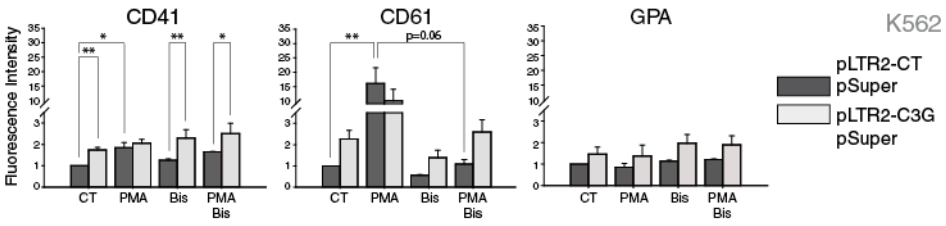

Figure R-24. Effect of the PKC inhibition on the expression of CD41, CD61 and GPA markers during PMA-induced MK differentiation. K562 cells were treated with 20 nM PMA for 48 hours in the presence or absence of 1 μM Bis. Histograms represent the mean ± SEM of the fluorescence intensity (relative units) of CD41, CD61 and GPA from at least 2 independent experiments with each clone, treated as indicated. 2-way ANOVA and Bonferroni t-test were done. *p<0.05, **p<0.01.

1.6.3. Role of ERK signaling pathway in the effect of C3G on MK differentiation

The role of the Raf/MEK/ERK signaling pathway, downstream of PKC in megakaryocytic differentiation, has been extensively studied and is considered one of the most important pathways that regulate this process. ERK1/2 (also called MAPK p44 and p42, respectively) is required for the expression of megakaryocyte surface markers but is not involved in cell endomitosis, suggesting that the ERK1/2 signaling pathway acts primarily at the onset of the megakaryocytic differentiation process (Conde, I. et al. 2010). In addition, it had been reported that inhibition of this pathway plays a role in the signal transduction mechanisms leading to erythroid differentiation (Jacquel, A. et al. 2006).

Based on the above, we wanted to study whether C3G is involved in the regulation of MK differentiation through the modulation of ERK1/2 activation. To do so, we performed a series of experiments in the presence of U0126 (U0), a selective inhibitor of MAP kinase kinases (MEK1 and MEK2), which acts by preventing the activation of ERK1 and ERK2.

Firstly, we analyzed, in our K562 clones transfected with the C3G constructs, the induction of ERK1/2 phosphorylation at short times or during several days of PMA treatment. Overexpression of C3G increased by two-fold the basal levels of phospho-ERK1/2 (**Figure R-25A**), indicating a role for C3G in this pathway. As expected, PMA stimulation increased ERK1/2 phosphorylation in both, control and pLTR2-C3G/pSuper cells, with no differences between clones being observed at short times (**Figure R-25A, left panel).** In addition, C3G depletion barely decreased ERK phosphorylation at short times of PMA stimulation (**Figure R-25A, right panel)**. On the other hand, while activation of ERK1/2 reached a peak in control cells after 24h of PMA treatment and then decreased, it was maintained for, at least, 72h in cells overexpressing C3G (**Figure R-25B, left panel)**. This effect was not observed in the absence of C3G (**Figure R-25B, right panel)**, indicating that C3G is required for the sustained activation of ERK1/2 induced by PMA.

Since Rap1-mediated sustained activation of ERK1/2 has been linked to cell differentiation in PC12 cells and other cellular models (York, R.D. et al. 1998, Conde, I. et al. 2010, Takahashi, M. et al. 2017), our results are in favor of a role for C3G-Rap1 in megakaryocytic differentiation through the sustained activation of the ERK1/2 pathway.

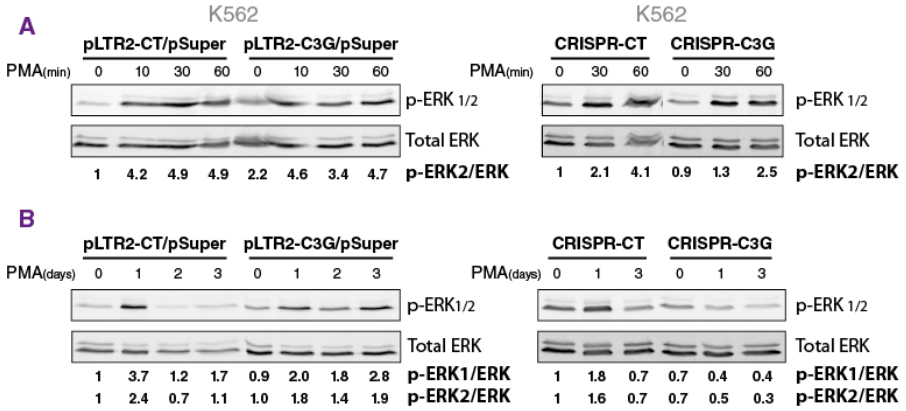

Figure R-25. Analysis of p-ERK1/2 levels in C3G transfected K562 cells at different times of PMA stimulation. Time course of p-ERK1/2, analyzed by Western Blot, in C3G-overexpressing and C3G knock-out clones treated with 20 nM PMA for 10, 30 and 60 min **(A)** or 1, 2 and 3 days **(B)** using anti-phospho-ERK1/2 antibodies. The expression of total ERK was used as a loading control. Relative p-ERK/ERK ratios are shown. All values are relative to control, non-treated cells.

Next, we analyzed the expression of CD61, CD41 and GPA markers in the same clones after treatment with PMA for 48h, in the presence or absence of 10 μM U0126 (**Figure R-26A**). Unexpectedly, the addition of U0 had no effect on the expression of the PMA-induced megakaryocytic markers in K562 cells, either in control cells or in C3G-overexpressing cells. However, GPA levels increased slightly upon inhibition of the MEK-ERK1/2 signaling pathway, mainly in C3G overexpressing cells, indicating that this pathway plays a negative role in the acquisition of erythroid markers in K562, in agreement with the literature (Jacquel, A. et al. 2006), and that C3G is involved. Pretreatment with U0 completely abolished basal ERK1/2 phosphorylation in both, control and C3G-overexpresing clones, and partially inhibited PMA-induced ERK1/2 phosphorylation (**Figure R-26B**). This indicates that the results in **Figure R-26A** were not due to poor inhibitor functioning.

The involvement of C3G in the PMA pathway downstream of PKC was further corroborated by the analysis of the activation of ERK1/2 in our C3G-overexpressing clones treated with PMA and Bis. Results in **Figure R-26B** showed that inhibition of PKC suppresses the phosphorylation of ERK1/2 induced by PMA in control cells. In contrast, Bis hardly affected PMA-induced ERK1/2 phosphorylation in pLTR2-C3G/pSuper cells, indicating that C3G is capable to activate ERK1/2 independently of PMA-PKC.

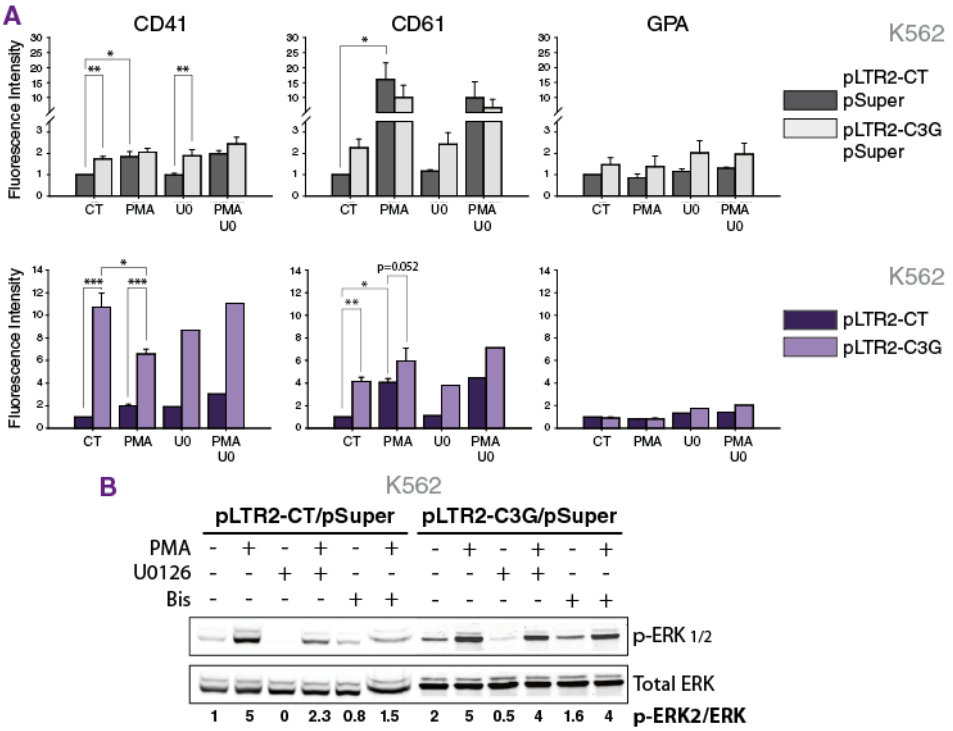

Figure R-26. Effect of the ERK1/2 inhibition on the expression of CD41, CD61 and GPA induced by PMA in C3G-overexpressing K562 clones. **A)** Histograms represent the mean ± SEM of the fluorescence intensity (relative units) of CD41, CD61 and GPA from at least 2 independent experiments with each clone, treated as indicated. 2-way ANOVA and Bonferroni t-test were done. *p<0.05, **p<0.01. **B)** Analysis of phospho-ERK1/2 by Western Blot in pLTR2/pSuper K562 clones treated with 20 nM PMA for 2 min in the presence or absence of 10 μM U0126 or 10 μM Bis. Total ERK was used as loading control. Relative p-ERK2/ERK ratios are shown. All values are relative to non-treated cells expressing the empty vector (pLTR2-CT/pSuper).

To corroborate the results obtained above, we analyzed the expression of CD41, CD61 and GPA in our C3G-silenced HEL clones treated with PMA in the presence or absence of U0 (**Figure R-27**). In contrast to the observed in K562 cells, U0 clearly inhibited PMA-induced CD41 and CD61 expression in control HEL cells. However, and according to the results in **Figure R-26**, U0 did not modify the increase in CD41 and CD61 markers induced by PMA in C3G-silenced HEL cells. In a similar way to that observed in C3G-silenced K562 cells, U0 induced an increase in GPA expression in these HEL clones, validating the negative effect of the ERK1/2 pathway on erythroid differentiation.

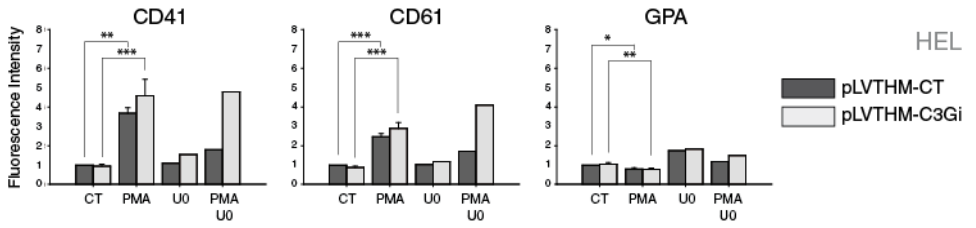

Figure R-27. Effect of the ERK1/2 inhibition, on the expression of CD41, CD61 and GPA induced by PMA in pLVTHM HEL clones. Histograms represent the mean ± SEM of the fluorescence intensity (relative units) of CD41, CD61 and GPA treated as indicated. 2-way ANOVA and Bonferroni t-test were done. *p<0.05, **p<0.01 and ***p<0.001.

Altogether, these data suggest that C3G can modulate the activation of ERK1/2 independently of PKC, and that ERK1/2 do not participate in the effect of C3G on the expression of MK markers.

1.6.4. Role of p38 MAPK signaling pathway in the effect of C3G on MK differentiation

Some studies suggest that p38 MAPK is upstream of the pathway that leads to ERK1/2 activation, acting as a negative regulator of MK differentiation by inhibiting the ERK signaling pathway (Herrera, R. et al. 1998, Jacquel, A. et al. 2006, Chang, Y.I. et al. 2010). In addition, our group has described a functional relationship between C3G and p38α MAPK in a pro-apoptotic context in K562 cells, in which the C3G-Rap1 pathway acts by inhibiting p38α MAPK activation, thus promoting the activation of ERK1/2 (Maia, V. et al. 2009). A negative regulation of p38 MAPK activity by C3G, independently of Rap1, has also been demonstrated (Gutierrez-Uzquiza, A. et al. 2010, Priego, N. et al. 2016).

The effect of p38α MAPK, the most common isoform, is generally studied by the use of its specific inhibitor, SB203580 (SB), which may also inhibit p38β isoform. It has been reported that SB can produce different effects on MK differentiation in a dose-dependent manner: at low doses (5-10 μM) it induces cells to differentiate into megakaryocytes, whereas at higher concentrations (20-50 μM) it drastically reduces MK differentiation and induces cell death (Jacquel, A. et al. 2006).

Considering these data, we wanted to elucidate whether p38 MAPK is involved in the effect of C3G on the differentiation of K562 and HEL cells to megakaryocytes, induced by PMA. For that, the megakaryocytic (CD41 and CD61) and erythroid (GPA) markers were analyzed in our transfected clones treated with PMA in the presence or absence of the p38 MAPK inhibitor, SB. Cell were treated with 20 nM PMA alone or in combination with 10 μM SB for 48 hours, and the cell markers were analyzed by flow cytometry. **Figure R-28A** shows

that SB did not affect the basal levels of these markers in the K562 clones, with the exception of the pLTR2-C3G-expressing clone, in which SB significantly increased CD41 levels. Moreover, SB modestly increased CD61 expression in K562 cells expressing pLTR2-C3G/pSuper. This is in favor of a negative role of p38 in the effect of C3G on MK differentiation. However, SB did not alter the expression of megakaryocyte markers induced by PMA, indicating that p38 MAPK does not seems to play a relevant role in MK differentiation induced by PMA in K562 cells. SB did not modify the expression of GPA either, despite the described role of p38 in the erythroid differentiation of K562 cells induced by imatinib (Jacquel, A. et al. 2006, Jacquel, A. et al. 2007).

To relate the flow cytometry results to the state of p38 phosphorylation, phospho-p38 levels were analyzed by Western Blot on C3G-overexpressing K562 and HEL cells treated with 20 nM PMA for 10 minutes, after SB treatment for 1 hour. Basal levels of phospho-p38 MAPK were increased by two-fold in both C3G-overexpressing cells (**Figure R-28B**). In addition, an increase in p-p38 levels was observed after PMA treatment, especially in HEL cells expressing the lentiviral construct pWpI-C3G, indicating that PMA promotes p38 activation in a C3G-dependent manner.

It is worthy to mention that SB does not inhibit p38 phosphorylation by its MAPKKs but it blocks p38 MAPK binding to ATP, thus preventing the phosphorylation of its direct targets (Cuenda, A. et al. 2007). However, it has been described a mechanism of p38 activation, independent of MAPKK, in which p38 can autophosphorylate (Ge, B. et al. 2002), which could explain our results in control cells. The increase in phospho-p38 MAPK, observed mainly in the PMA+SB-treated cells, could be related with the deactivation of a negative feed-back mechanism regulated by p38 MAPK.

Although it is not reflected in **Figure R-28**, the Anova results indicate that there is significant variability between pLTR2-C3G cells and control cells, independently of the treatment used ($p<0.001$ in CD41 expression results and $p<0.01$ in CD61 expression results).

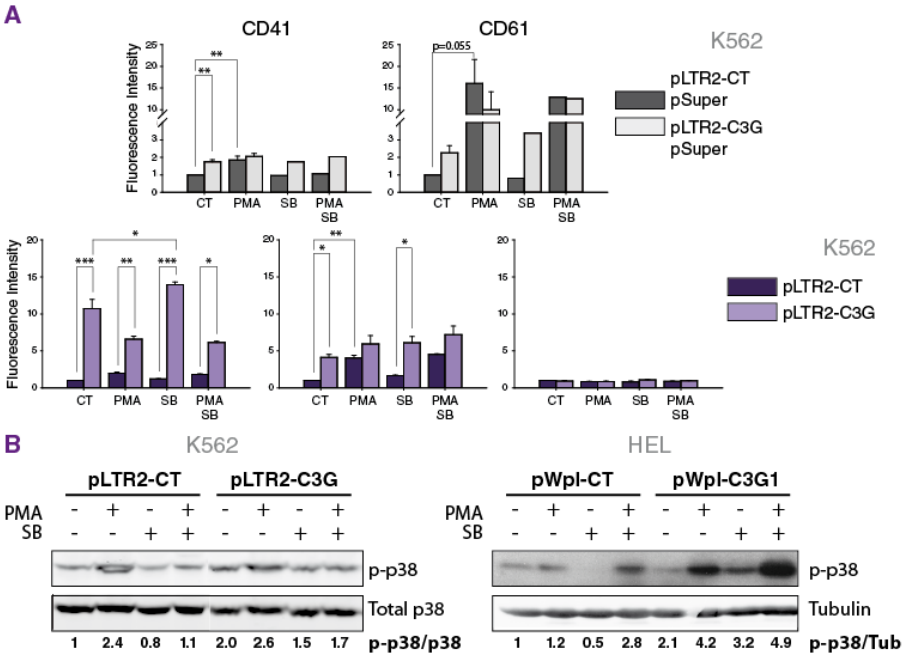

Figure R-28. Effect of the p38α/β MAPK inhibition on the expression of CD41, CD61 and GPA induced by PMA in C3G overexpressing K562 clones. **A)** Histograms represent the mean ± SEM of the fluorescence intensity (relative units) of CD41, CD61 and GPA treated as indicated. 2-way ANOVA and Bonferroni t-test were done. *p<0.05, **p<0.01, ***p<0.001. **B)** Analysis of phospho-p38 levels by Western Blot in K562 clones (left panel) and HEL clones (right panel). Total p38 and tubulin were used as loading controls respectively. Relative p-p38 levels are shown. All values are relative to non-treated cells expressing the empty vector (pLTR2-CT and pWpI-CT).

To reinforce the above data, we performed similar analysis in a HEL clone with silenced C3G expression (pLVTHM-C3Gi) and its control (pLVTHM-CT). In addition, we included in the analysis K562 clones with silenced expression for C3G (pSuper-C3Gi), p38α isoform (pSuper-p38αi) or both (pSuper-C3Gi-p38αi), together with control cells transfected with empty vector (pSuper-CT).

Results in **Figure R-29A**, show that SB pretreatment did not modify the expression of the markers induced by PMA in either the HEL clones or the single-silenced K562 clones, in agreement with results in **Figure R-28**. However, double C3G/p38α silencing induced a significant increase in GPA expression, in contrast with the positive role of p38 MAPK in erythroid differentiation (Jacquel, A. et al. 2006). This indicates a cooperative effect of C3G and p38 in the regulation of erythroid differentiation, where C3G would play an inhibitory role.

As mentioned above, p38 inhibition by low doses of SB enhances PMA-induced MK differentiation. This fact is in accordance with the modest increase in CD61 expression

observed in the pSuper-p38αi clone, under PMA+SB treatment. However, CD41 and CD61 levels decreased in PMA-treated pSuper-C3Gi-p38αi cells, while GPA levels showed the highest values in this clone with low expression of both proteins.

Figure R-29B shows the phosphorylation status of p38 in these C3G and p38α silenced clones treated with PMA and/or SB. As expected, p38 expression and phosphorylation were greatly diminished in pSuper-p38αi and pSuper-C3Gi-p38αi clones. Surprisingly, PMA induced a clear increase in phospho-p38 in control cells. Moreover, similarly to C3G overexpression, C3G silencing also increased basal levels of phospho-p38 MAPK, which were not modified by PMA treatment. These results suggest that the activation of p38 MAPK is modulated by the levels of C3G.

All these results support a regulatory role for C3G in p38 activation. In addition, although the involvement of p38 MAPK in MK differentiation induced by PMA is unclear, it is likely that p38 collaborate with C3G in this effect.

Although it is not reflected in **Figure R-29A**, the Anova analysis indicated that there is significant variability between pSuper-p38α and pSuper-CT, and between pSuper-C3Gi-p38αi and pSuper-CT clones, independently of the treatment used ($p<0.05$ in CD41 results).

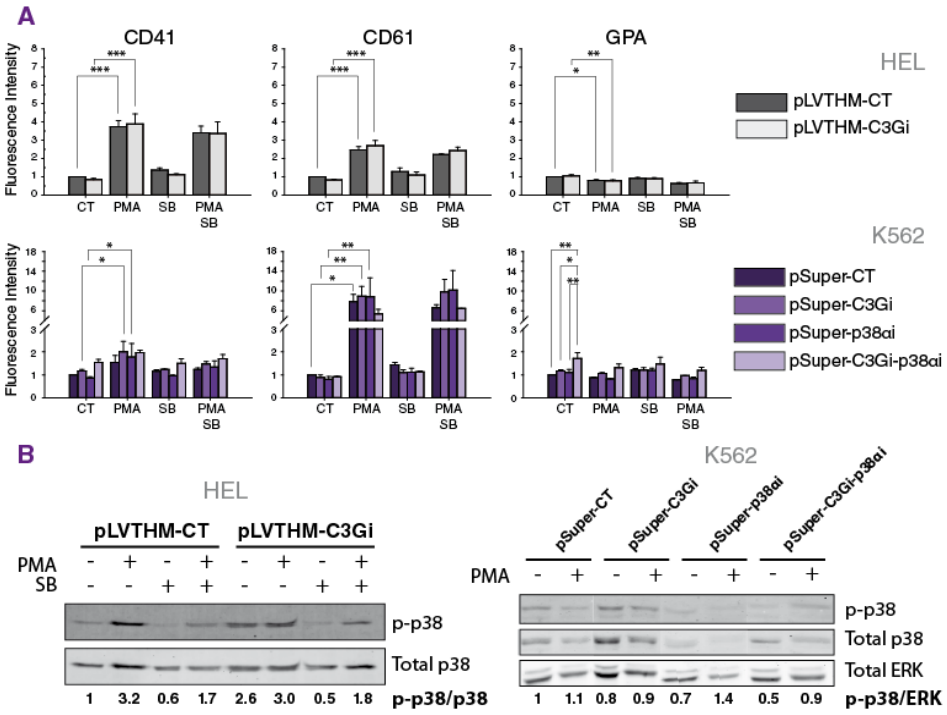

Figure R-29. Effect of the p38α/β MAPK inhibition on the expression of CD41, CD61 and GPA induced by PMA in C3G and/or p38α silenced clones. **A)** Expression of CD41, CD61 and GPA markers in C3G-silenced cells, pLVTHM HEL clones (up panels) and the indicated pSuper K562 clones (Bottom panels). Histograms represent the mean ± SEM of the fluorescence intensity (relative units) of CD41, CD61 and GPA from at least 2 independent experiments with each clone, treated as indicated. 2-way ANOVA and Bonferroni t-test were done. *p<0.05, **p<0.01 and ***p<0.001. **B)** Analysis of phospho-p38 and total p38 by Western Blot in HEL clones (left panel) and K562 clones (right panel). Total ERK was used as loading control. Relative p-p38/ERK ratios are shown. All values are relative to non-treated cells expressing the empty vector (pLVTHM-CT and pSuper-CT, respectively).

To better understand the regulation of p38 and ERK1/2 MAPK pathways in K562 and HEL cells, as well as the role played by C3G, we analyzed the levels of ERK phosphorylation in our C3G-overexpressing or silenced K562 and HEL clones, in combination with clones in which the p38 function has been downregulated by pretreatment with SB203580 or by gene silencing.

In general, treatment with SB caused an increase in basal levels of p-ERK (**Figure R-30)**. These data are in agreement with the literature, and indicate that p38 has an inhibitory effect on ERK (Li, S.P. et al. 2003). On the other hand, the fact that the treatment with PMA and SB together further increase the levels of phospho-ERK indicates that the activation of the MEK/ERK pathway is being reinforced by two different pathways, by direct activation through PKC and by elimination of p38 inhibition.

In addition, overexpression of C3G in HEL cells clearly increased SB-induced phospho-ERK levels **(Figure R-30B),** which were even higher in PMA+SB-stimulated cells. It is worthy to mention that the levels of phospho-ERK and phospho-p38 in HEL cells seem to be dependent on the levels of C3G expression, as already suggested by results in **Figures R-28B and R-29B**. Thus, the clone pWpI-C3G2, which expresses high levels of C3G (see C3G expression of pWpI clones in **Figure R-6B**), showed intermediate values of p-p38 and higher levels of p-ERK, compared to pWpI-C3G1 and pWpI-CT clones. In contrast, the clone pWpI-C3G1, whose C3G levels are intermediate, showed higher levels of p-p38 and lower levels of p-ERK, under the different stimuli (**Figure R-30B)**. These results strongly suggest that the levels of expression of C3G could modulate the levels of phospho-p38, which in turns, would regulate the activation of ERK1/2.

Additionally, we analyzed the expression of phospho-ERK1/2 in C3G- and/or p38α-silenced K562 clones. **Figures R-30C** and **R-30D** showed that the knock-down of p38α increased phospho-ERK levels in any experimental condition, in agreement with the results with SB and in concordance with the negative effect of p38 on ERK1/2 phosphorylation. C3G silencing slightly decreased phospho-ERK1/2 levels, mainly in PMA+SB treated cells and in

the p38αi silenced cells, probably through an increase in the levels of active p38, further confirming the regulatory role of C3G levels on p38 MAPK activity.

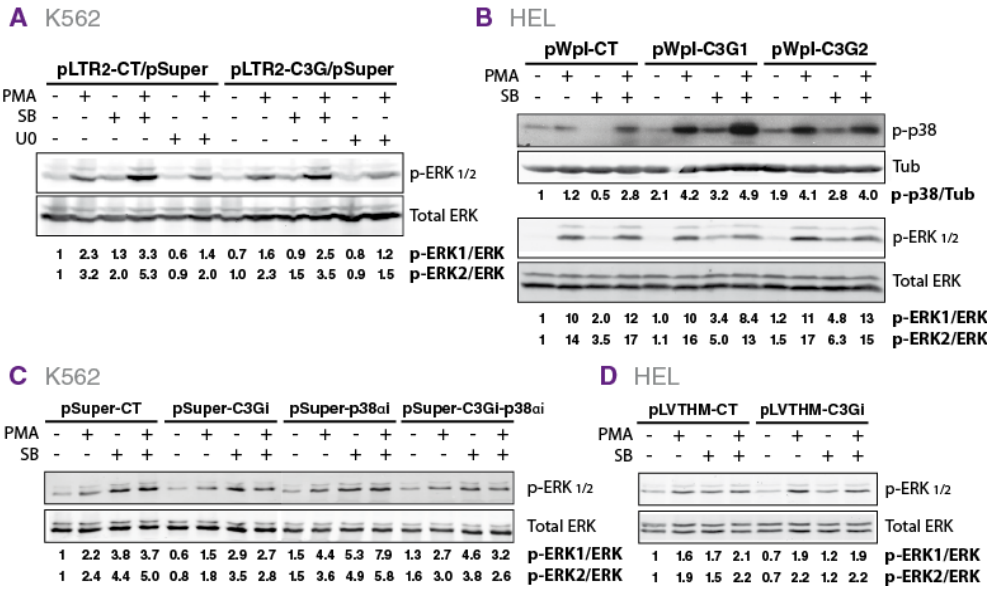

Figure R-30. Effect of the p38α/β MAPK inhibition on ERK1/2 phosphorylation in K562 and HEL clones treated with PMA. Levels of phospho-ERK1/2 and phospho-p38 in K562 pLTR2/pSuper clones (**A**), HEL pWpI clones (**B**), K562 pSuper clones (**C**) and HEL pLVTHM clones (**D**) pretreated with 10 μM U0126 or 10 μM SB203580 for 1 hour and/or 20 nM PMA for 10 minutes. Total ERK and total p38 were used as loading controls. Relative p-p38/p38 and p-ERK/ERK ratios are shown. All values are relative to non-treated cells expressing the empty vector.

1.6.5. Role of the PI3K signaling pathway in the effect of C3G on MK differentiation

It has been reported that activation of phosphoinositide 3-kinase (PI3K)-Akt signaling pathways is important for MK differentiation, specifically for the entry into the endomitosis cycle (Geddis, A.E. et al. 2001), although its role in MK marker expression is controversial (Jacquel, A. et al. 2006, Conde, I. et al. 2010, Sardina, J.L. et al. 2010). Based on that, we wanted to investigate in our clones whether this pathway is involved in the acquisition of megakaryocyte markers and whether C3G plays a role. For this, we analyzed the expression of CD41, CD61 and the erythroid marker GPA, by flow cytometry in K562-pLTR2-C3G and control clones, which were treated with the PI3K inhibitor, Wortmannin (W), and with PMA for 48 hours.

The results in **Figure R-31** show that W did not modify the expression of these markers in controls cells. However, the expression of the megakaryocyte markers, mainly CD41, decreased in W-treated cells overexpressing C3G, compared to the same untreated cells.

This suggests the involvement of PI3K in the C3G-mediated pathway that regulates MK differentiation.

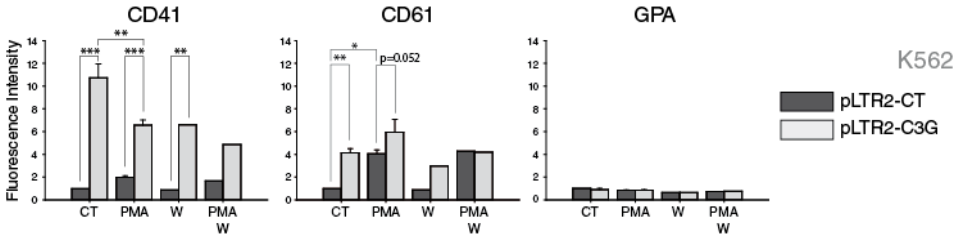

Figure R-31. Effect of PI3K inhibition on the expression of CD41, CD61 and GPA induced by PMA in C3G-overexpressing K562 clones. **A)** Expression of CD41, CD61 and GPA markers in pLTR2 clones treated with 20 nM PMA and/or 10 μM W for 48 hours. Histograms represent the mean ± SEM of the fluorescence intensity (relative units) of CD41, CD61 and GPA treated as indicated. 2-way ANOVA and Bonferroni t-test were done. *p<0.05, **p<0.01 and ***p<0.001.

A similar study was performed in HEL pLVTHM clones. According to the above results and, although the data were not significant, probably due to the low number of experiments, W induced a slight increase in the expression of CD61 in C3G-silenced cells treated with PMA (**Figure R-32).**

Although further studies should be performed to achieve statistical significance of the data, these results could indicate a positive role of PI3K in the PMA-C3G pathway leading to megakaryocytic differentiation in K562 and HEL cells.

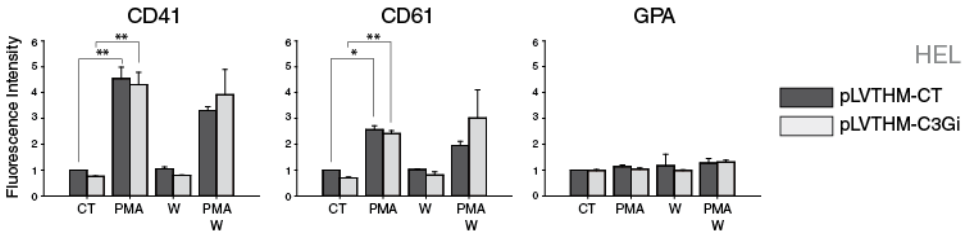

Figure R-32. Effect of PI3K inhibition on the expression of CD41, CD61 and GPA induced by PMA in C3G-silenced HEL clones. A) Expression of CD41, CD61 and GPA markers in C3G-silenced, pLVTHM, clones treated with 20 nM PMA and/or 10 μM W for 48 hours. Histograms represent the mean ± SEM of the fluorescence intensity (relative units) of CD41, CD61 and GPA from at least 2 independent experiments with each clone, treated as indicated. 2-way ANOVA and Bonferroni t-test were done. *p<0.05, **p<0.01 and ***p<0.001.

2. Analysis of the implication of C3G in megakaryocytic differentiation using mouse models

Megakaryopoiesis and thrombopoiesis are multistep processes through which hematopoietic progenitor cells become mature megakaryocytes and form proplatelets. The production of megakaryocytes from adult HSCs of bone marrow (BM) or from embryonic HSCs of liver and cord blood, cultured with certain cytokines, is an *ex vivo* model commonly used to study the mechanisms involved in the expansion and differentiation of megakaryocytic progenitors. Multiple cytokine cocktails and culture conditions have been developed for the production of MKs, but it is known that TPO, the main regulator of megakaryopoiesis, is sufficient to induce the differentiation and maturation of hematopoietic progenitors to MKs.

In this work, we have used two transgenic mouse lineages for C3G (Tg-C3G, lineages 2C1 and 6A6) and one for C3GΔCat (Tg-C3GΔCat, 8A3 lineage, in which C3G is deleted in its catalytic domain), which had been generated and characterized by our group in a previous work (Gutierrez-Herrero, S. et al. 2012). Both transgenes, C3G and C3GΔCat, are expressed under the control of the megakaryocyte and platelet specific PF4 (platelet factor 4) gene promoter. Therefore, with these mice we can specifically study the involvement of C3G in the development of mouse megakaryocytes.

2.1. Analysis of MK surface markers in transgenic BM cells

As first approach, we analyzed by flow cytometry the CD61 positive population in freshly isolated BM cells from Tg-C3G and Tg-C3GΔCat mice. This measurement was performed at basal conditions to determine whether C3G is able *perse* to stimulate the differentiation of megakaryocytes in our mouse models. Similar percentages of CD61-positive cells were observed in both Tg-C3G and in Tg-C3GΔCat BM cells, compared to their corresponding wild type (WT) cells (**Figure R-33**).

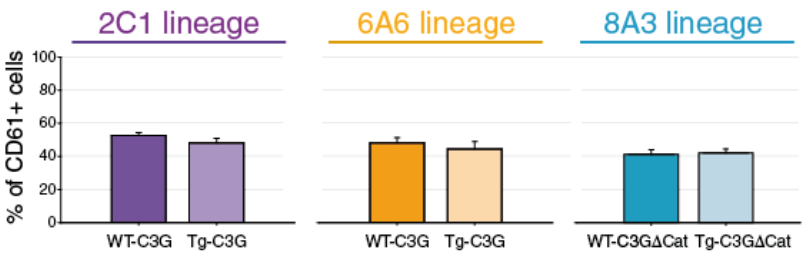

Figure R-33. Quantification of the percentage of CD61-positive cells in BM from our transgenic mice, at basal conditions. Freshly isolated bone marrow cells from the indicated genotypes were labeled

with anti-CD61 antibodies and analyzed by flow cytometry. Histograms represent the mean ± SEM of the percentage of CD61+ cells in at least, 3 different measures of each genotype. Mann-Whitney U test was done. No significant differences were observed between Tg-C3G or Tg-C3GΔCat *vs* WT.

Next, we studied the presence of megakaryocytes in mouse BM cultures of the different genotypes, stimulated with TPO, by flow cytometry analysis of the CD41 and CD61 positive cells. Since primary BM cultures include a mixture of different cell populations, it is more appropriate, in this context, to analyze the megakaryocytic markers by detecting the percentage of positive cells, rather than measuring fluorescence intensities.

Thus, freshly isolated BM cells from our transgenic mice were cultured with 50 µg/ml TPO for 6 days and then the levels of CD41 and CD61 positive cells measured by flow cytometry. The percentage of CD41+, CD61+ and double CD41/CD61+ megakaryocytes of each transgenic mouse are shown in **Figure R-34.** BM cultures from Tg-C3G mice harbored a higher percentage of megakaryocytes than WT or Tg-C3GΔCat mice, results being statistically significant in the CD41+ and double CD41+/CD61+ populations. On the other hand, there was a significant decrease in the percentage of CD41/CD61+ megakaryocytes in the bone marrow cultures of Tg-C3GΔCat mice, compared to WT and Tg-C3G cells. These results indicate that C3G plays a positive role in the acquisition of megakaryocyte markers, induced by TPO stimulation, which is dependent on its catalytic, GEF, activity, and are in agreement with our results in human cell lines.

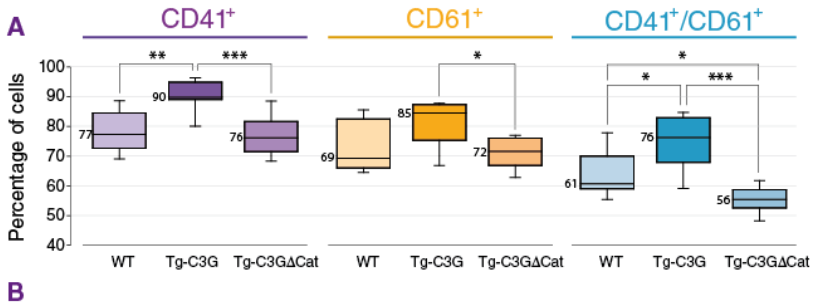

B

	Mean of cell percentage		
	CD41+ (± SEM)	CD61+ (± SEM)	CD41+/CD61+ (± SEM)
WT	78.1 ± 2.8	73.4 ± 4.0	64,0 ± 3.2
Tg-C3G	90.3 ± 1.8	81.2 ± 2.7	74.9 ± 3.2
Tg-C3GΔCat	76.9 ± 2.3	71.1 ± 1.8	55.6 ± 1.5

Figure R-34. Quantification of the percentage of CD41+ and/or CD61+ cells in BM from Tg-C3G, Tg-C3GΔCat and WT mice stimulated with TPO. Freshly isolated BM cells were cultured with thrombopoietin (TPO) for 6 days. The percentage of CD41+, CD61+ and double CD41+/CD61+ cells was analyzed by flow cytometry. **A)** Box plots representing the median ± SEM of the percentage of positive cells of 6 different measures from three independent cultures of each genotype. Mann-Whitney U test

was done. *p<0.05, **p<0.01 and ***p<0.001. **B)** Table indicating the mean (± SEM) of the percentage of positive cells of each genotype.

2.2. Analysis of ploidy in primary bone marrow cells

In order to establish whether, as in the K562 and HEL cell lines, C3G plays a role in increasing DNA content in megakaryocytes, *ex vivo*, we determined the ploidy status of megakaryocytes from our transgenic Tg-C3G and Tg-C3GΔCat mice. For this purpose, freshly isolated BM cells were cultured, for 6 days, in the presence of 50 ng/ml TPO and the following cocktail of cytokines: 10 ng/ml SCF, 10 ng/ml IL-3, 10 ng/ml IL-6 and 10 ng/ml IL-11. BM cells were removed at 2, 4, and 6 days and stained with CD41-FITC antibody, prior to staining with propidium iodide, to analyze the DNA content only in cells committed to the megakaryocytic lineage.

During the 6 days of MK differentiation a progressive increase in the percentage of CD41+ cells was observed by flow cytometry (**Figure R-35A**). Since the increase in the number of megakaryocytes over time was accompanied by an increase in cell size, two different populations of megakaryocytes could be distinguished; small cells expressing CD41 (FSC^{low}/CD41+) and large cells expressing high levels of CD41 (FSC^{high}/CD41+). Results in **Figure R-35B,** showing the ploidy distribution of each population separately, indicated that the small MKs were predominantly 2n (less mature), while the large MKs were polyploid cells (more mature). Therefore, we evaluated the ploidy of large, CD41+, BM cells.

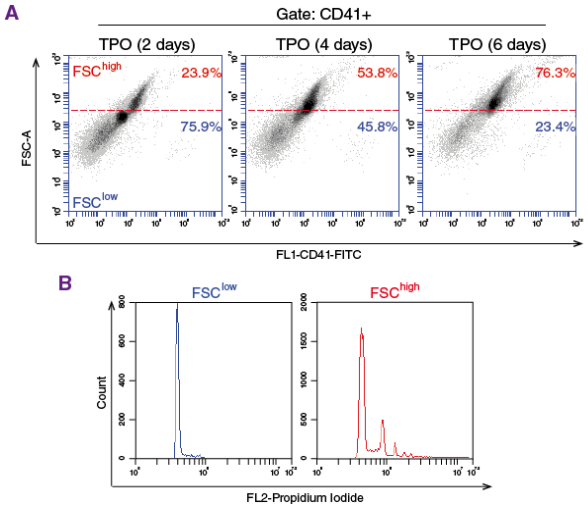

Figure R-35. Analysis of CD41+ populations in BM cultures differentiated to MKs. A) Flow cytometry dot plots showing forward-scatter and CD41 profiles of CD41+ BM cells. Cells were harvested after 2, 4 and 6 days of treatment with TPO plus cytokines cocktail. In each plot, two gates are shown containing

small megakaryocytes (FSC^{low}) and large megakaryocytes (FSC^{high}). **B)** Representative flow cytometry plots of ploidy distribution of small and large MKs, left and right panel, respectively.

2.2.1. Effect of C3G overexpression on TPO-induced polyploidization *ex vivo*

Next, we examined the polyploidization status of MKs of BM cells from Tg-C3G (2C1 and 6A6 lineages), as described above. Overexpression of C3G increased the polyploidization of MKs (**Figure R-36**). Specifically, a significant increase in CD41+ cells with a DNA content ≥8n (14% in Tg-C3G *vs* 9% in WT) was observed in Tg-C3G 2C1 lineage, which was coupled to a significant decrease in 2n CD41+ cells (64% in Tg-C3G *vs* 71% in WT). Similar tendency was observed in the 6A6 lineage (12% in Tg-C3G vs 8% in WT). These results indicate that C3G overexpression in megakaryocytes induces a higher rate of DNA replication.

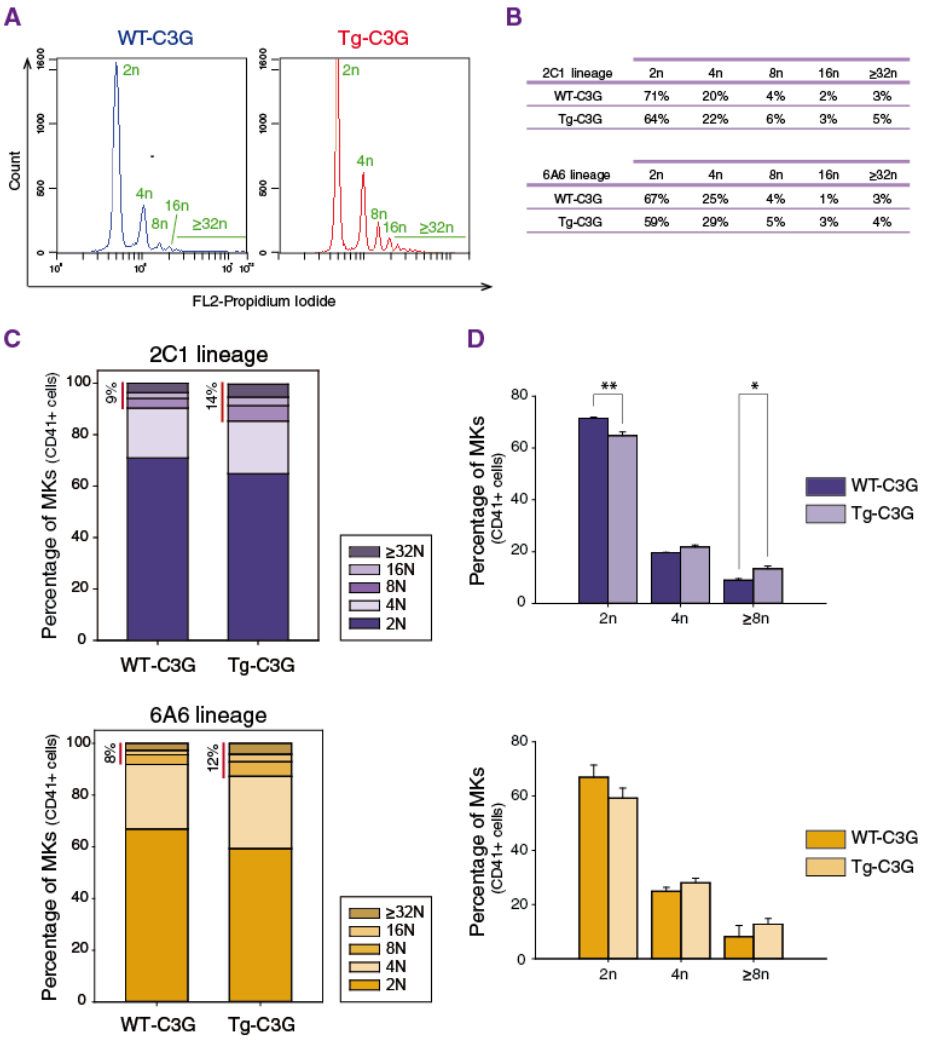

2C1 lineage	2n	4n	8n	16n	≥32n
WT-C3G	71%	20%	4%	2%	3%
Tg-C3G	64%	22%	6%	3%	5%

6A6 lineage	2n	4n	8n	16n	≥32n
WT-C3G	67%	25%	4%	1%	3%
Tg-C3G	59%	29%	5%	3%	4%

Figure R-36. Transgenic C3G expression increases MK polyploidization. Freshly isolated BM cells were cultured with TPO, SCF, IL-3, IL-6 and IL-11 for 6 days. DNA content in CD41+ cells was measured by flow cytometry. **A)** Representative flow cytometry plots of ploidy distribution of FSC^{high}/CD41+ MKs from 2C1 lineage (WT and Tg) are shown. We identified 5 different populations; 2n, 4n, 8n, 16n and ≥32n. **B)** Table indicating the percentage of FSC^{high}/CD41+ MKs of the different clones corresponding to each population. **C)** Stacked bar histograms of the percentage of MKs of each genotype belonging to the different ploidy populations (2n, 4n, 8n, 16n and ≥32n) of BM cells from 2C1 mice (top panel) and 6A6 mice (bottom panel). Red bars indicate the percentage of cells with a DNA content ≥8n. **D)** Histograms represent the mean ± SEM of the percentage of individual ploidy populations of BM cells from 2C1 (top panel) and 6A6 (bottom panel) mice lineages. Data correspond to 3 different experiments from 3 mouse of each genotype. Data were analyzed using the t-test. *p<0.05 and **p<0.01.

2.2.2. Effect of C3GΔCat overexpression on TPO-induced polyploidization *ex vivo*

To verify the results obtained with the Tg-C3G mice, polyploidization was analyzed in mature CD41+ megakaryocytes of the Tg-C3GΔCat mice. The results shown in **Figure R-37** indicate a DNA distribution of mature Tg-C3GΔCat megakaryocytes similar to that of the WT (12% in Tg-C3GΔCat *vs* 13% in WT). Additionally, the distribution of the different ploidy populations, ranging from 2n to 32n, was similar in Tg-C3GΔCat and WT megakaryocytes, indicating that overexpression of this mutant did not affect endomitosis.

These results, together with the results obtained with the Tg-C3G mice, suggest a regulatory role for C3G in the acquisition of polyploid features that seems to be dependent on its GEF activity. In addition, these results also suggest that, in this context, Tg-C3GΔCat does not behave as a dominant negative mutant.

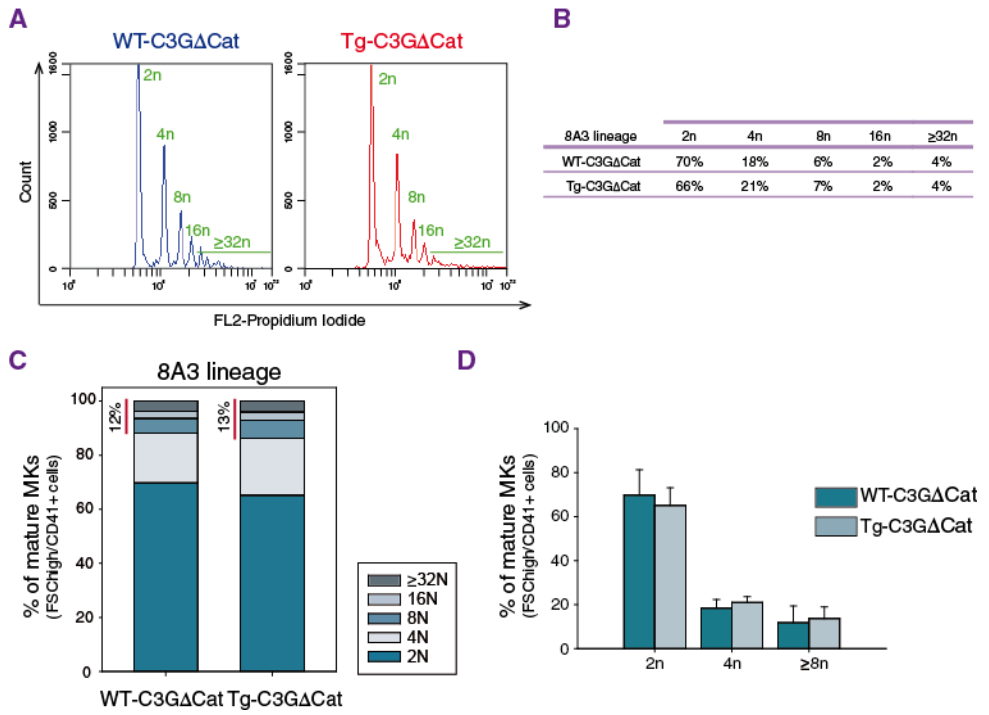

8A3 lineage	2n	4n	8n	16n	≥32n
WT-C3GΔCat	70%	18%	6%	2%	4%
Tg-C3GΔCat	66%	21%	7%	2%	4%

Figure R-37. Transgenic C3GΔCat expression does not affect MK polyploidization. Freshly isolated BM cells were cultured with TPO, SCF, IL-3, IL-6 and IL-11 for 6 days. DNA content in CD41+ cells was measured by flow cytometry. **A)** Two representative flow cytometry plots of ploidy distribution of FSC^{high}/CD41+ cells are shown. We identified 5 different populations; 2n, 4n, 8n, 16n and ≥32n. **B)** Table indicating the percentage of FSC^{high}/CD41+ MKs, corresponding to each population in the two genotypes. **C)** Stacked bar histograms of the percentage of FSC^{high}/CD41+ MKs of each genotype belonging to the different ploidy populations (2n, 4n, 8n, 16n and ≥32n) of BM cells from 8A3 mice lineage. Red bars indicate the percentage of cells with a DNA content ≥8n. **D)** Histograms represent the mean ± SEM of the percentage of individual ploidy populations of bone marrow MKs from 8A3 mice. Data correspond to 3 different experiments from 3 mouse of each genotype. Data were analyzed using the t-test. No significant differences were observed between Tg-C3GΔCat and WT.

2.3. Analysis of the microenvironment in transgenic BM cells

BM microenvironment plays an important role during the differentiation of hematopoietic lineages. Specifically, the interaction of megakaryocytic progenitors with the microenvironment is essential for proper megakaryopoiesis and subsequent development of megakaryocytes into platelets. Therefore, we aimed at studying the effect of the BM microenvironment on MK differentiation and its interplay with C3G.

As previously commented in the Introduction, the processes of megakaryopoiesis and platelet production involve two distinct BM niches: osteoblastic and vascular. Gradients of cytokines and growth factors, as well as different protein-protein interactions regulate the migration of hematopoietic progenitors between the two niches, throughout their differentiation

and maturation. It has been hypothesized that the dynamic interaction of MKs with extracellular matrix proteins in the bone marrow allows their maturation from HSCs and their subsequent migration to the vascular niche, where the process of proplatelet formation would begin (Machlus, K.R. et al. 2013). Integrins, that are highly expressed on the surface of megakaryocytes, are crucial for cell migration and adhesion during MK differentiation, particularly integrin αIIbβ3, whose activation is mediated by Rap1 (Deutsch, V.R. et al. 2013). In this line, our group has reported that C3G participates in the activation of integrin αIIbβ3 by Rap1 in platelets (Gutierrez-Herrero, S. et al. 2012).

Taking into account the importance of migration from the osteoblastic niche to the vascular niche during the differentiation and maturation of megakaryocytes, we analyzed the motility of megakaryocytes of our transgenic mice. Due to the importance of the microenvironment in MK migration, we need a model in which the microenvironment that supports megakaryocytic maturation is minimally modified.

For that, we used bone marrow explants, which are prepared by collecting the intact bone marrow from the mouse femur, cutting it transversely into small sections and keeping it in a physiological buffer for several hours. During this time, the cells migrate progressively at the periphery of the explant and due to the large size of mature MKs, we can follow them through optical microscopy (Strassel, C. et al. 2009, Gibbins, J.M. et al. 2011). Over time, the MKs change their morphology and we can classify them according to this: spherical MKs, MKs with protrusions and MK with extending proplatelets (**Figure R-38**).

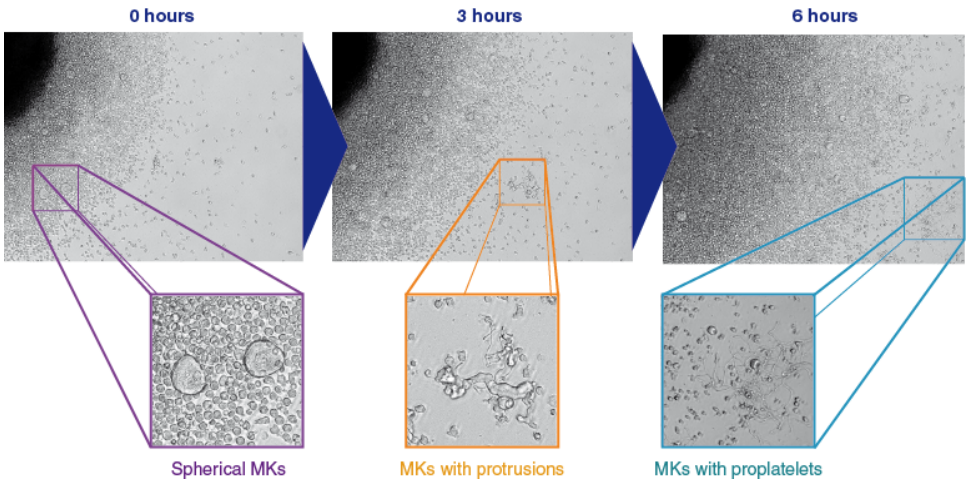

Figure R-38. Bone marrow explants. Representative optical microscopy images of migration and differentiation of megakaryocytes from BM explants at 0, 3 and 6 hours. Boxes show the amplification of representative regions from each time point. Three different morphologies can be distinguished over time: spherical MKs, MKs with protrusion and MKs with proplatelets.

2.3.1. Role of C3G on the migration of mature megakaryocytes

To study whether C3G regulates megakaryocyte motility, we analyzed the migration capacity of mature MKs in bone marrow explants of the different genotypes. The results of the velocity of migration and the distance covered are summarized in **Figures R-39A** and **R-39B**, respectively. The migration velocity of MKs released from the bone marrow of 6A6 mice was significantly higher in the Tg-C3G explants than in their WT. Similar results were obtained with the 2C1 lineage, although in this case differences were not statistically significant. On the other hand, Tg-C3GΔCat MKs showed a significant decrease in motility, compared to their WT MKs (8A3 lineage). These data were correlated with the results obtained when analyzing the distance covered, although only in 6A6 and 8A3 lineages the results were statistically significant (**Figure R-39B**).

These results suggest that C3G, through its catalytic activity, is able to positively modulate the motility of MKs during their maturation, at least in this context.

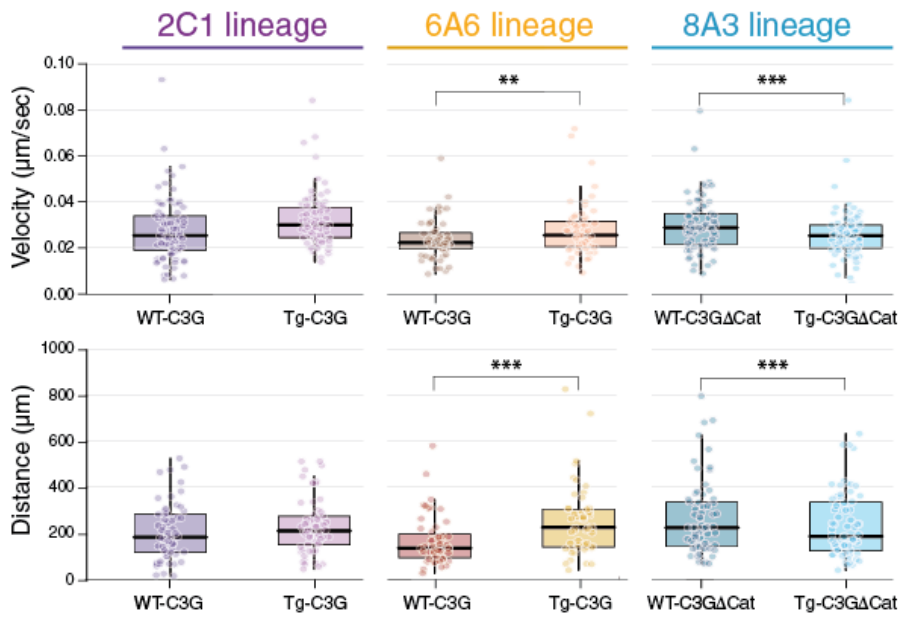

Figure R-39. C3G regulates megakaryocyte motility. Transverse sections of bone marrows from the different genotypes were plated in an incubation chamber and maintained at 37ºC for 6 hours. MKs at the periphery of the explants were tracked under the microscope and images were acquired at 10 min intervals. **A)** Box plots represent the mean ± SEM velocity (µm/second) of individual megakaryocytes 6 hours after their release from bone marrow explants. Three mice of each genotype were analyzed. Mann Whitney U test were done. **B)** Box plot represent the mean distance (µm) covered by megakaryocytes from bone marrow explants. **p<0.01, ***p<0.001.

2.3.2. Effect of C3G on the adhesion of MKs to the osteoblastic matrix

Proplatelet formation by megakaryocytes *in vivo* is temporarily regulated by interactions with the extracellular matrix. Type I collagen, which is particularly abundant in the osteoblastic niche, strongly inhibits proplatelet formation, whereas types IV and III collagens, which are located around the bone marrow vessels, support it. It is possible that these antagonistic events act by preventing the premature release of platelets into the circulation prior to the localization of megakaryocytes at the vascular interface of the bone marrow. Similarly, adhesion to perivascular fibronectin and vitronectin enhance megakaryopoiesis and proplatelet formation (Psaila, B. et al. 2012).

In order to analyze the interaction of our transgenic megakaryocytes with the extracellular matrix of the bone marrow, we studied the megakaryocyte progenitors that are most strongly associated with the bone matrix. To do this, after isolating the bone marrow from femurs, small fragments of bone were incubated with collagenase and dispase to release the progenitors that are attached to the bone. The released cells were stained with anti-CD61 antibodies and the presence or megakaryocytes was detected by flow cytometry. The results shown in **Figure R-40** indicate that C3G overexpression modestly decreases the percentage of MK progenitors that are bound to the bone matrix, whereas overexpression of the C3GΔCat mutant showed no effect.

Overall, our data suggest a role for C3G in the mobilization of mature megakaryocytes into the circulation.

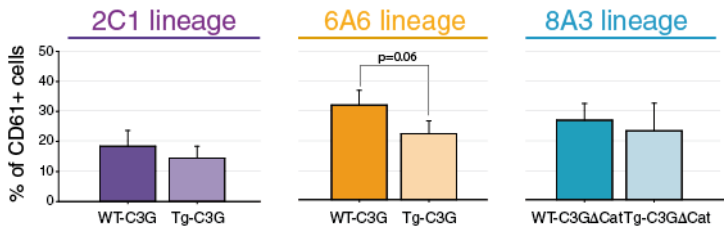

Figure R-40. Percentage of MKs most strongly associated to the osteoblastic niche. After extraction of the bone marrow, small pieces of femur were treated with collagenase and dispase for 2 hours and the presence of CD61+ cells was analyzed by flow cytometry. Mann-Whitney U test was done.

2.4. Effect of C3G on proplatelet formation

Initially, we attempted to study the final stage of the differentiation and maturation of megakaryocytes, the formation of proplatelets, using megakaryocytes cultured in coverslips coated with fibronectin or collagen. However, the experiments performed were unsuccessful because this process occurs, *in vivo*, in close association with cellular and extracellular

components of the bone marrow. Therefore, it is necessary to use a more physiological system, such as the bone marrow explants. Bone marrow explants were obtained in the same manner as previously indicated, except that in this case, an anti-CD41 specific fluorescence antibody was added to the physiological buffer. This improvement in the experimental approach allowed a better visualization of the megakaryocytes by fluorescence microscopy, which enabled to distinguish different morphologies (**Figure R-41A**).

The results in **Figure R-42B** show that the overexpression of C3G increased the proportion of cells capable of producing proplatelets, by 10% in Tg-C3G of the 2C1 lineage, and by 20% in Tg-C3G of the 6A6 lineage, compared to their WT. In addition, the implication of the catalytic domain of C3G in this effect was verified by the decrease of about 20% in the ability of the C3GΔCat mice to form proplatelets, as compared to its control. These results indicate that the overexpression of C3G, through its catalytic domain, promotes the formation of proplatelets in mature megakaryocytes.

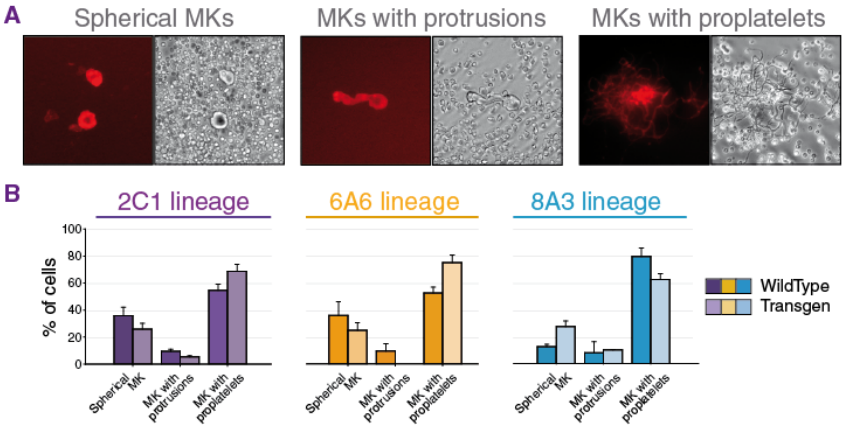

Figure R-41. C3G promotes the formation of proplatelets from mature megakaryocytes. A) Representative images of the different stages of MK maturation: spherical megakaryocytes, megakaryocytes with extending protrusions and megakaryocytes with proplatelets. Fluorescence microscope images (Left panels) and brightfield inverted microscope images (right panels). **B)** The histograms represent the mean ± SEM of the percentage of cells of each phenotype measured in two different experiments, with at least 4 explants from each genotype.

2.5. Analysis of the number of platelet in blood

The above results suggest that C3G may induce the formation of a greater number of platelets. Therefore, we performed platelet counts in periphery blood collected from mice of the different genotypes using the Hemavet Counter. Surprisingly, the overexpression of C3G in our transgenic mice did not affect the final number of platelets (**Figure R-42**). Additionally, no differences were found in platelet counts between males and females (data not shown).

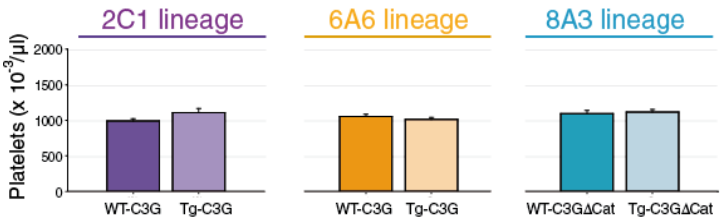

Figure R-42. C3G did not modify platelet counts. Counts were performed in peripheral blood collected from 6-month mice of the different genotypes using Hemavet Counter HV950FS. The histograms represent the mean ± SEM of the number of platelets. Mann-Whitney U test was done, but no significant differences were observed between Tg-C3G or Tg-C3GΔCat *vs* WT.

Discussion

In the present work, we have examined the implication of C3G in the modulation of different stages of megakaryopoiesis leading to platelet formation. These include acquisition of surface markers, changes in morphology, polyploidization, migration from the osteoblastic niche to the vascular niche and proplatelet formation. For this purpose, we have used two different experimental models: (i) hematopoietic cell lines K562 and HEL, in which C3G has been proven to modulate the expression of CD41, CD61 and GPA membrane glycoproteins, as well as changes in morphology and ploidy status, and (ii) primary bone marrow cells from C3G transgenic mice, where, in addition to the above, we have demonstrated that C3G promotes MK migration from the osteoblastic to the vascular niche, and proplatelet formation.

A role for C3G in differentiation has been demonstrated in many other systems, such adipocytes (Jin, S. et al. 2000), neuroblastoma cells (Radha, V. et al. 2008), monocytes to macrophages (Radha, V. et al. 2011) and mesenchymal cells to myotubes (Sasi Kumar, K. et al. 2015), which is probably a reflect of its essential role during embryogenesis (Ohba, Y. et al. 2001).

1. Implication of C3G in MK differentiation using transgenic cell lines

Megakaryocytic differentiation, induced by PMA, has been extensively studied in hematopoietic cell lines, such as K562 and HEL. PMA mimics TPO, the physiological inducer of megakaryopoiesis, in the *in vitro* stimulation of the morphological changes that take place during this process (Long, M.W. et al. 1990, Jacquel, A. et al. 2006, Conde, I. et al. 2010, Sardina, J.L. et al. 2010). Through the use of PMA, numerous signaling pathways have been described that are involved in modulating the acquisition of the MK features. However, certain mechanisms are not completely decrypted.

K562 and HEL cells behave as a pluripotent hematopoietic precursor, expressing in undifferentiated conditions, features of both erythroid and megakaryocytic lineages. In fact, both cell lines can be induced to undergo erythroid or megakaryocytic differentiation depending on the stimuli (Long, M.W. et al. 1990). Thus, K562 and HEL cells treated with PMA exhibit characteristic features of megakaryocytes, including large size, presence of vacuoles and long extensions. These same features were observed in unstimulated K562 cells overexpressing C3G, which provided the first evidence that C3G could be involved in the modulation of morphological changes accompanying MK differentiation, presumably acting downstream of PKC. Moreover, the expression of C3G was increased in K562, and specially

in HEL cells, upon treatment with PMA for several days, further suggesting that C3G could be involved in the actions of PMA leading to MK differentiation. In this regard, we have previously demonstrated the participation of C3G in the PMA-PKC pathway leading to integrin αIIbβ3 activation in mouse platelets (Gutierrez-Herrero, S. et al. 2012).

In agreement with a possible role of C3G in MK differentiation, expression of the megakaryocyte markers, CD41 and CD61, dramatically increased in K562 cells with stable overexpression of C3G, with no other stimuli. This indicates that C3G, per se, is capable of triggering the process by which these erythroid cell lines commit to the megakaryocytic lineage.

However, and contrarily to the expected, neither C3G-silencing, nor even C3G ablation, induced a decrease in the expression of these markers below the control levels, neither in basal conditions nor under PMA treatment. This, indicates that in K562 and HEL cells C3G modulates the acquisition of these megakaryocytic markers but is not essential. Assuming that C3G functions are, at least partially, mediated by its GEF activity on Rap1, a possible explanation for the lack of effect on the expression of MK markers in C3G-silenced cells is that a compensatory mechanism might be produced in which, the absence of C3G is countervailed by other Rap1-GEFs. A potential candidate is CALDAG-GEFI, which is one of the most abundant GEFs in murine platelets and plays a significant role in their function (Crittenden, J.R. et al. 2004, Schultess, J. et al. 2005). However, there are no indications about a possible role of CalDAG-GEFI in MK differentiation.

On the other hand, according to the existence of a common precursor for the erythroid and megakaryocytic lineages, the acquisition of the megakaryocytic markers in these cell lines was linked to the downregulation of the erythroid ones. In accordance, expression of α-globin was completely abrogated by C3G-overexpression in K562 cells, which was even able to inhibit that induced by Imatinib. Similarly, although to a lesser extent, the expression of GPA also decreased in the C3G-overexpressing K562 cells. In addition, although we did not observed changes in the expression of megakaryocytic markers in cells with C3G silencing, we observed a clear increase in the expression of GPA mRNA in K562-pSuper-C3Gi cells. All these results suggest a role for C3G in the regulation of early stages in the erythroid/megakaryocytic commitment.

Interestingly, untreated C3G-overexpressing cells showed levels of MK markers similar or even higher than control cells treated with PMA. The fact that PMA did not further increase the expression of these markers induced by C3G, suggests that both effects are not synergistic and that, therefore, C3G must be acting in the PMA-PKC pathway. In fact, while

inhibition of PKC, by treatment with Bis, completely abolished PMA-induced CD41 and CD61 expression in control cells, it slightly affected the induced by C3G, indicating that C3G is downstream of PKC in this pathway, as observed in platelets (Gutierrez-Herrero, S. et al. 2012). Also, these results indicate that C3G overexpression is sufficient to trigger downstream pathways involved in MK differentiation without the participation of upstream elements.

Treatment with PMA induces morphological changes in K562 and HEL cells reminiscent of megakaryocytes (Long, M.W. et al. 1990, Jacquel, A. et al. 2006, Conde, I. et al. 2010, Sardina, J.L. et al. 2010). We have observed that the overexpression of C3G induces the acquisition of MK differentiation features similar to those induced by PMA, including increase in size, appearance of large nuclei and long cytoplasmic extensions. However, contrarily to its role on the expression of CD41 and CD61, the effect of C3G in morphology is enhanced by treatment with PMA.

An important process that occurs along the differentiation and maturation of megakaryocytes is the increase of the DNA content through repeated cycles of endomitosis (Geddis, A.E. et al. 2006). The increase in polyploid state is accompanied by an increase in cell and nuclei size (Tomer, A. 2004). As indicated above, an increase in nuclear size was observed in C3G-overexpressing K562 cells, suggesting that C3G could be facilitating the exit of normal cell cycle and the entry into an endomitotic cycle. The analysis of the DNA content in C3G overexpressing and C3G silenced K562 and HEL cells indicate that C3G plays an important role in the modulation of polyploidy in these cells. Thus, overexpression of C3G increase the proportion of polyploid cells in both cell lines, while its ablation induced a clear decrease in the proportion of polyploid K562 cells. It should be highlighted that, although these results did not reach statistical significance, they were consistent in the two cell lines used and in both experimental conditions, i.e. C3G overexpression and C3G knock-out. The role of C3G in the regulation of ploidy was PMA-dependent, since no changes in ploidy status were observed in untreated clones. We have shown that treatment with PMA induces an increase in the phosphorylation of C3G in Y504. It has been described that phosphorylation of C3G in this residue, and possible in others, although is not essential, plays an important role in its full activation, probably through the release of some autoinhibitory mechanisms (Ichiba, T. et al. 1999, Mitra, A. et al. 2010). It is possible that an increase in C3G phosphorylation is required in later stages during MK differentiation, but not during the initial phases involved in the expression of the MK markers.

Additionally, overexpression of C3G in K562 cells induces an increase in the expression of p21, a negative regulator of the normal cell cycle, which is up-regulated during

MK differentiation (Matsumura, I. et al. 1997). Upregulation of p21 by C3G overexpression, through the ERK signaling pathway, has been also reported in neuronal differentiation (Radha, V. et al. 2008). However, p21 levels in our C3G knock-out K562 cells remained similar to those in control cells. This fact could not explain why these cells reach lower levels of ploidy. A plausible explanation is that the function of C3G in the induction of the endomitotic cycle requires other cell cycle regulators, in addition to p21. In fact, it has been shown that p21 knock-out does not rescue the mitotic arrest during differentiation, indicating that its role in endomitosis is not essential (Baccini, V. et al. 2001).

As mentioned, C3G is a Guanine Nucleotide Exchange Factor (GEF), so its main functions dependent on its catalytic, GEF domain. However, C3G also participates in the regulation of multiple cellular events through protein-protein interactions involving its central polyproline region (SH3-binding) and its N-terminal (E-cadherin-binding) domains, regardless of its catalytic function. In addition, these domains can contribute to the modulation of the catalytic activity (Ichiba, T. et al. 1999). Our results obtained using C3G deletion mutants indicate that both functions seem to be relevant in the acquisition of MK markers. That is, C3G could modulate MK differentiation through interactions with other proteins and additionally, through its function as GEF, modulating the activation of GTPases, presumably Rap1, considering its important role in megakaryocyte and platelet biology (Stork, P.J. et al. 2005). Additionally, the results of α-globin expression, which gave us a more precise view of the changes occurred in the erythroid markers than the flow cytometric data, clearly indicate that these three C3G domains contribute to the regulation of the levels of α-globin and, therefore to the prevention of erythroid differentiation following induction with Imatinib.

MK differentiation signaling pathways modulated by C3G

As previously commented, our results indicate that C3G is downstream PKC in the PMA pathway, as demonstrated by the lack of effect of Bisindolylmaleimide on the expression of MK markers, or in the activation of ERK1/2, induced by C3G overexpression. In fact, C3G is phosphorylated in a PKC-dependent manner, probably through Src, since activation of Src by PKC has been documented (Tatin, F. et al. 2006), as well as phosphorylation of C3G by Src-family kinases (SFK) and other non-receptor tyrosine kinases (NRTK), such as Abl or Bcr-Abl (Shivakrupa, R. et al. 2003, Radha, V. et al. 2004, Gutierrez-Berzal, J. et al. 2006, Mitra, A. et al. 2010). It should not be forgotten that Bcr-Abl is the main kinase that regulates signaling in K562 cells.

The Raf/MEK/ERK1/2 signaling pathway is considered one of the most important pathways that modulate MK differentiation. In K562, ERK1/2 is rapidly phosphorylated by PMA

and its activity has been related to early stages of MK differentiation and maturation. Specifically, transient phosphorylation of ERK1/2 is required to induce proliferation of progenitors and expression of surface markers (Jacquel, A. et al. 2006, Conde, I. et al. 2010), whereas a more sustained activation is needed during MK maturation. However, our analysis of the expression of MK surface markers, using the ERK inhibitor U0126, did not suggest a clear implication of ERK1/2 in this early differentiation event, as U0 inhibited the expression of these markers in HEL, but not in K562, control cells. However, what was clear is that U0 did not modify the expression of these markers modulated by C3G in any of these cell lines. The increase in GPA expression observed in both cell types upon treatment with U0 is in agreement with the negative effect of ERK signaling on erythroid differentiation described by other authors (Jacquel, A. et al. 2006).

On the other hand, we have observed that at short times of PMA stimulation, there are no differences in ERK1/2 phosphorylation between C3G-overexpressing, or silencing clones, and control clones. This indicates, that C3G does not participate in the transient activation of ERK1/2 by PMA. However, at longer PMA exposure times, C3G overexpression induced a sustained ERK1/2 phosphorylation, which was completely abrogated in cells with C3G ablation. These results indicate that C3G is involved in the activation of pathways leading to sustained ERK1/2 activation, which are needed for the maturation of megakaryocytes.

Moreover, these results are in agreement with the lack of effect of U0 in the expression of MK markers regulated by C3G, since this is an early event during MK differentiation. Therefore, our results indicate that C3G can modulate early stages of MK differentiation, such as marker expression, with independence of the ERK1/2 activation. Furthermore, C3G is able to activate ERK1/2 independently of PMA-PKC, as assessed by the lack of effect of Bis on C3G-induced ERK phosphorylation, indicating an uncoupling between PKC and C3G in the activation of ERK1/2.

TPO-induced MK differentiation requires an initial transient activation of ERK, which is mediated by the Shc/SOS/Ras/Raf signaling pathway. At later stages during MK differentiation a more sustained activation of ERK1/2 through the Rap1-B-Raf pathway, is produced (Stork, P.J. et al. 2005). Our results suggest that C3G could be the Rap1-GEF modulating this process in megakaryocytes. In fact, while Rap1 was transiently activated by PMA in K562 control cells, rapidly decaying after 2 min, Rap1-GTP levels were maintained for 10 min in C3G overexpressing cells, in correlation with a sustained C3G phosphorylation. Rap1 activity assays in PMA-stimulated K562 clones, expressing different C3G mutants, showed that N-terminal and the SH3-binding domains of C3G regulate its catalytic activity, reflecting the

complexity of the regulation of C3G activation by PMA. In addition, the observed increase in Rap1-GTP produced by the overexpression of a C3G mutant harboring only the SH3-binding domain, could be the result of the sequestration of Rap1 inhibitors interacting with this domain, or, alternatively could be due to the interaction of this domain with other proteins, forming complexes that stimulate the activation of Rap1 by other GEFs.

Interestingly Sos1/2 double KO mice show significant increase in platelet counts, without alteration of other blood parameters (Baltanas, F.C. et al. 2013). In hematopoietic cells Sos1/2 is the main Ras regulator leading to transient ERK1/2 activation, while sustained activation of ERK1/2 is driven by a CrkL-C3G-Ras pathway (Nosaka, Y. et al. 1999). Therefore, we can speculate that this increase in platelet count could be due to a higher megakaryopoiesis in these KO mice as a result of an increase in C3G-Ras or C3G-Rap1 pathways leading to a sustained ERK activation in the hematopoietic precursors.

Altogether, all the above results indicate that PMA induces the phosphorylation of C3G resulting in activation of the Rap1 signaling pathway that leads to the sustained activation of ERK1/2, which is necessary for MK maturation. Furthermore, our results suggest that C3G/Rap1 could modulate ERK1/2 in a PKC-independent manner and that the transient activation of ERK by PMA is not involved in the effect of C3G on the expression of MK surface markers.

The involvement of p38 MAPK pathway in MK differentiation is well documented. It has been suggested that p38 MAPK can play opposite roles during MK differentiation depending on its levels of activation. Thus, high levels of active p38 MAPK inhibits MK differentiation through its inhibitory effect on ERK1/2 phosphorylation, which, as mentioned is needed during early MK differentiation events. A functional relationship between p38 and ERK, in which p38 would act as a negative regulator of the activation of ERK1/2, has been extensively described (Ding, B.C. et al. 2001, Li, S.P. et al. 2003, Liu, Q. et al. 2004). However, it has been reported that low levels of phospho-p38 MAPK are needed during the initial stages of PMA-induced MK differentiation, while a drastic reduction in the levels of activated p38 MAPK blocked MK differentiation and increase cell death (Jacquel, A. et al. 2006). It has been proposed that transient p38 activation may induce cell cycle arrest, triggering a differentiation program in which sub-sequent p38 down-regulation is required for the acquisition of MK features (Conde, I. et al. 2010).

Our results using double C3G and p38α silenced K562 clones suggest that C3G and p38 collaborate in the regulation of the expression of megakaryocytic and erythroid markers, although the implication of this relationship in the regulation of early MK differentiation is not

clear. A functional relationship between C3G and p38 MAPK has been already described (Maia, V. et al. 2009, Gutierrez-Uzquiza, A. et al. 2010, Maia, V. et al. 2013, Priego, N. et al. 2016). Moreover, treatment with SB increased the expression of MK surface markers in cells with C3G overexpression, indicating a negative role of p38 MAPK in C3G actions.

PMA slightly increase p38 MAPK phosphorylation, indicative of its contribution to the regulation of PMA-induced MK differentiation. In addition, C3G overexpression also increased basal levels of phospho-p38, both in K562 and HEL cells, in agreement with the need for certain levels of p38 during MK differentiation. Moreover, the effect of PMA and C3G on p38 MAPK activation seems to be additive, indicating a possible dissociation between PMA-PKC and C3G pathways in the regulation of p38 MAPK. In any case, these results are in apparent contradiction with a negative role of p38 MAPK in the C3G actions. However, the use of two clones of HEL cells, expressing different levels of C3G, indicate that C3G modulates phospho-p38 levels, so that high levels of C3G could induce a decrease in the levels of phospho-p38. In this line, an interesting aspect is that p38 MAPK seems to be a mediator in the regulatory effect of C3G on ERK1/2 phosphorylation, at least in HEL cells stimulated with PMA. Thus, HEL cells with high levels of C3G, showed intermediate levels of phospho-p38. Similarly, cells with intermediate levels of C3G (higher than control) present higher levels of phospho-p38. Therefore, the increase in p-ERK levels observed in the clone with high C3G expression could be an indirect effect due to the lower levels of phospho-p38 MAPK in these cells. A negative regulatory effect of C3G over p38 MAPK activity has been observed in many systems (Maia, V. et al. 2009, Gutierrez-Uzquiza, A. et al. 2010, Maia, V. et al. 2013, Priego, N. et al. 2016).

Our results also showed a positive effect of SB on p38 MAPK phosphorylation. This apparently contradictory result can be explained by a p38 autophosphorylation mechanism, independent on MEKK (Ge, B. et al. 2002). In addition, we can not rule out the existence of negative feed-back mechanisms, hitherto unknown, regulated by p38 MAPK.

Regarding the role of PI3K-Akt in the effect of C3G on MK differentiation, our results, using PI3K inhibitor wortmannin (W), suggest a contribution of this pathway to the C3G-induced MK marker expression. However, W did not show any effect in PMA-stimulated control cells. The involvement of PI3K-Akt pathway in MK differentiation has not been completely clarified. Some authors have claimed that this pathway is necessary, but not sufficient, to induce endomitosis (Geddis, A.E. et al. 2001, Conde, I. et al. 2010), although it seems to also stimulate expression of MK surface markers, in cooperation with the ERK1/2 pathway (Conde, I. et al. 2010). However, according to other authors, Akt, but not PI3K, would be the one involved in the regulation of the expression of CD41 and CD61 during MK

differentiation in K562 and HEL cells (Sardina, J.L. et al. 2010). Finally, other authors, using two different PI3K inhibitors, Wortmannin (a covalent, irreversible, PI3K inhibitor) and LY294002 (a reversible PI3K inhibitor), did not observed any contribution of this pathway to MK differentiation in K562 cells (Jacquel, A. et al. 2006). Our results in control cells would be in accordance with these last two authors. In contrast, PI3K would be involved in the effect of C3G, independently of PMA. This is an interesting aspect that deserves more investigation.

2. Implication of C3G in MK differentiation using mouse model

In this part of the work we have used primary bone marrow cells, isolated from our transgenic C3G and C3GΔCat mice and their corresponding wild type siblings, in which, besides analyzing the process of acquisition of megakaryocytic markers and polyploidy status, we have also performed studies focused on the stages of megakaryopoiesis and thrombopoiesis that are probably more dependent of the microenvironment, such as migration of MKs and formation of proplatelets.

Analysis of the percentage of megakaryocytes in transgenic bone marrow (BM) cells, cultured in the presence of TPO, showed a higher proportion of CD41/CD61 positive cells in Tg-C3G mice, and a lower percentage in Tg-C3GΔCat mice, compared to wild type animals. This indicates that C3G plays a positive role in the early stages of MK differentiation induced by TPO, which depends on its GEF domain. This in agreement with the increase in CD41 and CD61 expression in K562 and HEL clones with C3G overexpression. However, the percentage of megakaryocytes in untreated mouse BM cells were similar in Tg-C3G, Tg-C3GΔCat mice and their controls. These results indicate that, in contrast to the observed in the cell lines, C3G alone is not able to modulate the acquisition of MK markers in a more physiological context, requiring an additional stimulation, such as TPO, to potentiate this process.

K562 and HEL cell lines behave like MEP (megakaryocyte-erythroid progenitor cells). So, they are multipotent cells that, depending on the stimulus they receive, commit to the megakaryocytic or erythroid lineage. As we have demonstrated, C3G induces the expression of MK markers, an early event in the MK differentiation program, being therefore, involved in the commitment of these cell lines into the megakaryocytic lineage. Hence, it would be interesting to study *ex vivo* whether C3G is also involved in the proliferation and differentiation of MEPs into HPP-CFU-MKs, the less differentiated MK progenitor, which follows the MEPs. However, since Rap1 expression has been reported to occur during maturation, rather than

differentiation, of megakaryocytes from cord blood progenitor cells (Balduini, A. et al. 2008), a participation of C3G, through Rap1 activation, in the early differentiation of MK progenitors is unlikely.

Our results, showing a higher proportion of mature megakaryocytes (large CD41+ cells) with a DNA content ≥8n in the bone marrow of our transgenic mice, confirmed our previous data in cell lines. In both Tg-C3G lineages (2C1 and 6A6), C3G overexpression induced a higher ratio of DNA replication, being statistically significant in the 2C1 mice. In contrast, the levels of polyploidy of large CD41+ cells from the BM of Tg-C3GΔCat mice were very similar to those of the control mice. These results corroborate the positive role played by C3G in the acquisition of polyploid features, which seems to be dependent on its GEF activity.

An important stage in MK differentiation is the migration of megakaryocyte precursors from the osteoblastic to the vascular niche. The interaction of megakaryocytes with the matrix is an essential process for a proper migration. Type I collagen, is found in the extracellular matrix, being the most abundant component of the osteoblastic niche. It has been described that its interaction with immature megakaryocytes through its main receptors, integrin α2β1 and GPVI, inhibits the premature release of platelets (Pallotta, I. et al. 2009, Zou, Z. et al. 2009). For this reason, we found it interesting to analyze the megakaryocytes that are most closely linked to the bone in our transgenic mice, which would reveal whether C3G overexpression modifies the interaction of MKs with the endosteal collagen. The results indicated a lower proportion of MKs bound to the osteoblastic matrix in Tg-C3G mice, compared to wild type mice, indicating that C3G overexpression decreases the interaction between the megakaryocytes and the endosteal niche through collagen. Several explanations may account for these observations: i) C3G accelerates the onset of MK differentiation and maturation, and therefore, the pool of MK progenitors in the endosteum is smaller; ii) C3G decreases the proliferation of progenitors, resulting in a decrease in the pool of immature MKs in the osteoblastic niche; iii) C3G expression impairs a proper interaction between MKs and type I collagen, thereby MK are released prematurely. Since transgenic and wild type mice showed similar percentages of MK in the bone marrow *in vivo* (see **Figure R-33**) and we did not observe changes in platelet levels in peripheral blood, we discarded the first possibility (see **Figure R-42**). To discriminate between the two other options, it would necessary to perform a CFU-MKs assay.

Interestingly, the proteomic analysis of platelets from Tg-C3G 2C1 mice and their controls, revealed a differential expression of several proteins involved in adhesion and migration, such as Integrin-linked protein kinase, Rho GDP-dissociation inhibitors, Cofilin-1,

Tubulin β-1 chain or Actin-related protein 3 (unpublished results of the group), which is in favor of a role of C3G in the regulation of adhesion and migration during MK maturation.

This is reinforced by the observation that C3G expression in bone marrow explants increases the velocity of migration and the distance covered by megakaryocytes, being the catalytic activity of C3G responsible of this effect. In addition, the migration capacity and the formation of proplatelets are two processes that are highly related, since both involve cytoskeleton dynamics. This idea is reinforced by our last experiment in which, according to the migration results, we observed an increase in the number of proplatelet-forming megakaryocytes in our C3G transgenic mice, whereas C3GΔCat transgenic mice showed a reduced percentage of proplatelets, compared to wild type mice. We can conclude that C3G, through its catalytic, GEF, domain, modulates MK migration and proplatelet formation.

Several studies have demonstrated a role for C3G in migration. In Ba/F3 hematopoietic cell, C3G in complexes with CrkL and Cbl, induces migration in response to a SDF1α gradient through the activation of integrin β1 and ERK1/2 (Uemura, N. et al. 1999). C3G also plays an essential role in the migration of neural precursors during the cerebral cortex development (Voss, A.K. et al. 2008, Yip, Y.P. et al. 2012). More recently, it has been shown that C3G, in complexes with CrkII, regulate T lymphocyte adhesion and migration in response to immunophilins (Nath, P.R. et al. 2014). A negative regulation of migration by C3G has also been reported (Ohba, Y. et al. 2001, Priego, N. et al. 2016).

The increased proplatelet formation observed in Tg-C3G mice would suggest the production of a greater number of platelets in these animals. However, as stated above, this was not the case. This prompt us to speculate that C3G might play a role in MK differentiation and maturation under pathological conditions, such as cancer or wound injury, rather than in normal megakaryopoiesis. In this line, we have recently demonstrated a role for platelet C3G in tumor angiogenesis and metastasis (unpublished results of the group). Future experiments will be conducted to address this hypothesis.

In summary, from the results obtained in this study, and previous data on the signaling pathways activated by PMA that are involved in the regulation of MK differentiation, we propose a model in which C3G could act as an inducer or mediator of the megakaryocytic differentiation by PMA- dependent and independent pathways (**Figure D-1**). In addition,

Figure D-2 summarizes the stages of megakaryopoiesis in which we have shown that C3G plays a role.

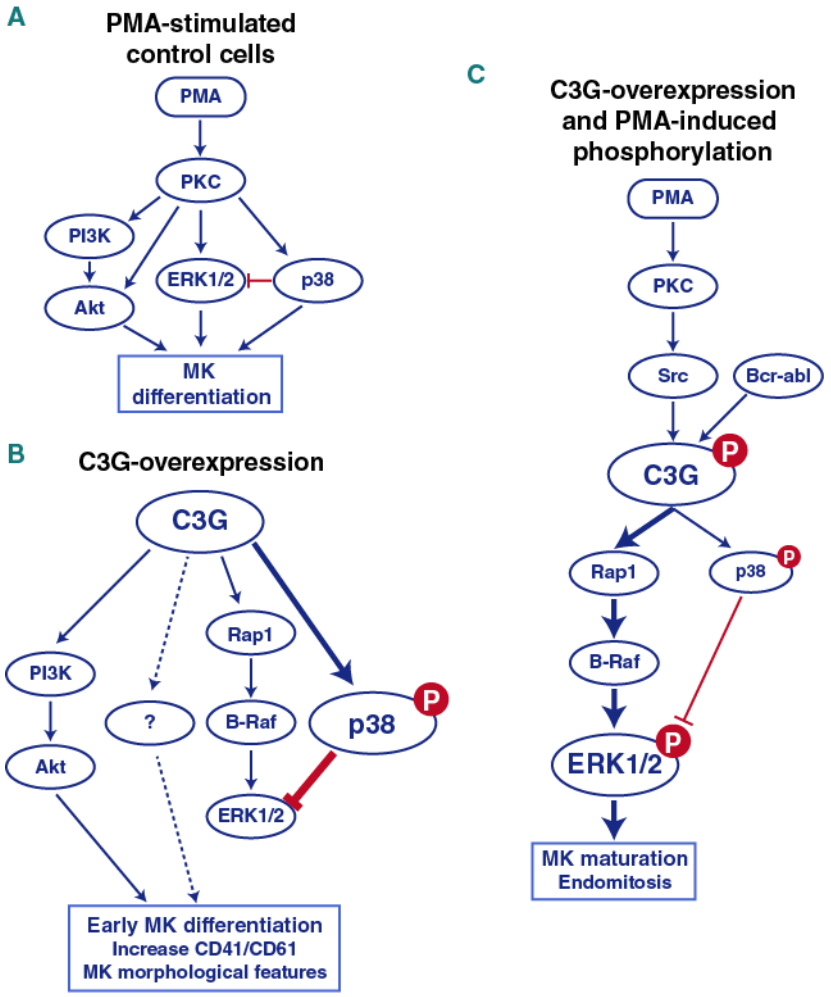

Figure D-1. Proposed model of the signaling pathways mediating the effect of C3G in MK differentiation and maturation. A) Previous proposed model of PMA-stimulated pathways during MK differentiation. B) Proposed model of signaling pathways induced by C3G overexpression; C3G would regulate early MK differentiation events by a PMA-PKC-independent pathway, involving the activation of PI3K-Akt, and possibly other pathways not yet identified C) Proposed model of the involvement of C3G in MK maturation. C3G would be phosphorylated by PMA through Src or other kinases. Overexpressed phosphorylated C3G induce a higher, sustained, activation of ERK by maintaining low levels of p38.

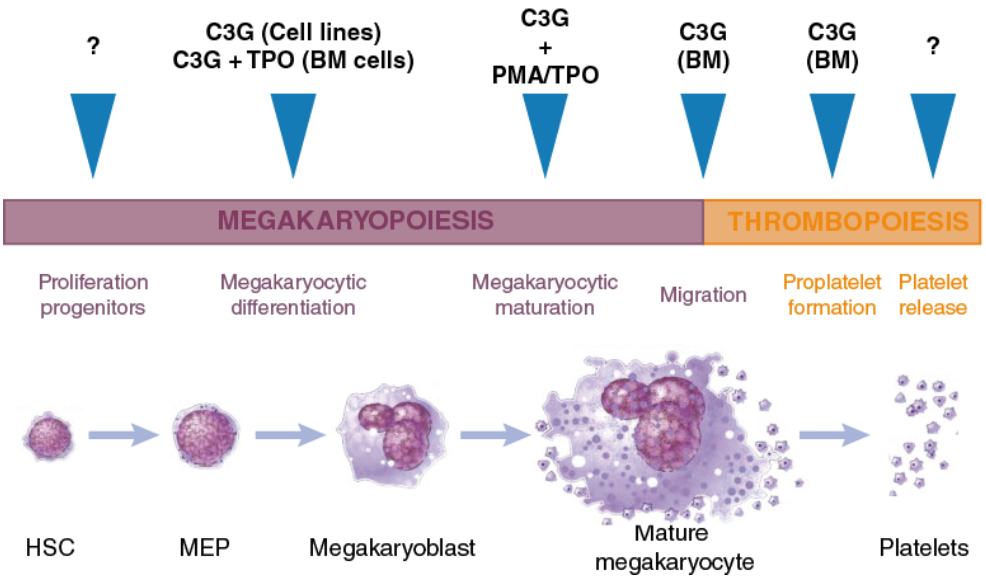

Figure D-2. Stages of megakaryopoiesis showing the processes in which C3G is involved. Arrowheads indicate the stages of megakaryopoiesis and thrombopoiesis in which our results in cell lines and primary bone marrow cells have demonstrated that C3G plays a role: acquisition of megakaryocytic features in early MK differentiation, increase in DNA content through endomitotic cycles after treatment with TPO or PMA, migration and proplatelet formation. BM: bone marrow.

Conclusions

1. C3G is involved in the regulation of megakaryocytic and erythroid surface markers, indicating its role in the early commitment of erythroid/megakaryocytic progenitors. In cell lines, this function is independent on stimulation, while in mouse bone marrow cells, it depends on TPO stimulation.

2. The role of C3G in the expression of megakaryocytic surface markers is mediated by Rap1 and PI3K but is independent on activation of PKC and transient activation of ERK1/2 and p38 MAPK. The N-terminal and SH3-binding domains of C3G play a role in the regulation of megakaryocytic and erythroid markers expression, probably through the modulation of the catalytic activity of C3G.

3. PMA induces the phosphorylation of C3G in Y504, leading to the sustained activation of the Rap1-ERK1/2 signaling pathway, which is probably involved in megakaryocytic maturation.

4. C3G regulates ERK1/2 activation through the modulation of phophos-p38 MAPK levels.

5. C3G modulates the increase in DNA content in cell lines treated with PMA through upregulation of p21 levels, and in bone marrow cells upon TPO stimulation.

6. In *ex vivo* models, C3G, through its catalytic activity, modulates megakaryocytic migration and proplatelet formation.

7. *In vivo*, the number of megakaryocytes in the bone marrow and the number of platelets in blood are not regulated by C3G overexpression.

Final Conclusion

C3G plays a role in the regulation of different stages in the megakaryocytic differentiation: acquisition of specific surface markers, changes in morphology, polyploidy, migration from de osteoblastic niche to the vascular niche and proplatelet formation. This effect of C3G on megakaryocytic differentiation does not lead to higher platelet counts under physiological conditions.

References

Akashi, K., D. Traver, T. Miyamoto and I. L. Weissman (2000). "A clonogenic common myeloid progenitor that gives rise to all myeloid lineages." Nature **404**(6774): 193-197.

Alsayed, Y., S. Uddin, S. Ahmad, B. Majchrzak, B. J. Druker, E. N. Fish and L. C. Platanias (2000). "IFN-gamma activates the C3G/Rap1 signaling pathway." J Immunol **164**(4): 1800-1806.

Arai, A., Y. Nosaka, E. Kanda, K. Yamamoto, N. Miyasaka and O. Miura (2001). "Rap1 is activated by erythropoietin or interleukin-3 and is involved in regulation of beta1 integrin-mediated hematopoietic cell adhesion." J Biol Chem **276**(13): 10453-10462.

Arai, A., Y. Nosaka, H. Kohsaka, N. Miyasaka and O. Miura (1999). "CrkL activates integrin-mediated hematopoietic cell adhesion through the guanine nucleotide exchange factor C3G." Blood **93**(11): 3713-3722.

Avruch, J., A. Khokhlatchev, J. M. Kyriakis, Z. Luo, G. Tzivion, D. Vavvas and X. F. Zhang (2001). "Ras activation of the Raf kinase: tyrosine kinase recruitment of the MAP kinase cascade." Recent Prog Horm Res **56**: 127-155.

Baccini, V., L. Roy, N. Vitrat, H. Chagraoui, S. Sabri, J. P. Le Couedic, N. Debili, F. Wendling and W. Vainchenker (2001). "Role of p21(Cip1/Waf1) in cell-cycle exit of endomitotic megakaryocytes." Blood **98**(12): 3274-3282.

Balduini, A., I. Pallotta, A. Malara, P. Lova, A. Pecci, G. Viarengo, C. L. Balduini and M. Torti (2008). "Adhesive receptors, extracellular proteins and myosin IIA orchestrate proplatelet formation by human megakaryocytes." J Thromb Haemost **6**(11): 1900-1907.

Balduini, A., A. Pecci, P. Lova, N. Arezzi, C. Marseglia, F. Bellora, C. Perotti, C. Balduini, C. L. Balduini and M. Torti (2004). "Expression, activation, and subcellular localization of the Rap1 GTPase in cord blood-derived human megakaryocytes." Exp Cell Res **300**(1): 84-93.

Baltanas, F. C., M. Perez-Andres, A. Ginel-Picardo, D. Diaz, D. Jimeno, P. Liceras-Boillos, R. L. Kortum, L. E. Samelson, A. Orfao and E. Santos (2013). "Functional redundancy of Sos1 and Sos2 for lymphopoiesis and organismal homeostasis and survival." Mol Cell Biol **33**(22): 4562-4578.

Behnke, O. (1968). "An electron microscope study of the megacaryocyte of the rat bone marrow. I. The development of the demarcation membrane system and the platelet surface coat." J Ultrastruct Res **24**(5): 412-433.

Benz, P. M., H. Laban, J. Zink, L. Gunther, U. Walter, S. Gambaryan and K. Dib (2016). "Vasodilator-Stimulated Phosphoprotein (VASP)-dependent and -independent pathways regulate thrombin-induced activation of Rap1b in platelets." Cell Commun Signal **14**(1): 21.

Bergmeier, W., T. Goerge, H. W. Wang, J. R. Crittenden, A. C. Baldwin, S. M. Cifuni, D. E. Housman, A. M. Graybiel and D. D. Wagner (2007). "Mice lacking the signaling molecule CalDAG-GEFI represent a model for leukocyte adhesion deficiency type III." J Clin Invest **117**(6): 1699-1707.

Bertoli, C., J. M. Skotheim and R. A. de Bruin (2013). "Control of cell cycle transcription during G1 and S phases." Nat Rev Mol Cell Biol **14**(8): 518-528.

Bertoni, A., S. Tadokoro, K. Eto, N. Pampori, L. V. Parise, G. C. White and S. J. Shattil (2002). "Relationships between Rap1b, affinity modulation of integrin alpha IIbbeta 3, and the actin cytoskeleton." J Biol Chem **277**(28): 25715-25721.

Besancenot, R., R. Chaligne, C. Tonetti, F. Pasquier, C. Marty, Y. Lecluse, W. Vainchenker, S. N. Constantinescu and S. Giraudier (2010). "A senescence-like cell-cycle arrest occurs during megakaryocytic maturation: implications for physiological and pathological megakaryocytic proliferation." PLoS Biol **8**(9).

Besancenot, R., D. Roos-Weil, C. Tonetti, H. Abdelouahab, C. Lacout, F. Pasquier, C. Willekens, P. Rameau, Y. Lecluse, J. B. Micol, S. N. Constantinescu, W. Vainchenker, E. Solary and S. Giraudier (2014). "JAK2 and MPL protein levels determine TPO-induced megakaryocyte proliferation vs differentiation." Blood **124**(13): 2104-2115.

Bhat, A., K. Kolibaba, T. Oda, S. Ohno-Jones, C. Heaney and B. J. Druker (1997). "Interactions of CBL with BCR-ABL and CRKL in BCR-ABL-transformed myeloid cells." J Biol Chem **272**(26): 16170-16175.

REFERENCES

Birge, R. B., C. Kalodimos, F. Inagaki and S. Tanaka (2009). "Crk and CrkL adaptor proteins: networks for physiological and pathological signaling." Cell Commun Signal **7**: 13.

Blair, P. and R. Flaumenhaft (2009). "Platelet alpha-granules: basic biology and clinical correlates." Blood Rev **23**(4): 177-189.

Bos, J. L., H. Rehmann and A. Wittinghofer (2007). "GEFs and GAPs: critical elements in the control of small G proteins." Cell **129**(5): 865-877.

Bradford, M. M. (1976). "A rapid and sensitive method for the quantitation of microgram quantities of protein utilizing the principle of protein-dye binding." Anal Biochem **72**: 248-254.

Broudy, V. C., N. L. Lin and K. Kaushansky (1995). "Thrombopoietin (c-mpl ligand) acts synergistically with erythropoietin, stem cell factor, and interleukin-11 to enhance murine megakaryocyte colony growth and increases megakaryocyte ploidy in vitro." Blood **85**(7): 1719-1726.

Buensuceso, C. S. and T. E. O'Toole (2000). "The association of CRKII with C3G can be regulated by integrins and defines a novel means to regulate the mitogen-activated protein kinases." J Biol Chem **275**(17): 13118-13125.

Conde, I., D. Pabon, A. Jayo, P. Lastres and C. Gonzalez-Manchon (2010). "Involvement of ERK1/2, p38 and PI3K in megakaryocytic differentiation of K562 cells." Eur J Haematol **84**(5): 430-440.

Crespo, P. and J. Leon (2000). "Ras proteins in the control of the cell cycle and cell differentiation." Cell Mol Life Sci **57**(11): 1613-1636.

Crittenden, J. R., W. Bergmeier, Y. Zhang, C. L. Piffath, Y. Liang, D. D. Wagner, D. E. Housman and A. M. Graybiel (2004). "CalDAG-GEFI integrates signaling for platelet aggregation and thrombus formation." Nat Med **10**(9): 982-986.

Cuenda, A. and S. Rousseau (2007). "p38 MAP-kinases pathway regulation, function and role in human diseases." Biochim Biophys Acta **1773**(8): 1358-1375.

Chang, Y., D. Bluteau, N. Debili and W. Vainchenker (2007). "From hematopoietic stem cells to platelets." J Thromb Haemost **5 Suppl 1**: 318-327.

Chang, Y. I., W. K. Hua, C. L. Yao, S. M. Hwang, Y. C. Hung, C. J. Kuan, J. S. Leou and W. J. Lin (2010). "Protein-arginine methyltransferase 1 suppresses megakaryocytic differentiation via modulation of the p38 MAPK pathway in K562 cells." J Biol Chem **285**(27): 20595-20606.

Che, Y. L., S. J. Luo, G. Li, M. Cheng, Y. M. Gao, X. M. Li, J. M. Dai, H. He, J. Wang, H. J. Peng, Y. Zhang, W. Y. Li, H. Wang, B. Liu and H. Linghu (2015). "The C3G/Rap1 pathway promotes secretion of MMP-2 and MMP-9 and is involved in serous ovarian cancer metastasis." Cancer Lett **359**(2): 241-249.

Chrzanowska-Wodnicka, M., S. S. Smyth, S. M. Schoenwaelder, T. H. Fischer and G. C. White, 2nd (2005). "Rap1b is required for normal platelet function and hemostasis in mice." J Clin Invest **115**(3): 680-687.

De Falco, V., M. D. Castellone, G. De Vita, A. M. Cirafici, J. M. Hershman, C. Guerrero, A. Fusco, R. M. Melillo and M. Santoro (2007). "RET/papillary thyroid carcinoma oncogenic signaling through the Rap1 small GTPase." Cancer Res **67**(1): 381-390.

Debili, N., C. Issaad, J. M. Masse, J. Guichard, A. Katz, J. Breton-Gorius and W. Vainchenker (1992). "Expression of CD34 and platelet glycoproteins during human megakaryocytic differentiation." Blood **80**(12): 3022-3035.

Deutsch, V. R. and A. Tomer (2006). "Megakaryocyte development and platelet production." Br J Haematol **134**(5): 453-466.

Deutsch, V. R. and A. Tomer (2013). "Advances in megakaryocytopoiesis and thrombopoiesis: from bench to bedside." Br J Haematol **161**(6): 778-793.

Ding, B. C., T. L. Witt, B. Hukku, H. Heng, L. Zhang and L. H. Matherly (2001). "Association of deletions and translocation of the reduced folate carrier gene with profound loss of gene expression in methotrexate-resistant K562 human erythroleukemia cells." Biochem Pharmacol **61**(6): 665-675.

Drachman, J. G., D. F. Sabath, N. E. Fox and K. Kaushansky (1997). "Thrombopoietin signal

transduction in purified murine megakaryocytes." Blood **89**(2): 483-492.

Dupuy, A. J., K. Morgan, F. C. von Lintig, H. Shen, H. Acar, D. E. Hasz, N. A. Jenkins, N. G. Copeland, G. R. Boss and D. A. Largaespada (2001). "Activation of the Rap1 guanine nucleotide exchange gene, CalDAG-GEF I, in BXH-2 murine myeloid leukemia." J Biol Chem **276**(15): 11804-11811.

Eckly, A., H. Heijnen, F. Pertuy, W. Geerts, F. Proamer, J. Y. Rinckel, C. Leon, F. Lanza and C. Gachet (2014). "Biogenesis of the demarcation membrane system (DMS) in megakaryocytes." Blood **123**(6): 921-930.

Feller, S. M., B. Knudsen and H. Hanafusa (1994). "c-Abl kinase regulates the protein binding activity of c-Crk." EMBO J **13**(10): 2341-2351.

Fernandez-Medarde, A. and E. Santos (2011). "The RasGrf family of mammalian guanine nucleotide exchange factors." Biochim Biophys Acta **1815**(2): 170-188.

Franke, B., M. van Triest, K. M. de Bruijn, G. van Willigen, H. K. Nieuwenhuis, C. Negrier, J. W. Akkerman and J. L. Bos (2000). "Sequential regulation of the small GTPase Rap1 in human platelets." Mol Cell Biol **20**(3): 779-785.

Fukuyama, T., H. Ogita, T. Kawakatsu, T. Fukuhara, T. Yamada, T. Sato, K. Shimizu, T. Nakamura, M. Matsuda and Y. Takai (2005). "Involvement of the c-Src-Crk-C3G-Rap1 signaling in the nectin-induced activation of Cdc42 and formation of adherens junctions." J Biol Chem **280**(1): 815-825.

Garcia, J., J. de Gunzburg, A. Eychene, S. Gisselbrecht and F. Porteu (2001). "Thrombopoietin-mediated sustained activation of extracellular signal-regulated kinase in UT7-Mpl cells requires both Ras-Raf-1- and Rap1-B-Raf-dependent pathways." Mol Cell Biol **21**(8): 2659-2670.

Ge, B., H. Gram, F. Di Padova, B. Huang, L. New, R. J. Ulevitch, Y. Luo and J. Han (2002). "MAPKK-independent activation of p38alpha mediated by TAB1-dependent autophosphorylation of p38alpha." Science **295**(5558): 1291-1294.

Geddis, A. E. (2010). "Megakaryopoiesis." Semin Hematol **47**(3): 212-219.

Geddis, A. E., N. E. Fox and K. Kaushansky (2001). "Phosphatidylinositol 3-kinase is necessary but not sufficient for thrombopoietin-induced proliferation in engineered Mpl-bearing cell lines as well as in primary megakaryocytic progenitors." J Biol Chem **276**(37): 34473-34479.

Geddis, A. E. and K. Kaushansky (2006). "Endomitotic megakaryocytes form a midzone in anaphase but have a deficiency in cleavage furrow formation." Cell Cycle **5**(5): 538-545.

Gibbins, J. M. and M. P. Mahaut-Smith (2011). Platelets and Megakaryocytes Volume 3, Additional Protocols and Perspectives. Methods in Molecular Biology Ser. New York

Secaucus, Humana Press

Springer Distributor.

Gotoh, T., S. Hattori, S. Nakamura, H. Kitayama, M. Noda, Y. Takai, K. Kaibuchi, H. Matsui, O. Hatase, H. Takahashi and et al. (1995). "Identification of Rap1 as a target for the Crk SH3 domain-binding guanine nucleotide-releasing factor C3G." Mol Cell Biol **15**(12): 6746-6753.

Gotoh, T., Y. Niino, M. Tokuda, O. Hatase, S. Nakamura, M. Matsuda and S. Hattori (1997). "Activation of R-Ras by Ras-guanine nucleotide-releasing factor." J Biol Chem **272**(30): 18602-18607.

Guerrero, C., A. Fernandez-Medarde, J. M. Rojas, J. Font de Mora, L. M. Esteban and E. Santos (1998). "Transformation suppressor activity of C3G is independent of its CDC25-homology domain." Oncogene **16**(5): 613-624.

Guerrero, C., S. Martin-Encabo, A. Fernandez-Medarde and E. Santos (2004). "C3G-mediated suppression of oncogene-induced focus formation in fibroblasts involves inhibition of ERK activation, cyclin A expression and alterations of anchorage-independent growth." Oncogene **23**(28): 4885-4893.

Gutierrez-Berzal, J., E. Castellano, S. Martin-Encabo, N. Gutierrez-Cianca, J. M. Hernandez, E. Santos and C. Guerrero (2006). "Characterization of p87C3G, a novel, truncated C3G isoform that is overexpressed in chronic myeloid leukemia and interacts with Bcr-Abl." Exp Cell Res **312**(6): 938-948.

Gutierrez-Herrero, S., V. Maia, J. Gutierrez-Berzal, N. Calzada, M. Sanz, C. Gonzalez-Manchon, M. Pericacho, S. Ortiz-Rivero, J. R. Gonzalez-Porras, M. Arechederra, A. Porras and C. Guerrero (2012). "C3G transgenic mouse models with specific expression in platelets reveal a new role for C3G in platelet clotting through its GEF activity." Biochim Biophys Acta **1823**(8): 1366-1377.

Gutierrez-Uzquiza, A., M. Arechederra, I. Molina, R. Banos, V. Maia, M. Benito, C. Guerrero and A. Porras (2010). "C3G down-regulates p38 MAPK activity in response to stress by Rap-1 independent mechanisms: involvement in cell death." Cell Signal **22**(3): 533-542.

Hamada, T., R. Mohle, J. Hesselgesser, J. Hoxie, R. L. Nachman, M. A. Moore and S. Rafii (1998). "Transendothelial migration of megakaryocytes in response to stromal cell-derived factor 1 (SDF-1) enhances platelet formation." J Exp Med **188**(3): 539-548.

Hasegawa, H., E. Kiyokawa, S. Tanaka, K. Nagashima, N. Gotoh, M. Shibuya, T. Kurata and M. Matsuda (1996). "DOCK180, a major CRK-binding protein, alters cell morphology upon translocation to the cell membrane." Mol Cell Biol **16**(4): 1770-1776.

Heijnen, H. F., N. Debili, W. Vainchencker, J. Breton-Gorius, H. J. Geuze and J. J. Sixma (1998). "Multivesicular bodies are an intermediate stage in the formation of platelet alpha-granules." Blood **91**(7): 2313-2325.

Herrera, R., S. Hubbell, S. Decker and L. Petruzzelli (1998). "A role for the MEK/MAPK pathway in PMA-induced cell cycle arrest: modulation of megakaryocytic differentiation of K562 cells." Exp Cell Res **238**(2): 407-414.

Hirata, T., H. Nagai, K. Koizumi, K. Okino, A. Harada, M. Onda, T. Nagahata, I. Mikami, K. Hirai, S. Haraguchi, E. Jin, O. Kawanami, K. Shimizu and M. Emi (2004). "Amplification, up-regulation and over-expression of C3G (CRK SH3 domain-binding guanine nucleotide-releasing factor) in non-small cell lung cancers." J Hum Genet **49**(6): 290-295.

Hogan, C., N. Serpente, P. Cogram, C. R. Hosking, C. U. Bialucha, S. M. Feller, V. M. Braga, W. Birchmeier and Y. Fujita (2004). "Rap1 regulates the formation of E-cadherin-based cell-cell contacts." Mol Cell Biol **24**(15): 6690-6700.

Hong, Y., J. F. Martin, W. Vainchenker and J. D. Erusalimsky (1996). "Inhibition of protein kinase C suppresses megakaryocytic differentiation and stimulates erythroid differentiation in HEL cells." Blood **87**(1): 123-131.

Howell, W. H. and D. D. Donahue (1937). "The Production of Blood Platelets in the Lungs." J Exp Med **65**(2): 177-203.

Ichiba, T., Y. Hashimoto, M. Nakaya, Y. Kuraishi, S. Tanaka, T. Kurata, N. Mochizuki and M. Matsuda (1999). "Activation of C3G guanine nucleotide exchange factor for Rap1 by phosphorylation of tyrosine 504." J Biol Chem **274**(20): 14376-14381.

Ichiba, T., Y. Kuraishi, O. Sakai, S. Nagata, J. Groffen, T. Kurata, S. Hattori and M. Matsuda (1997). "Enhancement of guanine-nucleotide exchange activity of C3G for Rap1 by the expression of Crk, CrkL, and Grb2." J Biol Chem **272**(35): 22215-22220.

Ikuta, K. and I. L. Weissman (1992). "Evidence that hematopoietic stem cells express mouse c-kit but do not depend on steel factor for their generation." Proc Natl Acad Sci U S A **89**(4): 1502-1506.

Italiano, J. E., Jr., P. Lecine, R. A. Shivdasani and J. H. Hartwig (1999). "Blood platelets are assembled principally at the ends of proplatelet processes produced by differentiated megakaryocytes." J Cell Biol **147**(6): 1299-1312.

Jacquel, A., P. Colosetti, S. Grosso, N. Belhacene, A. Puissant, S. Marchetti, J. P. Breittmayer and P. Auberger (2007). "Apoptosis and erythroid differentiation triggered by Bcr-Abl inhibitors in CML cell lines are fully distinguishable processes that exhibit different sensitivity to caspase inhibition." Oncogene **26**(17): 2445-2458.

Jacquel, A., M. Herrant, V. Defamie, N. Belhacene, P. Colosetti, S. Marchetti, L. Legros, M. Deckert, B. Mari, J. P. Cassuto, P. Hofman and P. Auberger (2006). "A survey of the signaling pathways involved in megakaryocytic differentiation of the human K562 leukemia cell line by molecular and c-DNA array analysis." Oncogene **25**(5): 781-794.

Jiang, F., Y. Jia and I. Cohen (2002). "Fibronectin- and protein kinase C-mediated activation of ERK/MAPK are essential for

proplateletlike formation." Blood **99**(10): 3579-3584.

Jin, S., B. Zhai, Z. Qiu, J. Wu, M. D. Lane and K. Liao (2000). "c-Crk, a substrate of the insulin-like growth factor-1 receptor tyrosine kinase, functions as an early signal mediator in the adipocyte differentiation process." J Biol Chem **275**(44): 34344-34352.

Junt, T., H. Schulze, Z. Chen, S. Massberg, T. Goerge, A. Krueger, D. D. Wagner, T. Graf, J. E. Italiano, Jr., R. A. Shivdasani and U. H. von Andrian (2007). "Dynamic visualization of thrombopoiesis within bone marrow." Science **317**(5845): 1767-1770.

Kaushansky, K. (2006). "Lineage-specific hematopoietic growth factors." N Engl J Med **354**(19): 2034-2045.

Kaushansky, K., V. C. Broudy, N. Lin, M. J. Jorgensen, J. McCarty, N. Fox, D. Zucker-Franklin and C. Lofton-Day (1995). "Thrombopoietin, the Mp1 ligand, is essential for full megakaryocyte development." Proc Natl Acad Sci U S A **92**(8): 3234-3238.

Kaushansky, K., S. Lok, R. D. Holly, V. C. Broudy, N. Lin, M. C. Bailey, J. W. Forstrom, M. M. Buddle, P. J. Oort, F. S. Hagen and et al. (1994). "Promotion of megakaryocyte progenitor expansion and differentiation by the c-Mpl ligand thrombopoietin." Nature **369**(6481): 568-571.

Kauts, M. L., C. S. Vink and E. Dzierzak (2016). "Hematopoietic (stem) cell development - how divergent are the roads taken?" FEBS Lett **590**(22): 3975-3986.

Kawaguchi, T., R. Hatano, K. Yamaguchi, K. Nawa, R. Hashimoto and H. Yokota (2012). "Fibronectin promotes proplatelet formation in the human megakaryocytic cell line UT-7/TPO." Cell Biol Int **36**(1): 39-45.

Kiel, M. J. and S. J. Morrison (2008). "Uncertainty in the niches that maintain haematopoietic stem cells." Nat Rev Immunol **8**(4): 290-301.

Kikuchi, J., Y. Furukawa, S. Iwase, Y. Terui, M. Nakamura, S. Kitagawa, M. Kitagawa, N. Komatsu and Y. Miura (1997). "Polyploidization and functional maturation are two distinct processes during megakaryocytic differentiation: involvement of cyclin-dependent kinase inhibitor p21 in polyploidization." Blood **89**(11): 3980-3990.

Kirito, K. and N. Komatsu (2002). "[Signal transduction in hematopoiesis: a functional role of Stat 1 and Stat 3 in erythropoiesis and megakaryopoiesis]." Rinsho Ketsueki **43**(4): 278-281.

Kirsch, K. H., M. M. Georgescu and H. Hanafusa (1998). "Direct binding of p130(Cas) to the guanine nucleotide exchange factor C3G." J Biol Chem **273**(40): 25673-25679.

Knudsen, B. S., S. M. Feller and H. Hanafusa (1994). "Four proline-rich sequences of the guanine-nucleotide exchange factor C3G bind with unique specificity to the first Src homology 3 domain of Crk." J Biol Chem **269**(52): 32781-32787.

Kondo, M., I. L. Weissman and K. Akashi (1997). "Identification of clonogenic common lymphoid progenitors in mouse bone marrow." Cell **91**(5): 661-672.

Ku, H., Y. Yonemura, K. Kaushansky and M. Ogawa (1996). "Thrombopoietin, the ligand for the Mpl receptor, synergizes with steel factor and other early acting cytokines in supporting proliferation of primitive hematopoietic progenitors of mice." Blood **87**(11): 4544-4551.

Larson, M. K. and S. P. Watson (2006). "Regulation of proplatelet formation and platelet release by integrin alpha IIb beta3." Blood **108**(5): 1509-1514.

Lee, C. H., H. J. Yun, H. S. Kang and H. D. Kim (1999). "ERK/MAPK pathway is required for changes of cyclin D1 and B1 during phorbol 12-myristate 13-acetate-induced differentiation of K562 cells." IUBMB Life **48**(6): 585-591.

Lefrancais, E., G. Ortiz-Munoz, A. Caudrillier, B. Mallavia, F. Liu, D. M. Sayah, E. E. Thornton, M. B. Headley, T. David, S. R. Coughlin, M. F. Krummel, A. D. Leavitt, E. Passegue and M. R. Looney (2017). "The lung is a site of platelet biogenesis and a reservoir for haematopoietic progenitors." Nature **544**(7648): 105-109.

Levine, R. F., A. Eldor, P. K. Shoff, S. Kirwin, D. Tenza and E. M. Cramer (1993). "Circulating megakaryocytes: delivery of large numbers of intact, mature megakaryocytes to the lungs." Eur J Haematol **51**(4): 233-246.

Li, J., Y. Xia and D. J. Kuter (1999). "Interaction of thrombopoietin with the platelet c-mpl receptor in plasma: binding, internalization,

stability and pharmacokinetics." Br J Haematol **106**(2): 345-356.

Li, S. P., M. R. Junttila, J. Han, V. M. Kahari and J. Westermarck (2003). "p38 Mitogen-activated protein kinase pathway suppresses cell survival by inducing dephosphorylation of mitogen-activated protein/extracellular signal-regulated kinase kinase1,2." Cancer Res **63**(13): 3473-3477.

Ling, L., T. Zhu and P. E. Lobie (2003). "Src-CrkII-C3G-dependent activation of Rap1 switches growth hormone-stimulated p44/42 MAP kinase and JNK/SAPK activities." J Biol Chem **278**(29): 27301-27311.

Liu, Q. and P. A. Hofmann (2004). "Protein phosphatase 2A-mediated cross-talk between p38 MAPK and ERK in apoptosis of cardiac myocytes." Am J Physiol Heart Circ Physiol **286**(6): H2204-2212.

Livak, K. J. and T. D. Schmittgen (2001). "Analysis of relative gene expression data using real-time quantitative PCR and the 2(-Delta Delta C(T)) Method." Methods **25**(4): 402-408.

Long, M. W., C. H. Heffner, J. L. Williams, C. Peters and E. V. Prochownik (1990). "Regulation of megakaryocyte phenotype in human erythroleukemia cells." J Clin Invest **85**(4): 1072-1084.

Lordier, L., J. Pan, V. Naim, A. Jalil, I. Badirou, P. Rameau, J. Larghero, N. Debili, F. Rosselli, W. Vainchenker and Y. Chang (2012). "Presence of a defect in karyokinesis during megakaryocyte endomitosis." Cell Cycle **11**(23): 4385-4389.

Lozzio, C. B. and B. B. Lozzio (1975). "Human chronic myelogenous leukemia cell-line with positive Philadelphia chromosome." Blood **45**(3): 321-334.

Machlus, K. R. and J. E. Italiano, Jr. (2013). "The incredible journey: From megakaryocyte development to platelet formation." J Cell Biol **201**(6): 785-796.

Maia, V., S. Ortiz-Rivero, M. Sanz, J. Gutierrez-Berzal, I. Alvarez-Fernandez, S. Gutierrez-Herrero, J. M. de Pereda, A. Porras and C. Guerrero (2013). "C3G forms complexes with Bcr-Abl and p38alpha MAPK at the focal adhesions in chronic myeloid leukemia cells: implication in the regulation of leukemic cell adhesion." Cell Commun Signal **11**(1): 9.

Maia, V., M. Sanz, J. Gutierrez-Berzal, A. de Luis, A. Gutierrez-Uzquiza, A. Porras and C. Guerrero (2009). "C3G silencing enhances STI-571-induced apoptosis in CML cells through p38 MAPK activation, but it antagonizes STI-571 inhibitory effect on survival." Cell Signal **21**(7): 1229-1235.

Marshall, C. J. (1995). "Specificity of receptor tyrosine kinase signaling: transient versus sustained extracellular signal-regulated kinase activation." Cell **80**(2): 179-185.

Martegani, E., M. Vanoni, R. Zippel, P. Coccetti, R. Brambilla, C. Ferrari, E. Sturani and L. Alberghina (1992). "Cloning by functional complementation of a mouse cDNA encoding a homologue of CDC25, a Saccharomyces cerevisiae RAS activator." EMBO J **11**(6): 2151-2157.

Martin-Encabo, S., E. Santos and C. Guerrero (2007). "C3G mediated suppression of malignant transformation involves activation of PP2A phosphatases at the subcortical actin cytoskeleton." Exp Cell Res **313**(18): 3881-3891.

Martin, P. and T. Papayannopoulou (1982). "HEL cells: a new human erythroleukemia cell line with spontaneous and induced globin expression." Science **216**(4551): 1233-1235.

Matsuda, M., Y. Hashimoto, K. Muroya, H. Hasegawa, T. Kurata, S. Tanaka, S. Nakamura and S. Hattori (1994). "CRK protein binds to two guanine nucleotide-releasing proteins for the Ras family and modulates nerve growth factor-induced activation of Ras in PC12 cells." Mol Cell Biol **14**(8): 5495-5500.

Matsuda, M., S. Tanaka, S. Nagata, A. Kojima, T. Kurata and M. Shibuya (1992). "Two species of human CRK cDNA encode proteins with distinct biological activities." Mol Cell Biol **12**(8): 3482-3489.

Matsumura, I., J. Ishikawa, K. Nakajima, K. Oritani, Y. Tomiyama, J. Miyagawa, T. Kato, H. Miyazaki, Y. Matsuzawa and Y. Kanakura (1997). "Thrombopoietin-induced differentiation of a human megakaryoblastic leukemia cell line, CMK, involves transcriptional activation of p21(WAF1/Cip1) by STAT5." Mol Cell Biol **17**(5): 2933-2943.

Mazharian, A., S. Roger, P. Maurice, E. Berrou, M. R. Popoff, M. F. Hoylaerts, F. Fauvel-Lafeve, A. Bonnefoy and M. Bryckaert (2005). "Differential Involvement of ERK2 and p38 in

platelet adhesion to collagen." J Biol Chem **280**(28): 26002-26010.

Mazharian, A., S. P. Watson and S. Severin (2009). "Critical role for ERK1/2 in bone marrow and fetal liver-derived primary megakaryocyte differentiation, motility, and proplatelet formation." Exp Hematol **37**(10): 1238-1249 e1235.

Melemed, A. S., J. W. Ryder and T. A. Vik (1997). "Activation of the mitogen-activated protein kinase pathway is involved in and sufficient for megakaryocytic differentiation of CMK cells." Blood **90**(9): 3462-3470.

Minamiguchi, H., T. Kimura, Y. Urata, H. Miyazaki, T. Bamba, T. Abe and Y. Sonoda (2001). "Simultaneous signalling through c-mpl, c-kit and CXCR4 enhances the proliferation and differentiation of human megakaryocyte progenitors: possible roles of the PI3-K, PKC and MAPK pathways." Br J Haematol **115**(1): 175-185.

Mitra, A. and V. Radha (2010). "F-actin-binding domain of c-Abl regulates localized phosphorylation of C3G: role of C3G in c-Abl-mediated cell death." Oncogene **29**(32): 4528-4542.

Miyazaki, R., H. Ogata, T. Iguchi, S. Sogo, T. Kushida, T. Ito, M. Inaba, S. Ikehara and Y. Kobayashi (2000). "Comparative analyses of megakaryocytes derived from cord blood and bone marrow." Br J Haematol **108**(3): 602-609.

Miyazaki, R., H. Ogata and Y. Kobayashi (2001). "Requirement of thrombopoietin-induced activation of ERK for megakaryocyte differentiation and of p38 for erythroid differentiation." Ann Hematol **80**(5): 284-291.

Mochizuki, N., Y. Ohba, S. Kobayashi, N. Otsuka, A. M. Graybiel, S. Tanaka and M. Matsuda (2000). "Crk activation of JNK via C3G and R-Ras." J Biol Chem **275**(17): 12667-12671.

Moosavi, M. A., R. Yazdanparast and A. Lotfi (2007). "ERK1/2 inactivation and p38 MAPK-dependent caspase activation during guanosine 5'-triphosphate-mediated terminal erythroid differentiation of K562 cells." Int J Biochem Cell Biol **39**(9): 1685-1697.

Munoz-Alonso, M. J., L. Ceballos, G. Bretones, P. Frade, J. Leon and A. Gandarillas (2012). "MYC accelerates p21CIP-induced megakaryocytic differentiation involving early mitosis arrest in leukemia cells." J Cell Physiol **227**(5): 2069-2078.

Nakao, K. and A. A. Angrist (1968). "Membrane surface specialization of blood platelet and megakaryocyte." Nature **217**(5132): 960-961.

Nakao, T., A. E. Geddis, N. E. Fox and K. Kaushansky (2008). "PI3K/Akt/FOXO3a pathway contributes to thrombopoietin-induced proliferation of primary megakaryocytes in vitro and in vivo via modulation of p27(Kip1)." Cell Cycle **7**(2): 257-266.

Nath, P. R., G. Dong, A. Braiman and N. Isakov (2014). "Immunophilins control T lymphocyte adhesion and migration by regulating CrkII binding to C3G." J Immunol **193**(8): 3966-3977.

Nosaka, Y., A. Arai, N. Miyasaka and O. Miura (1999). "CrkL mediates Ras-dependent activation of the Raf/ERK pathway through the guanine nucleotide exchange factor C3G in hematopoietic cells stimulated with erythropoietin or interleukin-3." J Biol Chem **274**(42): 30154-30162.

Oda, A., Y. Miyakawa, B. J. Druker, A. Ishida, K. Ozaki, H. Ohashi, M. Wakui, M. Handa, K. Watanabe, S. Okamoto and Y. Ikeda (1996). "CrkI is constitutively tyrosine phosphorylated in platelets from chronic myelogenous leukemia patients and inducibly phosphorylated in normal platelets stimulated by thrombopoietin." Blood **88**(11): 4304-4313.

Ohba, Y., K. Ikuta, A. Ogura, J. Matsuda, N. Mochizuki, K. Nagashima, K. Kurokawa, B. J. Mayer, K. Maki, J. Miyazaki and M. Matsuda (2001). "Requirement for C3G-dependent Rap1 activation for cell adhesion and embryogenesis." EMBO J **20**(13): 3333-3341.

Okada, S., H. Nakauchi, K. Nagayoshi, S. Nishikawa, Y. Miura and T. Suda (1992). "In vivo and in vitro stem cell function of c-kit- and Sca-1-positive murine hematopoietic cells." Blood **80**(12): 3044-3050.

Okada, S. and J. E. Pessin (1997). "Insulin and epidermal growth factor stimulate a conformational change in Rap1 and dissociation of the CrkII-C3G complex." J Biol Chem **272**(45): 28179-28182.

Okino, K., H. Nagai, H. Nakayama, D. Doi, K. Yoneyama, H. Konishi and T. Takeshita (2006). "Inactivation of Crk SH3 domain-

binding guanine nucleotide-releasing factor (C3G) in cervical squamous cell carcinoma." Int J Gynecol Cancer **16**(2): 763-771.

Olson, T. S., A. Caselli, S. Otsuru, T. J. Hofmann, R. Williams, P. Paolucci, M. Dominici and E. M. Horwitz (2013). "Megakaryocytes promote murine osteoblastic HSC niche expansion and stem cell engraftment after radioablative conditioning." Blood **121**(26): 5238-5249.

Pallotta, I., M. Lovett, W. Rice, D. L. Kaplan and A. Balduini (2009). "Bone marrow osteoblastic niche: a new model to study physiological regulation of megakaryopoiesis." PLoS One **4**(12): e8359.

Pannekoek, W. J., M. R. Kooistra, F. J. Zwartkruis and J. L. Bos (2009). "Cell-cell junction formation: the role of Rap1 and Rap1 guanine nucleotide exchange factors." Biochim Biophys Acta **1788**(4): 790-796.

Patel, S. R., J. H. Hartwig and J. E. Italiano, Jr. (2005). "The biogenesis of platelets from megakaryocyte proplatelets." J Clin Invest **115**(12): 3348-3354.

Pear, W. S., G. P. Nolan, M. L. Scott and D. Baltimore (1993). "Production of high-titer helper-free retroviruses by transient transfection." Proc Natl Acad Sci U S A **90**(18): 8392-8396.

Pendaries, C., S. P. Watson and J. C. Spalton (2007). "Methods for genetic modification of megakaryocytes and platelets." Platelets **18**(6): 393-408.

Priego, N., M. Arechederra, C. Sequera, P. Bragado, A. Vazquez-Carballo, A. Gutierrez-Uzquiza, V. Martin-Granado, J. J. Ventura, M. G. Kazanietz, C. Guerrero and A. Porras (2016). "C3G knock-down enhances migration and invasion by increasing Rap1-mediated p38alpha activation, while it impairs tumor growth through p38alpha-independent mechanisms." Oncotarget **7**(29): 45060-45078.

Psaila, B., D. Lyden and I. Roberts (2012). "Megakaryocytes, malignancy and bone marrow vascular niches." J Thromb Haemost **10**(2): 177-188.

Racke, F. K., K. Lewandowska, S. Goueli and A. N. Goldfarb (1997). "Sustained activation of the extracellular signal-regulated kinase/mitogen-activated protein kinase pathway is required for megakaryocytic differentiation of K562 cells." J Biol Chem **272**(37): 23366-23370.

Radha, V., A. Mitra, K. Dayma and K. Sasikumar (2011). "Signalling to actin: role of C3G, a multitasking guanine-nucleotide-exchange factor." Biosci Rep **31**(4): 231-244.

Radha, V., A. Rajanna, R. K. Gupta, K. Dayma and T. Raman (2008). "The guanine nucleotide exchange factor, C3G regulates differentiation and survival of human neuroblastoma cells." J Neurochem **107**(5): 1424-1435.

Radha, V., A. Rajanna, A. Mitra, N. Rangaraj and G. Swarup (2007). "C3G is required for c-Abl-induced filopodia and its overexpression promotes filopodia formation." Exp Cell Res **313**(11): 2476-2492.

Radha, V., A. Rajanna and G. Swarup (2004). "Phosphorylated guanine nucleotide exchange factor C3G, induced by pervanadate and Src family kinases localizes to the Golgi and subcortical actin cytoskeleton." BMC Cell Biol **5**: 31.

Radley, J. M. and C. J. Haller (1982). "The demarcation membrane system of the megakaryocyte: a misnomer?" Blood **60**(1): 213-219.

Radley, J. M. and C. J. Haller (1983). "Fate of senescent megakaryocytes in the bone marrow." Br J Haematol **53**(2): 277-287.

Raslova, H., V. Baccini, L. Loussaief, B. Comba, J. Larghero, N. Debili and W. Vainchenker (2006). "Mammalian target of rapamycin (mTOR) regulates both proliferation of megakaryocyte progenitors and late stages of megakaryocyte differentiation." Blood **107**(6): 2303-2310.

Ravid, K., J. Lu, J. M. Zimmet and M. R. Jones (2002). "Roads to polyploidy: the megakaryocyte example." J Cell Physiol **190**(1): 7-20.

Ren, R., Z. S. Ye and D. Baltimore (1994). "Abl protein-tyrosine kinase selects the Crk adapter as a substrate using SH3-binding sites." Genes Dev **8**(7): 783-795.

Rojnuckarin, P., J. G. Drachman and K. Kaushansky (1999). "Thrombopoietin-induced activation of the mitogen-activated protein kinase (MAPK) pathway in normal

megakaryocytes: role in endomitosis." Blood **94**(4): 1273-1282.

Rojnuckarin, P., Y. Miyakawa, N. E. Fox, J. Deou, G. Daum and K. Kaushansky (2001). "The roles of phosphatidylinositol 3-kinase and protein kinase Czeta for thrombopoietin-induced mitogen-activated protein kinase activation in primary murine megakaryocytes." J Biol Chem **276**(44): 41014-41022.

Roux, P. P. and J. Blenis (2004). "ERK and p38 MAPK-activated protein kinases: a family of protein kinases with diverse biological functions." Microbiol Mol Biol Rev **68**(2): 320-344.

Sabri, S., M. Jandrot-Perrus, J. Bertoglio, R. W. Farndale, V. M. Mas, N. Debili and W. Vainchenker (2004). "Differential regulation of actin stress fiber assembly and proplatelet formation by alpha2beta1 integrin and GPVI in human megakaryocytes." Blood **104**(10): 3117-3125.

Samuelsson, J., S. Alonso, T. Ruiz-Larroya, T. H. Cheung, Y. F. Wong and M. Perucho (2011). "Frequent somatic demethylation of RAPGEF1/C3G intronic sequences in gastrointestinal and gynecological cancer." Int J Oncol **38**(6): 1575-1577.

Sardina, J. L., G. Lopez-Ruano, L. I. Sanchez-Abarca, J. A. Perez-Simon, A. Gaztelumendi, C. Trigueros, M. Llanillo, J. Sanchez-Yague and A. Hernandez-Hernandez (2010). "p22phox-dependent NADPH oxidase activity is required for megakaryocytic differentiation." Cell Death Differ **17**(12): 1842-1854.

Sasi Kumar, K., A. Ramadhas, S. C. Nayak, S. Kaniyappan, K. Dayma and V. Radha (2015). "C3G (RapGEF1), a regulator of actin dynamics promotes survival and myogenic differentiation of mouse mesenchymal cells." Biochim Biophys Acta **1853**(10 Pt A): 2629-2639.

Schick, P. K., C. M. Wojenski, X. He, J. Walker, C. Marcinkiewicz and S. Niewiarowski (1998). "Integrins involved in the adhesion of megakaryocytes to fibronectin and fibrinogen." Blood **92**(8): 2650-2656.

Schultess, J., O. Danielewski and A. P. Smolenski (2005). "Rap1GAP2 is a new GTPase-activating protein of Rap1 expressed in human platelets." Blood **105**(8): 3185-3192.

Schumacher, C., B. S. Knudsen, T. Ohuchi, P. P. Di Fiore, R. H. Glassman and H. Hanafusa (1995). "The SH3 domain of Crk binds specifically to a conserved proline-rich motif in Eps15 and Eps15R." J Biol Chem **270**(25): 15341-15347.

Schwertz, H., S. Koster, W. H. Kahr, N. Michetti, B. F. Kraemer, D. A. Weitz, R. C. Blaylock, L. W. Kraiss, A. Greinacher, G. A. Zimmerman and A. S. Weyrich (2010). "Anucleate platelets generate progeny." Blood **115**(18): 3801-3809.

Seita, J. and I. L. Weissman (2010). "Hematopoietic stem cell: self-renewal versus differentiation." Wiley Interdiscip Rev Syst Biol Med **2**(6): 640-653.

Severin, S., C. Ghevaert and A. Mazharian (2010). "The mitogen-activated protein kinase signaling pathways: role in megakaryocyte differentiation." J Thromb Haemost **8**(1): 17-26.

Shakyawar, D. K., K. Dayma, A. Ramadhas, C. Varalakshmi and V. Radha (2017). "C3G shows regulated nucleocytoplasmic exchange and represses histone modifications associated with euchromatin." Mol Biol Cell **28**(7): 984-995.

Sher, N., J. R. Von Stetina, G. W. Bell, S. Matsuura, K. Ravid and T. L. Orr-Weaver (2013). "Fundamental differences in endoreplication in mammals and Drosophila revealed by analysis of endocycling and endomitotic cells." Proc Natl Acad Sci U S A **110**(23): 9368-9373.

Shivakrupa, R., V. Radha, C. Sudhakar and G. Swarup (2003). "Physical and functional interaction between Hck tyrosine kinase and guanine nucleotide exchange factor C3G results in apoptosis, which is independent of C3G catalytic domain." J Biol Chem **278**(52): 52188-52194.

Snow, J. W., N. Abraham, M. C. Ma, N. W. Abbey, B. Herndier and M. A. Goldsmith (2002). "STAT5 promotes multilineage hematolymphoid development in vivo through effects on early hematopoietic progenitor cells." Blood **99**(1): 95-101.

Stork, P. J. and T. J. Dillon (2005). "Multiple roles of Rap1 in hematopoietic cells: complementary versus antagonistic functions." Blood **106**(9): 2952-2961.

Strassel, C., A. Eckly, C. Leon, C. Petitjean, M. Freund, J. P. Cazenave, C. Gachet and F. Lanza (2009). "Intrinsic impaired proplatelet formation and microtubule coil assembly of megakaryocytes in a mouse model of Bernard-Soulier syndrome." Haematologica **94**(6): 800-810.

Szalai, G., A. C. LaRue and D. K. Watson (2006). "Molecular mechanisms of megakaryopoiesis." Cell Mol Life Sci **63**(21): 2460-2476.

Takahashi, M., Y. Li, T. J. Dillon and P. J. Stork (2017). "Phosphorylation of Rap1 by cAMP-dependent Protein Kinase (PKA) Creates a Binding Site for KSR to Sustain ERK Activation by cAMP." J Biol Chem **292**(4): 1449-1461.

Takai, S., M. Tanaka, H. Sugimura, K. Yamada, Y. Naito, I. Kino and M. Matsuda (1994). "Mapping of the human C3G gene coding a guanine nucleotide releasing protein for Ras family to 9q34.3 by fluorescence in situ hybridization." Hum Genet **94**(5): 549-550.

Tanaka, S., T. Morishita, Y. Hashimoto, S. Hattori, S. Nakamura, M. Shibuya, K. Matuoka, T. Takenawa, T. Kurata, K. Nagashima and et al. (1994). "C3G, a guanine nucleotide-releasing protein expressed ubiquitously, binds to the Src homology 3 domains of CRK and GRB2/ASH proteins." Proc Natl Acad Sci U S A **91**(8): 3443-3447.

Tanaka, S., T. Ouchi and H. Hanafusa (1997). "Downstream of Crk adaptor signaling pathway: activation of Jun kinase by v-Crk through the guanine nucleotide exchange protein C3G." Proc Natl Acad Sci U S A **94**(6): 2356-2361.

Tatin, F., C. Varon, E. Genot and V. Moreau (2006). "A signalling cascade involving PKC, Src and Cdc42 regulates podosome assembly in cultured endothelial cells in response to phorbol ester." J Cell Sci **119**(Pt 4): 769-781.

Tavassoli, M. and M. Aoki (1981). "Migration of entire megakaryocytes through the marrow--blood barrier." Br J Haematol **48**(1): 25-29.

Thon, J. N., A. Montalvo, S. Patel-Hett, M. T. Devine, J. L. Richardson, A. Ehrlicher, M. K. Larson, K. Hoffmeister, J. H. Hartwig and J. E. Italiano, Jr. (2010). "Cytoskeletal mechanics of proplatelet maturation and platelet release." J Cell Biol **191**(4): 861-874.

Tomer, A. (2004). "Human marrow megakaryocyte differentiation: multiparameter correlative analysis identifies von Willebrand factor as a sensitive and distinctive marker for early (2N and 4N) megakaryocytes." Blood **104**(9): 2722-2727.

Trakala, M. and M. Malumbres (2014). "The functional relevance of polyploidization in the skin." Exp Dermatol **23**(2): 92-93.

Uchida, M., K. Kirito, R. Shimizu, Y. Miura, K. Ozawa and N. Komatsu (2001). "A functional role of mitogen-activated protein kinases, erk1 and erk2, in the differentiation of a human leukemia cell line, UT-7/GM: a possible key factor for cell fate determination toward erythroid and megakaryocytic lineages." Int J Hematol **73**(1): 78-83.

Uchida, N., A. Tsukamoto, D. He, A. M. Friera, R. Scollay and I. L. Weissman (1998). "High doses of purified stem cells cause early hematopoietic recovery in syngeneic and allogeneic hosts." J Clin Invest **101**(5): 961-966.

Uddin, S., J. Ah-Kang, J. Ulaszek, D. Mahmud and A. Wickrema (2004). "Differentiation stage-specific activation of p38 mitogen-activated protein kinase isoforms in primary human erythroid cells." Proc Natl Acad Sci U S A **101**(1): 147-152.

Uemura, N. and J. D. Griffin (1999). "The adapter protein Crkl links Cbl to C3G after integrin ligation and enhances cell migration." J Biol Chem **274**(53): 37525-37532.

Voss, A. K., J. M. Britto, M. P. Dixon, B. N. Sheikh, C. Collin, S. S. Tan and T. Thomas (2008). "C3G regulates cortical neuron migration, preplate splitting and radial glial cell attachment." Development **135**(12): 2139-2149.

Voss, A. K., P. Gruss and T. Thomas (2003). "The guanine nucleotide exchange factor C3G is necessary for the formation of focal adhesions and vascular maturation." Development **130**(2): 355-367.

Voss, A. K., D. L. Krebs and T. Thomas (2006). "C3G regulates the size of the cerebral cortex neural precursor population." EMBO J **25**(15): 3652-3663.

Whalen, A. M., S. C. Galasinski, P. S. Shapiro, T. S. Nahreini and N. G. Ahn (1997). "Megakaryocytic differentiation induced by

constitutive activation of mitogen-activated protein kinase kinase." Mol Cell Biol **17**(4): 1947-1958.

Witthuhn, B. A., F. W. Quelle, O. Silvennoinen, T. Yi, B. Tang, O. Miura and J. N. Ihle (1993). "JAK2 associates with the erythropoietin receptor and is tyrosine phosphorylated and activated following stimulation with erythropoietin." Cell **74**(2): 227-236.

Woo, T. H., B. K. Patel, M. Cinco, L. D. Smythe, M. L. Symonds, M. A. Norris and M. F. Dohnt (1998). "Real-time homogeneous assay of rapid cycle polymerase chain reaction product for identification of Leptonema illini." Anal Biochem **259**(1): 112-117.

Woolthuis, C. M. and C. Y. Park (2016). "Hematopoietic stem/progenitor cell commitment to the megakaryocyte lineage." Blood **127**(10): 1242-1248.

Yang, L., D. Bryder, J. Adolfsson, J. Nygren, R. Mansson, M. Sigvardsson and S. E. Jacobsen (2005). "Identification of Lin(-)Sca1(+)kit(+)CD34(+)Flt3- short-term hematopoietic stem cells capable of rapidly reconstituting and rescuing myeloablated transplant recipients." Blood **105**(7): 2717-2723.

Yip, Y. P., T. Thomas, A. K. Voss and J. W. Yip (2012). "Migration of sympathetic preganglionic neurons in the spinal cord of a C3G-deficient mouse suggests that C3G acts in the reelin signaling pathway." J Comp Neurol **520**(14): 3194-3202.

Yoder, M. C. (2002). "Embryonic hematopoiesis in mice and humans." Acta Paediatr Suppl **91**(438): 5-8.

Yokote, K., U. Hellman, S. Ekman, Y. Saito, L. Ronnstrand, Y. Saito, C. H. Heldin and S. Mori (1998). "Identification of Tyr-762 in the platelet-derived growth factor alpha-receptor as the binding site for Crk proteins." Oncogene **16**(10): 1229-1239.

York, R. D., H. Yao, T. Dillon, C. L. Ellig, S. P. Eckert, E. W. McCleskey and P. J. Stork (1998). "Rap1 mediates sustained MAP kinase activation induced by nerve growth factor." Nature **392**(6676): 622-626.

Yu, M. and A. B. Cantor (2012). "Megakaryopoiesis and thrombopoiesis: an update on cytokines and lineage surface markers." Methods Mol Biol **788**: 291-303.

Zhai, B., H. Huo and K. Liao (2001). "C3G, a guanine nucleotide exchange factor bound to adapter molecule c-Crk, has two alternative splicing forms." Biochem Biophys Res Commun **286**(1): 61-66.

Zhu, T., E. L. Goh and P. E. Lobie (1998). "Growth hormone stimulates the tyrosine phosphorylation and association of p125 focal adhesion kinase (FAK) with JAK2. Fak is not required for stat-mediated transcription." J Biol Chem **273**(17): 10682-10689.

Zimmet, J. and K. Ravid (2000). "Polyploidy: occurrence in nature, mechanisms, and significance for the megakaryocyte-platelet system." Exp Hematol **28**(1): 3-16.

Zimmet, J. M., D. Ladd, C. W. Jackson, P. E. Stenberg and K. Ravid (1997). "A role for cyclin D3 in the endomitotic cell cycle." Mol Cell Biol **17**(12): 7248-7259.

Zou, Z., A. A. Schmaier, L. Cheng, P. Mericko, S. K. Dickeson, T. P. Stricker, S. A. Santoro and M. L. Kahn (2009). "Negative regulation of activated alpha-2 integrins during thrombopoiesis." Blood **113**(25): 6428-6439.